Activated zeolite as operational environment in anaerobic fermentation processes

DOCTORAL THESIS

In partial fulfillment of the requirements for the degree of
Doctor rerum naturalium (Dr. rer. nat.)

by
Stefan Weiß

born in
Schwerin (Mecklenburg-Western Pomerania, Germany)

born on the
27th of October in 1981

Dissertation submitted to the Faculty of Chemistry, Chemical- and Process Engineering, Biotechnology, Institute of Environmental Biotechnology at Graz University of Technology
Thesis supervisor: Univ.-Prof. Dr. Georg Gübitz

in the period of
February 2009 to March 2012

1. Referee: Univ.-Prof. Dr. Georg M. Gübitz, Graz University of Technology, Institute of Environmental Biotechnology
2. Referee: Univ.-Prof. Dr. Michael Narodoslawsky, Graz University of Technology, Institute for Process and Particle Engineering

Abstract

Renewable energy production on the basis of biomass and its conversion to energy and heat via the formation of combustible methane as an alternative to fossil energy sources and nuclear power becomes inevitable these days to cope with the global energy turnaround for sustainability. The arguable trend to grow energy crops such as maize and other grasses solely for energy recovery through fermentation did not vanish so far, but utilisation of organic wastes and residues from municipal and agricultural sources become more imposing than ever. In biogas production processes the hydrolysis of biopolymers represents a bottle neck since recalcitrant plant cell structures such as crystalline cellulose and lignocellulosic compounds represent a barrier in the degradation of biomass and its conversion to biomethane. Since eubacterial and archaeal microorganisms do act syntrophically in a consortium to accomplish the hydrolysis, acidification, acetogenesis and methanogenesis as a whole process, each phase contributes to a stable working chain. Consequently, approaches concerning a more efficient de-polymerisation of cellulose and hemicellulose to monomeric sugars are required.

Here, we show a strategy using natural zeolites (i.e. trace metal activated clinoptilolites) as natural carrier material supporting microbial growth and enzyme activity enhancing the biomass degrading step and thus increasing the methane productivity. Microscopy techniques proofed dense biofilm formation on the surface of clinoptilolite particles (Scanning electron microscopy) and as well approved bacteria inhabiting voids of the nano-porous zeolitic framework (Confocal laser scanning microscopy) during batch and continuous operated fermentation experiments. Furthermore, computer-assisted cluster analyses based on an unweighted pairwise grouping method applied to 16S rRNA-based PCR-SSCP fingerprints revealed the occurrence of specific clusters for clinoptilolite colonisers. Herein, 104 bacterial sequences could be identified including members with relative abundance of the orders Clostridiales (32.2%), Bacteroidales (28.8%), Bacillales (18.6%) and Pseudomonadales (10.2%). Immobilised populations showed a unique fingerprint pattern, which was significantly different from those clusters specifically formed on grass silage or found as free populations. Investigations of the biofilm's role in the biodegradation process exposed populations associated with clinoptilolites to develop pronounced hydrolytic enzyme activities, i.e. cellulase, pectinase and

xylanase, shortly after re-incubation in sterilised sludge on grass silage and model substrate. 36 enzymes were identified via sequencing analysis (Mass spectroscopy), allocating most affiliations to endo- and exo-acting cellulases (75%), i.e. exocellobiohydrolases and glucanases; sugar isomerases (31%) and hemicellulolytic enzymes (22%) including xylanase. An increase of hemicellulolytic activity and corresponding populations, i.e. foremost *Clostridium* spp. and *Bacteroides* spp. could also been provoked through cultivation and enrichment from inoculation with an energy plant derived natural biogas consortium on powderous xylan as sole carbon source in synthetic medium. However, the presence of plant cell wall devourers was accompanied by the methanogenic hydrogenotrophic genera *Methanoculles bourgensis* and *Methanolinea tarda*, but also *Methanosarcina barkeri* when clinoptilolite particles were exposed to complex inoculating mixed populations during *in sacco* incubation under anaerobic mesophilic conditions.

Our results demonstrate that members of hydrolytical and methanogenic populations do naturally inhabit the clinoptilolite matrix to dwell in co-existence and how ‘immobilisation by purpose’ can be realised efficiently. In either case, clinoptilolites proofed to be eminently suitable mineral carriers for microorganisms. We anticipate our findings to be the starting point for more sophisticated applications of combined action of microbial advanced clinoptilolite in order to enhance the biogas production from organic biomass and to overcome degradation and conversion derived bottle necks by supporting syntrophical relationships.

Table of Contents

1. Introduction

1.1 Objectives of the work

The present thesis deals with the applicability of a natural mineral as inorganic carrier for microorganisms. During the conversion of plant biomass for energy production, recalcitrant cell wall structures represent a barrier for hydrolysis – a rate limiting step towards the final production of combustible methane. In large-scale processes unwanted extension of hydraulic retention times and process inhibition through acidification are the consequences. In high performance systems such as upflow anaerobic sludge blanket or expanded granular sludge bed reactors, dysfunctions in the formation of activated sludge are observed during fermentation of recalcitrant biomass, i.e. substrates rich in biopolymer contents. Therefore, enzymatic hydrolysis of the world´s most abundant biopolymer cellulose and of other plant polysaccharides has a tremendous potential for bioenergy and renewable building block production. Though the majority of enzymes from aerobic fungi and some bacteria involved in biomass degradation have been described, there are still remaining questions considering anaerobic organisms occurring in the biogas process. Thus, investigations were focussed on anaerobic cellulose degrading enzyme producers. It was furthermore assumed that the use of hydrolytically active enzymes can be maximised by applying whole microbes, rather than costly non-selfreproducing pure enzyme additives. Therefore, colonisation and immobilisation of whole organisms on a carrier material, i.e. zeolite was intensively studied. Since food based substrates and energy crops become more and more banned in biogas production, lignocellulose based agricultural wastes are favoured. Consequently, the optimisation of hydrolysis under anaerobic conditions is gaining a lot of importance from both, the scientific and practical point of view.

The following paragraphs attempt to provide the reader with basic and complex information on the thematic background of the scientific publications that constitute the major core of this work. Going through the publication’s headlines and data contents, the reader might get a feel that the chronological order is putting the cart before the horse. Instead of fully evolving theoretical backgrounds before all, application approaches in small-scaled lab experiments were done first to accomplish a proof of principle, then to be followed by detailed basic research approaches in order to fully understand the mechanisms behind.

1.2 Bio-energy recovery through fermentation

(Co-Authorship, Book Chapter, Springer, Berlin, Heidelberg, 2010)

1.2.1 Fermentation conditions

The fermentation of biomass for sustainable energy production, i.e. the production of combustible methane involves several parameters of crucial importance for the process interpretation, i.e. substrate concentration, hydraulic retention time, volume loading rate, metabolic production of volatile fatty acids, just to mention some. Variations in these values, especially of the hydraulic retention time (HRT) depend on whether the process is operated under mesophilic or thermophilic temperature conditions. Co-fermentation of liquid and solid substrate fractions such as manures and silages as well as thermophilic temperature conditions usually result in shorter HRTs (Schöftner et al., 2007). A change in substrate composition containing higher proportions of fibrous and cellulosic substrates leads to an increase in recirculation demand of diluting process liquids, which lowers the HRT and generates more solid digestion residues (SDR) as reported by Resch et al. (2008). Since SDRs provide the largest source of residual methane potential (expressed as non-converted volatile solids) their reduction is demanded. Out of extensive collections of empirical data a variety of biological key values has been selected for the assessment of optimal fermentation conditions for biogas producing plants. The assessment system gives operational parameter ranges for optimal (green range) and suboptimal conditions (yellow and red range) considering energy crop and co-fermentation processes (table 1-1).

Tab. 1-1 Evaluation of operational parameters for optimal fermentation conditions for energy crop and co-fermentation processes obtained from empirical data (Schöftner et al., 2007, study by IFA Tulln Institute of Environmental Biotechnology, 2005 and 2006).

parameter	green range		yellow range		red range	
	from	to	from	to	from	to
pH	7.5	8.1	7.1	7.5	< 7.1	> 8.1
OD [%]	3	9	-	< 3	> 9	-
ODM [%]	3	6	<3	7	> 7	-
Total VFA [mg l^{-1}]	0	1500	1500	4500	> 4500	-
VS [%]	2.4	6	> 2.4	7	> 7	-
Propionic acid [mg l^{-1}]	0	250	250	1000	> 1000	-
Acetic acid [mg l^{-1}]	0	1000	1000	3000	> 3000	-
UVA [mg l^{-1}]	0	2.5	2.5	20	> 20	-
UAN [mg l^{-1}]	-	< 600	600	800	> 800	-
TKN [g l^{-1}]	-	< 6	> 6	-	-	-
TAN [g l^{-1}]	-	< 5	> 5	-	-	-

OD = organic solids; ODM = total organic solids; VFA = volatile fatty acids; VS = volatile solids; UVA = undissociated volatile acids; UAN = undissociated ammonia nitrogen; TKN = total Kjedahl nitrogen; TAN = total ammonia nitrogen

Simulated and experimental studies (Angelidaki et al., 1993; Biswas et al., 2005) indicate that initial concentrations of slurry, carbohydrate, protein and fat affect the performance of anaerobic digester based on feed consisting of municipal wastes significantly. Methane concentration and the calorific value of biogas decrease with increasing concentrations of slurry, carbohydrate and protein, while increased fat concentration has the opposite effect. One of the most important parameters for bacterial growth is the ratio of nutrients provided by the substrate, which are carbon (C), nitrogen (N) and phosphate (P). Bacterial communities producing biogas demand a ratio of carbon to nitrogen to phosphate between 75:5:1 to 125:5:1 (Eder and Schulz, 2006). Furthermore, optimum total carbon to total nitrogen ratio is considered to be between 10:1 and 30:1. Depending on the given substrate composition the C:N:P ratio can be calculated and responded to through setting up the mixture whereby an optimal plant feeding mixture is ascertainable. The methane energy value system (MEVS) enables the calculation of nutrient content specific methane production potential for certain organic substrates e.g. maize and

clover grass as assumed by Amon et al. (2003). Due to the determination of nutrient contents MEVS includes the estimation of methane yield per hectare of energy crops, varieties and crop rotations, as well as the estimation of nutrient requirements of microorganisms that are responsible for the anaerobic digestion. Furthermore MEVS allows recommendations on varieties and optimum harvesting time for energy crops.

1.2.2 By-product formation

Under anaerobic conditions biological processes in biogas plants produce several by-products. The hydrogen sulfide (H_2S) content in the biogas ranges from 500 to 20000 ppm (2% v/v) depending on the given substrate (Woodcock and Gottlieb, 2004). Because of its corrosive and harmful properties it has to be removed from the produced biogas in order to protect power engines and human life. Nowadays biofiltration is being studied and considered as an interesting alternative for classical chemical methods. Biotrickling filters can be described as vessels, in most cases filled with a porous, inert solid support over which active microorganisms develop by using pollutants as nutrient and energy sources, thus resulting in biodegradation (biological oxidation) of the contaminants (Gabriel and Deshusses, 2003; Devinny, 1999). Redondo et al. (2008) introduced an automated online H_2S analyser which can be applied to the monitoring of biotrickling filters. A single-channel flow injection analyser (FIA) detects S^{2-} in the liquid phase and is coupled with a continuous flow analyser (CFA) including a gaseous diffusion step (GD-CFA) for detecting H_2S in the gas phase. The formation of undissociated ammonia nitrogen, which has inhibiting properties for the microbial community can be controlled by adjusting the pH value between 7.5 and 8.1 to keep the total concentration belong 600 mg NH_4^+ l^{-1}.

1.2.3 Mass & energy balances

Even if agricultural areas in europe are predominantly cultivated with annual crops, energy balance and cost-benefit analyses suggest perennial crops for energy production in biogas plants (Uellendahl et al., 2008). The energy input for the cultivation of e.g. miscanthus and willow resulting from field preparation, planting, fertiliser and pesticide needs, etc. is much lower compared to e.g. corn (Møller et al., 2008; Heller et al., 2003). At the same time, their annual solar energy conversion efficiency is often higher than that of annual plants due to longer growing seasons resulting in higher biomass yields (Uellendahl et al., 2008).

Since perennial crops show high dry matter and lignocellulosic biomass concentrations a suitable pretreatment like alki or acid treatment, predigestion, ensilage usage, thermo-chemical or ultrasonic treatment are necessary to gain appropriate methane yields (Yadvika et al., 2004). Uellendahl et al. (2008) showed input:output ratios ranging from 6.9 to 9.5 for corn, miscanthus and willow respectively. Via pretreatment the input:output ratio increased up to ~13 resulting in an higher biogas productivity. An example for high efficiency substrates is switchgrass. Its input:output ratio ranges from 10.8 to 11.3 (Vadas et al., 2008) and can be considered as formidable co-substrate in order to increase the net energy yield per hectare through balanced co-fermentation with less efficient crops.

1.2.4 Biofuel

Biogas usage as a fuel becomes more attractive since it meets the European and international target changes concerning the replacement of fossil fuels. The comparison of energy values of methane, ethanol and other common fuels (also relevant for combined heat and power plants) reveals the outstanding potential of methane as biofuel (table 1-2).

Tab. 1-2 Minimum calorific values of biogas and other fuels in comparison and their equivalence to methane (Constant et al., 1989).

fuel	MJ kg^{-1}	MJ Nm^3	volumetric equivalence to CH_4
Methane	50.0	35.9	1.0
Purified biogas (90%)	45.0	32.3	0.9
Biogas (60%)	30.0	21.5	0.6
Butane	45.7	118.5	3.3
Propane	46.4	90.9	2.5
Methanol	19.9	$15.9 * 10^3$	442.9
Ethanol	26.9	$21.4 * 10^3$	596.1
Gasoline	45.0	$33.3 * 10^3$	927.6
Diesel	42.1	$34.5 * 10^3$	961.0

Nm^3 = volume at standard ambient temperature and pressure

Properties for the usage biogas as biofuel must be: a minimal calorific value (21.5 MJ m^{-3} considering CH_4 content of 60%), a stoichiometric air to fuel ratio of 7.5 (flammable biogas to air mixture is between 8 to 20% considering CH_4 content of 5-12%), a flame velocity of 25 cm s^{-1} and a minimum auto-ignite temperature of 600°C (Noyola et al., 2006). Biogas will not burn if more than 75% of CO_2 is present. Natural gas (NG) and bio-methane operated vehicles perform fully equivalent to petrol or diesel driven ones. With minor modifications present technology allows EURO 6/VI emission level values. Methane is used in two forms that are liquefied natural gas (LNG) and compressed natural gas (CNG), which can be used to substitute diesel in dual-fuel engines. According to the report of the European expert group on future transport fuel (Söldner et al., 2011) diesel could be feasibly reduced by up to 85% when co-combustion of NG/bio-methane is applied. Besides comparably lower pollutant emission levels, CO_2 is drastically reduced (up to 24% compared to petrol) when bio-methane is used as fuel. LNG could cover long distance transports via road, water ways or rail transport systems, wherever diesel engines are used currently. Considering a market share of 20% for CNG and LNG vehicles in transport fuels a reduction of CO_2 emissions by 7% would be possible, assuming only 20% of the total gas content to be bio-methane. Prognoses presume a market share of 5% in the EU by 2020, which would account for approximately 15 million cars.

1.3 Cellulosic biomass composition

In general the term biomass is defined as the sum of all biological matter naturally produced by living or recently living organisms. In the circumstance of bioenergy and sustainability it rather describes renewable energy sources based on the primary product of photosynthesis. At this, biopolymers constitute major components of terrestrial plant cell wall matrices (figure 1-1), wherein cellulose and hemicelluloses are produced in large amounts (table 1-3). Cellulose is the most abundant renewable natural carbon source in the biosphere, generating around 100 billion dry tons per year (Jarvis, 2003). Consequently, cellulosic biomass is an enormously important bioresource for the production of biobased products and bioenergy. Cellulosic biomass includes all kinds of domesticated natural sources, either purposely planted like energy crops or resulting from domestic consumption chains as biowastes. Another aspect could be added, when unused natural sources such as greenery wastes and autumn foliage are considered as substrates for biogas production.

Tab. 1-3 Chemical composition of common natural cellulosic biomass sources in [%] of dry matter.

agricultural and industrial residues	cellulose [%]	hemicellulose [%]	lignin [%]	reference
bermuda grass	25	36	6	Sun and Cheng (2002)
birch wood	38	20	23	Wiselogel et al. (1996)
corn cobs	45	35	15	Sun and Cheng (2002)
corn stover	36	23	7	Wiselogel et al. (1996)
grasses	25-45	15-50	6-30	Sun and Cheng (2002)
hardwood stems	40-55	24-40	18-25	Sun and Cheng (2002)
leaves	15-20	80-85	0	Sun and Cheng (2002)
maize	19-37	25-38	4-9	Amon et al. (2007)
newspaper	40-55	25-40	18-30	Sun and Cheng (2002)
paper	85-99	0	0-15	Sun and Cheng (2002)
pulp waste papers	60-70	10-20	5-10	Sun and Cheng (2002)
softwood stems	45-50	25-33	25-35	Sun and Cheng (2002)
switch grass	45	31	12	Sun and Cheng (2002)
wheat straw	30	50	15	Sun and Cheng (2002)

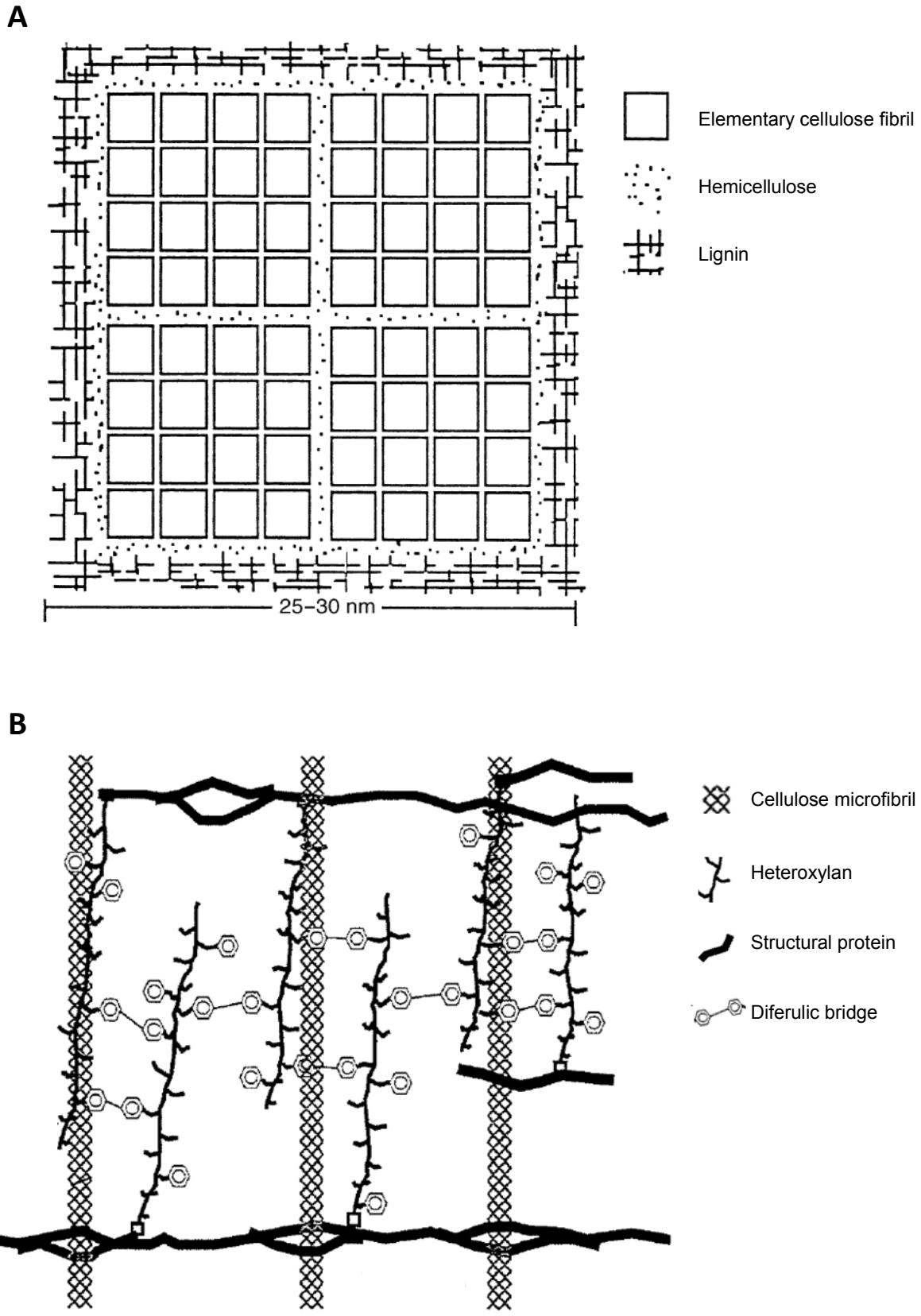

Fig. 1-1 **A** Cross-sectional model of the ultrastructural organisation of wood cell wall components (Fengel, 1971), **B** Model of corn fibre cell walls, exemplary for energy crops (Saulnier and Thibault, 1999).

1.3.1 Cellulose

Cellulose is a polymorph structure which shows six different derivatives that can be interconverted (O'Sullivan, 1997). Celluose I (figure 1-2A) is the native form to be found in nature from which cellulose II and III to IV can be formed directly via regeneration or mercerisation or indirectly via heat exposure. Cellulose derivatives are basically differentiated by alterations in the organisation of the fibrillar structure, i.e. the orientation of microfibril bundles (unidirectional in cellulose I vs. mixed directions of microfibril chains in cellulose II) or the variability of hydroxymethyl conformation that determines two aspects: the degree of crystallinity (non-uniform in cellulose I vs. defined structure in cellulose III) and the arrangement of hydrogen bonding patterns. Cellulose I has two intramolecular hydrogen bonds at (OH)3-(*O*)5 and (OH)2-(*O*)6 and an interchain bond between (*O*)6 and (*O*)3, while cellulose II has an intrachain hydrogen bonding at (OH)3-(*O*)6 and two intermolecular bonds at (OH)6-(*O*)2 for corner chains and (OH)6-(*O*)3 for centre chains. Other referred derivatives of cellulose such as methylcellulose, (sodium)-carboxymethylcellulose (CMC) or hydroxypropyl cellulose (HPC) are simply discriminated by altered substitutions derived from alkylation, but what's more important, these compounds are soluble in water and organic solvents. However, native cellulose is water-insoluble, fibrous and tough in order to protect the cell wall of plants, particularly stems, stalks and woody plant parts are cellulose-rich to preserve the structural morphology. Biosynthesis is suggested to be taking place at or outside the plasma membrane (Brett and Waldorn, 1990; Lamport, 1970) where collections of cellulose chains (microfibrils) are elongated by terminal complexes (TCs) which are thought to be cellulose synthase complexes (Macchi and Palma, 1969). Cellulose chains are composed of β-D-glucopyranose units linked by β-1,4-glucosidic bonds with a degree of polymerisation (DP) ranging from 100 to 200,000 glucopyranose units (e.g. wood DP = 10,000) as summarised by Zhang et al. (2006). DP in primary cell walls is supposed to be lower compared with secondary cell walls. The repeating unit in cellulose is also often referred to as cellobiose, a dimer of β-D-glucopyranosyl-D-glucose. Material strength is furthermore given by criss-cross like arrangement of cellulose microfibrils. Crystalline cellulose is formed by crystallisation of pre-formed TC-directed cellulose chains through a protein (top protein) or just by coupling of adjacent cellulose chains and sheets by hydrogen bonds (Zhang et al., 2006). Van der Waal's forces result consequently in a parallel alignment (crystalline structure)

with straight supra-molecular fibres of high tensile strength and low accessibility (Notley et al., 2004, Nishiyama et al., 2003). Armorphous cellulose is suggested to be microfibril parts which consist mostly of small amounts of straight surface chains with a low degree of substitution around 1 or 2% (Debzi et al., 1991, Verlhac et al., 1990). Overall cellulose molecules are very stable, i.e. the estimated half-life is between 5 to 8 million years for β-glucosidic bond cleavage at a temperature of 25°C (Wolfenden and Snider, 2001).

1.3.2 Hemicellulose

Hemicelluloses are found in the primary cell wall of all vascular plants and constitute a group of polysaccharides that are associated with cellulose microfibrils via hydrogen bonds (Nevell and Zeronian, 1985; Haigler, 1985). Compared to cellulose, hemicelluloses' solubility in water is higher, which is due to a lower degree of polymerisation (DP) ranging from 100 to 200 of several different hexoses, pentoses and glucoronic acid (Kuhad et al., 1997). They constitute the second most abundant polysaccharide in nature. Even if non-covalently bound to cellulose, hemicelluloses cannot be extracted easily by hot water treatment or chelating agents, but in contrast to cellulose (hence the name hemicellulose) are soluble in strong alkali solutions such as 4M potassium hydroxide (Wilkie, 1979). These heteropolymers consist of pentoses (xylose, arabinose) and hexoses (glucose and its epimers) with highly substituted sugar backbones (xylan, arabinan, glucomannan etc.). In sweet grasses (Graminiae) like maize, the major hemicelluloses are acidic arabinoxylans and neutral mixed-linkage β-1,3-1,4-glucans (figure 1-2B). A characteristic feature of monocots is the presence of a linear polysaccharide backbone composed of a β-1,4-linked D-xylopyranose residues (Wilkie, 1979), so called xylans. In Graminiae heteroxylans dominate, where approximately half of the xylose residues are substituted at (*O*)2 and (*O*)3 positions with mainly acetyl groups (50-70%), other pentoses or hexoses such as D-glucose and its diastereomers galactose and mannose. L-arabinofuranosyl, D-glucopyranosyluronic acid or 4-*O*-methylglucopyrano-syluronic acid groups are also often attached to the xylan backbone via D-xylosyl residues, forming single units (glucuronic acid) or more extended di- or trisaccharide side chains (arabinofuranose). In many cases, side chains are linked to the backbone through arabinofuranosyl residues (Stephen, 1983; Wilkie, 1979). Furthermore, heteroxylans are highly cross linked with other xylans via

diferulic bridges or structural cell wall proteins through isodityrosine bridges (Saha, 2003). Besides sweet grasses, xylans are found in hardwoods, whereas softwoods consist prevalently of glucomannans. The ultrastructural organisation of wood cell walls shows single hemicellulose molecules which are intercepting cellulose fibrils and even whole monomolecular layers of hemicellulose between elementary fibrils (Fengel, 1971). Particular binding of xyloglucan has been suggested to regulate the cellulose fibrillar size (Sasaki and Taylor, 1984).

1.3.3 Lignin

Lignins are another group of polymers in the plant cell wall architecture (figure 1-2C) formed of aromatic compounds to which substituents are connected by ether and carbon-carbon linkages. They are composed of three phenolic alcohols: *p*-coumaryl, coniferyl and sinapyl propanol that are polymerised through various types of linkages (Chesson and Forsberg, 1988) via a free radical coupling mechanism (Freudenberg, 1968) forming so called dehydrogenative polymers (DHP). Lignification is thus due to oxidase enzymes generated polymer-polymer coupling of is achieved by cross-linking reactions of a monomer with a polymer. Structural units are formed by ether and C-C linkages including β-*O*-4, β-1 or 5, dimerization β-β resinol, diaryl ether 5-*O*-4 and biphenyl 5-5 linkages (Wong, 2009). One of the most abundant linkages in e.g. softwoods is the β-arylether (Higuchi, 1990) constituting a substructure by binding a free benzyl hydroxyl group in the α-position and a free phenolic hydroxyl group in the γ-position. Both of these hydroxyl groups were proposed to be possible sites for lignin-carbohydrate bonds. In grasses *p*-couramic acid is esterified to terminal hydroxyl groups of propyl side chains, whereas ferulic acids are bound via ester linkages to structural carbohydrates and even serve to crosslink hemicellulose chains (Hartley and Jones, 1976; Higuchi et al., 1967). These couplings of carbohydrates such as galactomannan, arabino-4-*O*-methylglucurono-xylan and arabinogalactan linked to lignin at benzyl positions (Azuma et al., 1981; Mukoyoshi et al., 1981) are forming Lignin-carbohydrate complexes (LCCs). LCCs are found in many plant species as heterogeneous and irregular structures, wherein lignin is bound covalently to carbohydrates resulting in highly intractable materials limiting the biodegradation (Wallace et al., 1991). Most bonds were suggested to be ester or ether linkages, e.g. Watanabe and Koshijima (1988) proposed that the 4-*O*-methylglucuronic acid residue in arabinoglucuronoxylan binds to lignin by an ester

linkage between the (*O*)2 and (*O*)3 positions of the xylose units and the α- or conjugated γ-position of phenyl propane or propene units of the lignin. Furthermore, p-hydroxyl and p-alkoxy structures can be substituted with either lignin or sugar (mannose, galactose, glucose and xylose) via *O*-2 or 3 or 6-ether linkages.

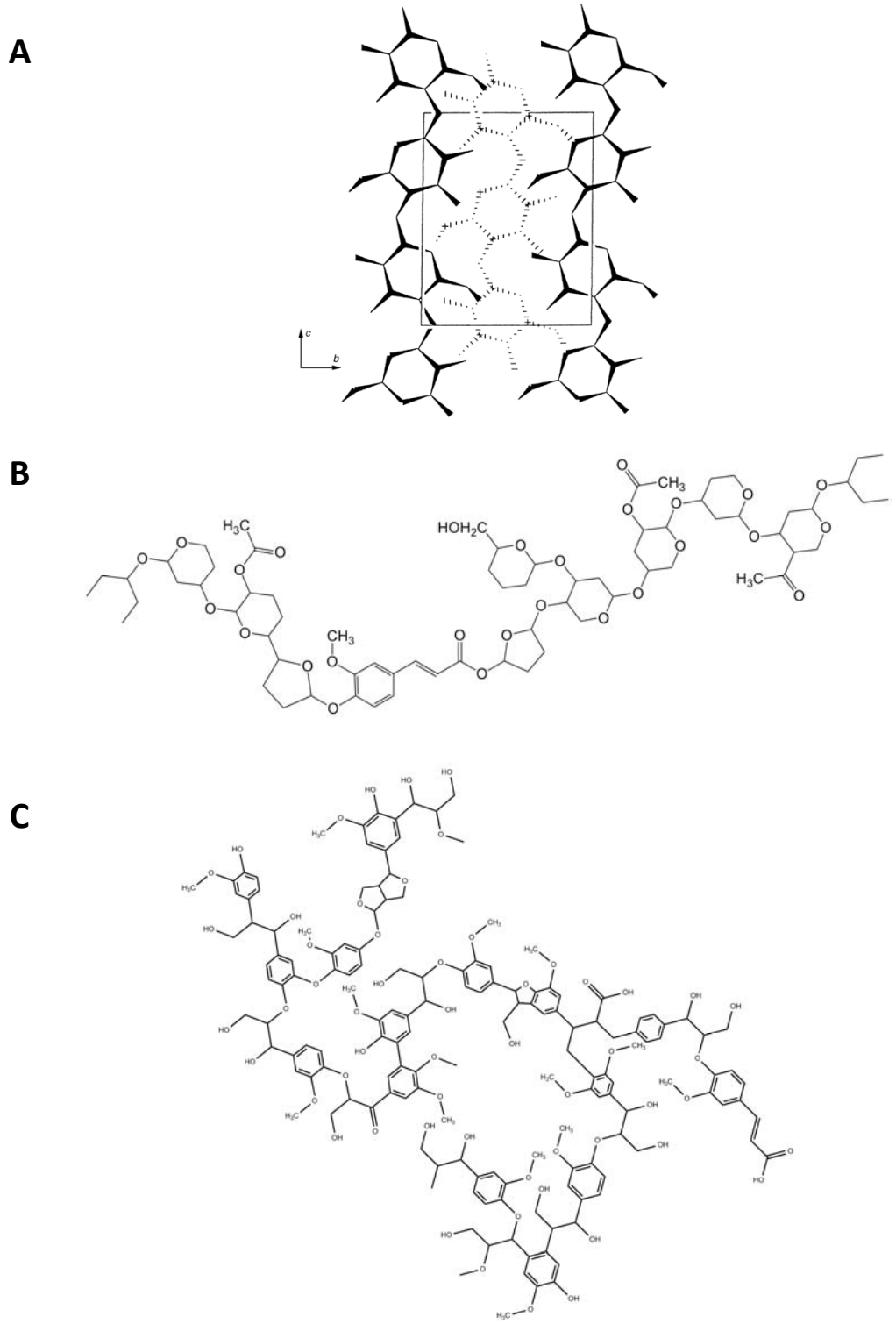

Fig. 1-2 Comparison of native biopolymer structures: **A** cellulose I (projections of a two-chain model by Woodcock and Sarko, 1980), **B** substituted xylan from monocotyledonous cell walls (modified model from Fry, 1986; Aspinall, 1981 and Wilkie, 1979), **C** hypothetical model of lignin.

Although chemical compositions of cellulose, hemicellulose and lignin and ultrastructural organisations of cell wall structures are well described or at least hypothesised in detail, heterogeneity and unclear dynamic interactions between different insoluble components, e.g. lignocellulose formation and the overall complexity limits rational strategies on total degradation.

1.4 Enzymatic biomass degradation

Plant materials constitute a major proportion of ruminants' diets, where symbioses with microorganisms are essential. The rumen environment is strictly anaerobic, operates in a temperature range of 38 to 40°C, continuously mixed by muscle contractions. Indigenous microbial community consists of about 10^{10} ml^{-1} bacteria and 10^{6} ml^{-1} protozoa (Hespell, 1988). It was assumed, that 70 to 80% of the total rumen microbial cell mass is associated with the particulate food fraction shortly after entering the rumen (Forsberg, 1977), although microbial attachment mechanisms were unknown for a long time. Plant polysaccharides are converted to soluble oligosaccharides and monomers by various fibrolytic species, which results in varying degrees of digestibility. 60% of the plant cell walls are degraded in average by domestic ruminants, which can be further split into cellulose degradation (58% digestibility in average) and hemicellulose/xylan degradation (49% diegestibility in average) as reported by Van Soest (1982).

1.4.1 Cellulose degradation

The resistance of cellulose to enzymatic attack depends on the ratio of crystalline regions to amorphous, easily degradable regions (Robson and Chambliss, 1989). Cellulolytic microorganisms produce a variety of different enzyme modules (catalytic and non-catalytic), which form cellulases that act synergistically on their substrate. More recently multi-enzyme-complexes, so called cellulosomes are discussed in circumstance of anaerobic biomass degradation (Ohmiya et al., 2003, Schwarz, 2001). The cellulosome was found first on the surface of *Clostridium thermocellum* (later on *C. cellulolyticum*, *C. josui*, *Ruminococcus albus*) and originally proposed by Bayer et al. (1998), even earlier in the 1980s by Bayer and Lamed, which were not using the term cellulosome at that time. However, the cellulosomal structure is a macromolecule machine, where components interact in a synergistic manner to catalyse the efficient degradation of cellulose (figure 1-3B).

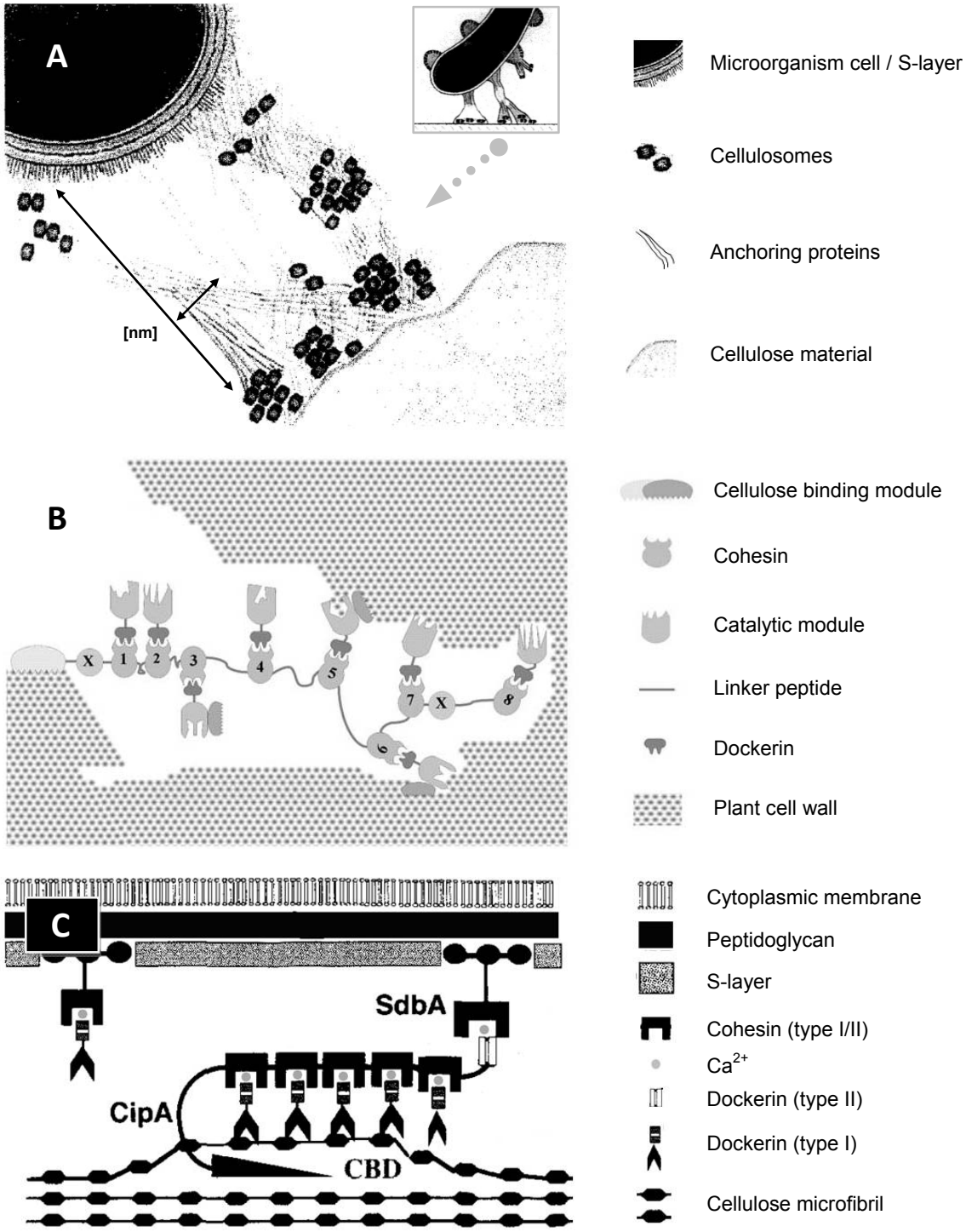

Fig. 1-3 Schematic diagrams of the interaction of a cellulolytic bacterium on cellulose. **A** Cell surface bears protuberance-like surface organelles (anchoring proteins) that contain multiple copies of the cellulosomes for their deposition along the cellulose surface (Ohmiya et al., 2003); **B** After an extended period of growth the cell detaches from the cellulose, leaving cell-free cellulosome clusters on the surface of the residual substrate (Hammel et al., 2005); **C** Cellulosome dockerin and cohesin interaction to form multi-enzyme complexes, CipA and dockerins bind on the catalytic domains (type I) where cellulose is bound by the cellulosome binding domain (CBD), while attachment to the bacterial cells is realised via cohesin-dockerin bindings (type II) at the C-terminus of SdbA (Ohmiya et al., 2003).

Some cellulosomes appear to be tethered to the bacterial cell envelope via similarly intricate, multiple-domain anchoring proteins. Scaffoldin (a non-catalytic scaffolding protein) assembles xylanase and mannanase into the complex, where more than 15 enzymes with molecular weights of 40 to 250 kDa are bound, comprising a multi-enzyme complex. Each cellulosomal subunit consists of a multiple set of modules: Two classes (dockerin domains on the enzymes and cohesin domains on the scaffoldin protein) govern the incorporation of the enzymatic subunits into the cellulosome complex (figure 1-3C). Another scaffolding module (cellulose-binding domain) is responsible for binding to the substrate. The anchoring proteins are organised in so called proturburances, which protract and deposit the cellulosomes that they are carrying along the cellulose surface. Proturburance dimensions (figure 1-3A) were described to be around 550 nm in length and ranging from 50 to 300 nm in width (Shoham et al., 1999, Bayer et al., 1998). The enzymes on the cellulosomes then commence the cellulose degradation, which involves synergistic actions by three main enzymes (Zhang et al., 2006):

1. endoglucanase (EC 3.2.1.4)
2. exoglucanase or cellobiohydrolase (EC 3.2.1.91)
3. β-glucosidase (EC 3.2.1.21)

The endoglucanase action (1) covers the hydrolysis of accessible intramolecular β-1,4-glucosidic bonds of cellulose chains randomly to produce new chain ends (reduces dramatically the DP, i.e. decreases specific viscosity of CMC). Exoglucanases (2) processively cleave cellulose chains at the accessible ends to release soluble cellobiose or glucose molecules. Cellobiohydrolase I (CBH I) acts on the reducing end (C1-CH_2OH), while CBH II acts on the non-reducing end (C4-OH). Last but not least, β-glucosidases (3) catalyse the hydrolysis of cellobiose units and other soluble cellodextrins with a DP up to 6 to produce glucose monomers in the aqueous phase, in order to eliminate cellobiose inhibition (figure 1-4).

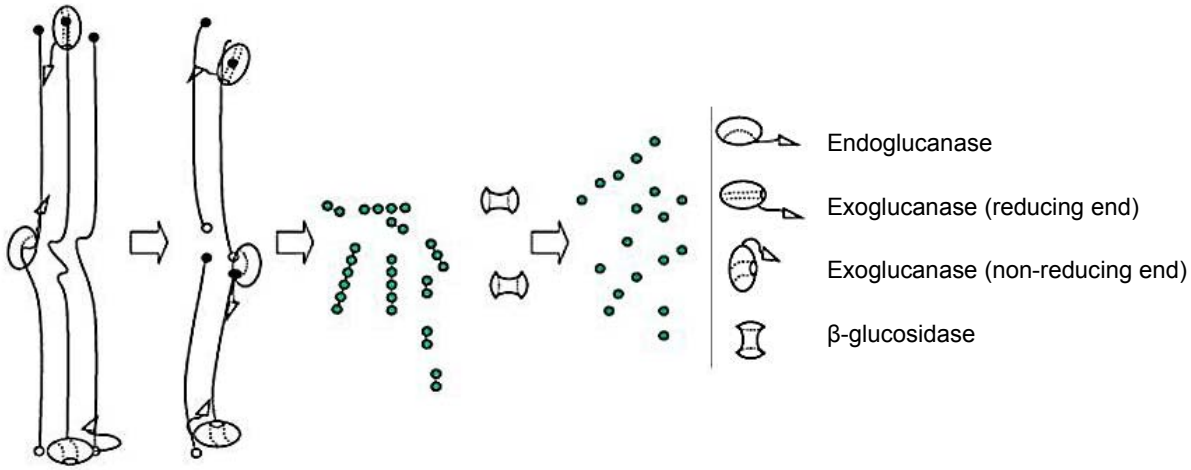

Fig. 1-4 Mechanistic scheme of enzymatic cellulose degradation activity (i.e. hydrolysis) by a non-complexed cellulase system of *Trichoderma* spp. (Zhang et al. 2006). Before Hydrolysis of insoluble cellulose chains takes place, amorphogenesis of crystalline cellulose parts, i.e. dispersion and swelling of cellulose fibres appears.

1.4.2 Hemicellulose degradation

Hemicellulose degradation is realised by several synergistically acting enzymes, which are classified according to the substrate they act upon. Since native hemicelluloses (especially xylan) are often esterified or acetylated, higher hydrophobicity and less extensive intrachain hydrogen bonding are observed, which leads to precipitation. Thus accessory enzymes are needed for the hemicellulose utilisation. Besides (1), (2) and (3) listed below, ferulic and *p*-coumaric esterases are involved.

1. acetylxylan esterase (EC 3.1.1.72)
2. arabinofuranosidase (EC 3.2.1.55)
3. xylanase
   a) endo-β-1,4-xylanase (EC 3.2.1.8)
   b) exo-β-1,4-xylosidase (EC 3.2.1.32)
4. xylobiase (EC 3.2.1.37)
5. α-glucuronidase (EC 3.2.1.131)
6. endo-β-1,4-/1,6-mannosidase (3.2.1.78/101)
7. α-galactosidase (EC 3.2.1.22)
8. endo-α-1,5-arabinosidase (3.2.1.99)

Esterases (1) catalyse the de-acetylation of xylans and xylo-oligosaccharides an act in a cooperative manner with xylanases (Biely et al., 1986) and are involved in the LC-bond cleavage. Arabino-furanosidases (2) realise the hydrolysis of terminal non-reducing α-L-arabinofuranoside residues and appear strongly induced by xylan. Xylanases (3) catalyse the hydrolysis of β-1,4-glucosidic bonds of the xylose-based backbone, which leads to the cleavage of β-1,4-D-xylans and the successive release of D-xylose residues from the non-reducing termini (a) or from within the back-bone chain (b). Most β-xylosidases are cell-bound and show activity over a broad pH range of acidic to alkaline milieus and high temperatures. Free endo-xylanases are more common, but less effective in xylose production. Xylobiases (4) act specifically on cellulose single units, i.e. xylobiose, which describes the hydrolysis of β-1,4-D-xylans into D-xylose residues as known for xylanases. Glucuronidases (5) catalyse the hydrolysis of α-D-1,2-(4-*O*-methyl)-glucuronosyl links in the main chain of hardwood xylans. Besides xylanases, there are enzymes specifically degrading glycosidic bondages of backbones based on aldohexoses (mannans [6], e.g. [7] for galactoglucomannan) or other aldopentoses (arabinans [8]).

1.4.3 Lignin degradation

Unlike cellulose or hemicellulose, no chains containing repeating subunits are present in lignin, which makes the enzymatic hydrolysis of this polymer tremendously difficult. The cleavage by enzymatic activity may require certain cofactors and inducers. As known from wood lignin, mild alkali treatment releases about 50% of the total carbohydrate components of LCC regions, whereat xylan is removed to a greater extent than any other carbohydrate constituents (Lundquist et al., 1983). Since most carbohydrate chains or side groups appear to be attached to lignin through the non-reducing part, exo-splitting enzyme activity is constrained and attack cannot take place completely. Digestion of LCCs by endo-splitting enzymes leaves residual polysaccharide oligomers with a DP ≥ 4, which remain attached to the lignin. Even though LCCs may constitute a barrier in the degradation of lignin complex structures, they can be degraded through the activity of endo-xylanases, endo-cellulases etc. by their specific mechanisms described above. However, lignin itself is degraded by extracellular oxidative enzymes that act synergistically on C-C bond and ether bonds (C-*O*-C). Lignolytic enzymes include a set of different peroxidases, i.e.

lignin peroxidases (liginase), manganese peroxidases and versatile peroxidases, but also laccases (Wong, 2009) and several accessory enzymes:

1. ligninase (EC 1.11.1.14)
2. manganese peroxidase (EC 1.11.1.13)
3. versatile peroxidase (EC 1.11.1.16)
4. laccase (EC 1.10.3.2)
5. glyoxal oxidase (EC 1.2.3.5)
6. veratryl alcohol oxidase (EC 1.1.3.7)
7. glucose oxidase (EC 1.1.3.4)
8. cellobiose/quinone oxidoreductase (EC 1.1.5.1)
9. cellobiose dehydrogenase (EC 1.1.99.18)

Ligninases act relatively unspecific on a variety of substrates, including phenolic and non-phenolic lignin parts as well as organic compounds in the presence of H_2O_2, which is common for all peroxidases. The depolymerisation leads to the cleavage of 1,2-bis-(3,4-dimethoxyphenyl)-propane-1,2-diol to 3,4-dimehtoxybenzaldehyde and 1-(3,4-dimethoxypheny)ethane-propane-1,3-diol (Hammel et al., 1993; Tien and Kirk, 1983). Manganese peroxidases oxidise Mn(II) to Mn (III), which in turn oxidises a variety of monomeric phenols and phenolic lignin model compounds. Laccases belong to a family of multi-copper enzymes produced by fungi and bacteria catalysing the oxidation of benzenediol to benzosemiquinone in the presence of O_2 and are therefore also known as benzendiol:oxygen oxidoreductases. Versatile peroxidases possess the ability to oxidise phenolic and non-phenolic substrates which are typical for Ligninases, but also can act specifically on Mn(II) as manganese peroxidases.

1.5 Natural zeolites

Oxygen and silicon followed by Al, Fe, Ca, Na, Mg and K are the most abundant elements in the Earth's crust. Along with hydrogen, Ba and Sr these are the major elements in most zeolite minerals, which altogether belong to the silicate minerals. Zeolites occur in volcaniclastic and sedimentary deposits. Most available are sources near to the surface, which can be mined. Such open-system deposits for natural zeolites are common in the Tertiary silicic tephra of the United States, e.g. located in the Death Valley Junction of California, southeastern Oregon, southeastern Texas and New Mexico (Bowie et al., 1987; Sheppard, 1985). European deposits have been found in southern Italy, northeastern Greece and are spread widely over eastern Europe, e.g. Slovakia, Serbia, Georgia, Hungary and in the Capathian Mountains of the south-western Ukraine, where mainly clinoptilolite and mordenite zeolites occur. These deposits have been attributed to geoautoclave genesis or burial diagenesis, whereas zeolite deposits in silicic tuffs may have formed at relatively mild temperatures in an open hydrologic system (Sheppard and Hay, 2001). Geologic or hydrogeologic systems are saline/alkaline lakes, soils or land surfaces, deep-sea sediments, closed tephra systems or hydrothermal alteration spots. Natural zeolites are principally formed in alkaline environments, e.g. lakes with pH of 9.5 to 10 in the presence of an high activity ratio of $(Na^+ + K^+ + Ca^{2+}):H^+$ from a variety of precursor materials, i.e. volcanic and impact glasses, aluminosilicate gels or minerals. Mined material can be crushed and sized into a desired particle-size range, e.g. sand-sized particles of 0.05 to 2.0 mm to suit any specific kind of application (figure 1-5).

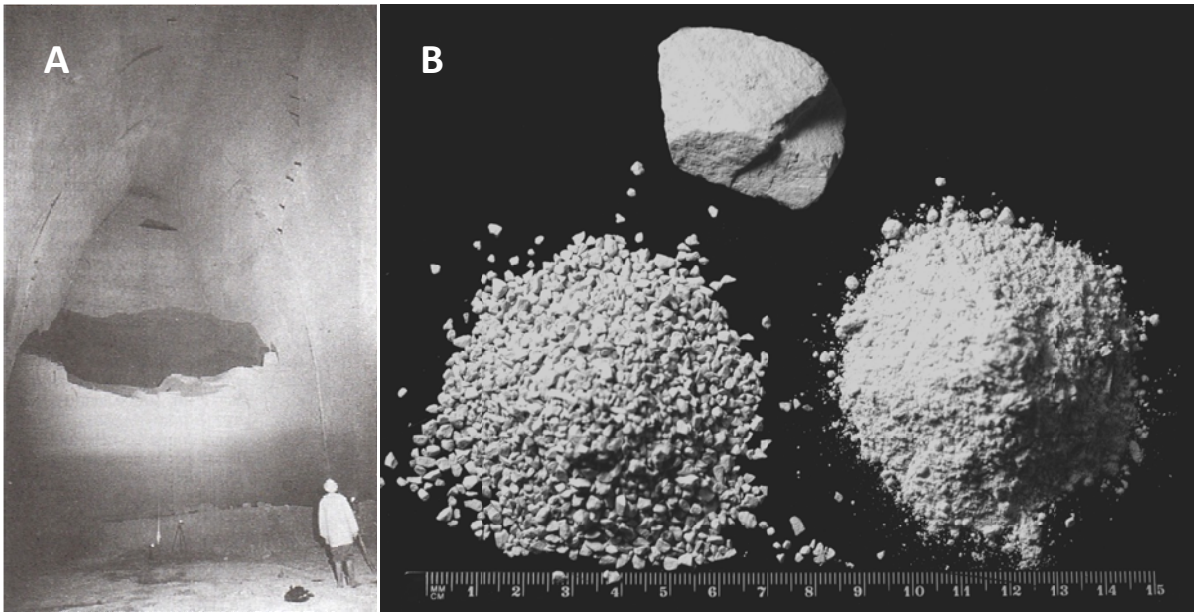

Fig. 1-5 A Gallery mining of Neapolitan yellow tuff in Capodimonte, Neaples, Italy (Geochemical and Mineralogical Society of America); **B** Clinoptilolite in different particle sizes: 4 cm, 1.0-2.5 mm, < 100 µm in diameter (available at IPUS GmbH, Paltentaler Holding, Rottenmann, Austria).

Zeolites are crystalline, hydrated aluminosilicates of alkali and alkaline earth cations characterised by hydration/dehydration reversibility, an adsorption capacity and the ability to exchange some of their constituent cations in aqueous solutions. Zeolites, feldspars and quartz show one identical tetrahedral framework structure, which is described as TO_4 tetrahedron, where every single O is furthermore shared with another adjacent tetrahedron. The T stands for Si (in cases of quartz or any other SiO_2 polymorph) or Al, which can be found in zeolites and feldspars substituting for Si. Since the charge balance must be maintained, Na^+ or K^+ cations are needed, when e.g. Si in Si_4O_8 is replaced by Al, forming $[AlSi_3O_8]^{1-}$, in order to balance the formal valence charges of the ions in the chemical formula, which must be zero to keep up the stability of the silicate. Zeolites are formed in nature at low pressures and temperatures in the presence of water. Their structure possesses channels, cages and voids. Thus zeolites have a more open framework with lower densities than other silicates, possessing open volumes of up to 50% of the total framework size. Na^+ and K^+ ions can be found occupying the structural voids, surrounded by six to eight oxygen atoms, resulting in $(Na,K)[Al_2Si_2O_8]$ (Loewenstein, 1954). The greater the substitution of Al for Si atoms, the larger the charge deficiency resulting from Al's lower electrostatic bond strength to oxygen compared to Si-O bonds (Pauling, 1939).

This means that extra cations such as Ca^{2+} or Mg^{2+} are required to compensate the underbonded oxygen atoms and restore electrostatically neutrality of the total framework. A possible formula would be $(Na,K)Ca_4[Al_9Si_{27}O_{72}] \cdot 24\ H_20$. The water is additionally needed to balance local lacks of charge satisfaction, which result from one or more exposed sides of the channel cations in the framework. H_2O can enter the structure and form partial hydration spheres around the cation's positive portion with its negative dipoles pointing at. The more divalent ions are involved as channel ions, the more H_2O can be found in the framework, which is due to the fact that one e.g. Mg^{2+} is smaller than two K^+ ions and also absorbs larger hydration spheres. In case of clinoptilolites, the type of zeolite used in the studies presented in this work, the general formula can be written as $(Na,K)_6[Al_6Si_{30}O_{72}] \cdot 20\ H_20$.

1.5.1 Clinoptilolites

The classification of zeolites is based upon specifically defined aspects of the crystal structure or physical properties (e.g. morphology). According to Breck (1974) the classification of zeolites can be accomplished by comparing the secondary building units (SBUs), a structural method, that lists seven groups of zeolites based on the geometry of these SBUs. They describe the arrangement of tetrahedra such as rings, chains, sheets or frameworks, which often tend to control the morphology of the zeolite. Following this scheme, clinoptilolites belong to group 7, which building blocks are chains of $T_{10}O_{20}$ (Al, Si)O_4 tetrahedra running parallel to the a-axis of the three-dimensional structure. Group 7 also includes heulandite (HEU – stands also for clinoptilolite), stilbite (STI) and brewsterite (BRE). The abbreviations are framework codes according to Meier et al. (1996). The parallel chain planes are cross-linked to form three different framework topologies, resulting in several types of channels that are all interconnected with each other (figure 1-6). A tabular morphology is observed because cross-linking of the $T_{10}O_{20}$ chains parallel to the c-axis is much stronger exhibited than that one to the b-axis.

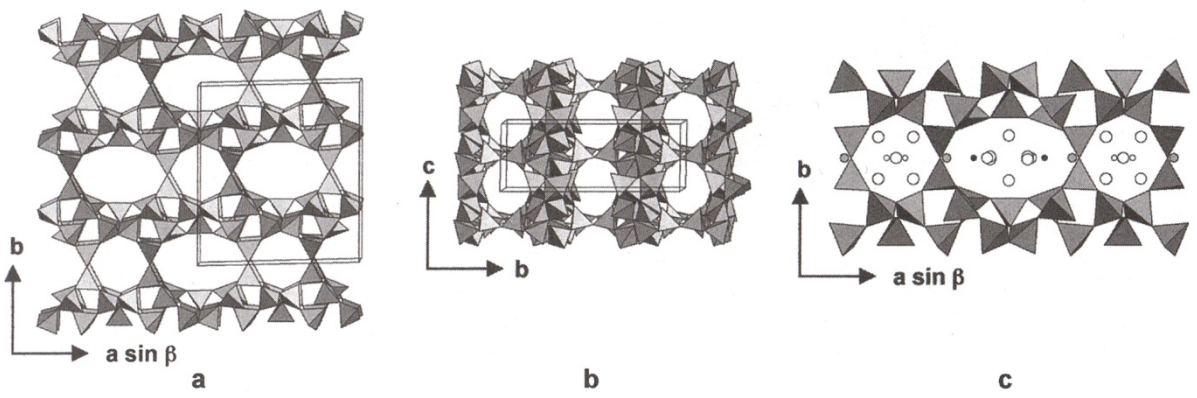

Fig. 1-6 Heulandite/clinoptilolite (HEU) structure, (**a**) projection looking down the c-axis with the b-axis vertical, showing the elliptical ten-membered A rings forming one set of channels (A channels) and the near circular eight-membered rings forming the smaller B channels; (**b**) projection looking down the a-axis with the c-axis vertical (flipping projection [a] upright), showing the C channels which are parallel and formed by elliptical eight-membered rings; (**c**) projection a zoomed in, showing three different cation sites and H_2O: the elliptical A channel has two different metal sites – the small black dot represents a channel cation site usually occupied by Na^+ whereas the larger gray-shaded atoms at the outer ellipse side represent the K^+ binding site, H_2O are variable; the smaller B Channels to the left and right are occupied by Ca^{2+} (small white dots) and H_2O (larger white circles), (Gunter et al., 1994).

The crystal structures of heulandite and clinoptilolite are foremost monoclinic, but also including triclinic sectors, with higher and lower symmetry space groups (*C*2/*m, Cm, C*$\bar{1}$) defining the distances in the orientations a, b and c as 17.7, 17.8 and 7.4 Å. Two of the three channels A-C are parallel to the c-axis (A and B). A channels are formed of strongly compressed ten-membered rings (3.0 x 7.6 Å) which are occupied by Na^+, K^+ and H_2O. B channels are confined by eight-membered rings (3.3 x 4.6 Å) accommodating Ca^{2+} ions and also H_2O. In contrast, C channels are parallel to the a-axis and are formed of smaller eight-membered rings (2.6 x 4.7 Å). Further main sites for Na^+ and K^+ are close to the intersection of the A and C channels. The Na^+ site of channel A often contains Ca instead, whereas the Ca site in channel B is Na^+ free. Na^+, K^+ and Ca^{2+} are in the mirror plane, coordinate to the framework oxygens and channel H_2O molecules through the structure. Mg^{2+} usually resides in the center of the A channel (summarised by Armbruster and Gunter, 2001).

1.5.2 Cation-exchange properties

To understand the ion-exchange ability, the following general formula for natural zeolites points out constituent variability: $(M_x^+,M_y^{2+})[Al_{(x+2y)}Si_{n-(x+2y)}O_{2n}] \cdot mH_2O$ (Gottardi and Galli, 1985). M represents cations either monovalent (+) or divalent (2+) with stoichiometry *x* or *y*, which are exchangeable. Those elements within the second set of brackets represent structural cations and oxygen that make up the framework of the zeolites structure. The *m* stands for the number of possible water molecules and gives an idea of the volume of channels relative to the total volume – the higher the number of bound H_2O under hydrated conditions (maximum m < n/2), the more space is possibly there for the adsorption of other molecules under dehydrated conditions. The (Si + Al):O ratio is 1:2 and the number of tetrahedral Al^{3+} is equal to the sum of positive charges of exchangeable cations (x + y). Thus theoretical cation-exchange capacity (CEC) is primarily a function of the degree of Al^{3+} substitution for Si^{4+}, i.e. the charge density of the anionic structure. That means, the higher the Al substitution is, the more cations are needed for electrical neutrality, hence, the higher the CEC. The unit of CEC values is milliequivalents per gram of solid (meq g^{-1}). Exchangeable cations are loosely held in the zeolite's framework and can be easily removed by washing the zeolites with high concentrations of cations of another kind, but the exchange also depends on a whole set of factors (channel dimension, polarisability, charge density, ionic charge, temperature). The thermodynamics of cation-exchange includes e.g. the so called "concentration-valency effect". It explains that the total concentration of the aqueous solution does not influence the selectivity of the zeolites for ions of equal charges, but does have a strong effect, when ions of different valences contribute to the system. Then the selectivity for ions of higher valences becomes progressively greater with increasing dilution. The thermo-dynamics of ion-exchange can be further described by the equilibrium constant, which involves activities of the aqueous species and the activities of the zeolite components. The resulting K value logarithm (*ln*) is used in the Gibbs free energy equation in order to estimate the preference of the zeolite for the hypothetical ion A^{Z_A+} relative to an ion B^{Z_B+} for a certain temperature T and gas constant R (equations 1a and b). At this, the zeolite can be considered as a solid solution of two components AL_{Z_A} and $BL_{Z_{AB}}$, where L_{Z_A} is the amount of anionic framework (negatively charged) associated with the positively charged A^{Z_A+} ion and so on for ion B (summarised by Pabalan and Bertetti, 2001).

$$K_{(A,B)} = \frac{(\bar{a}_A)^{Z_B}\,(a_B)^{Z_A}}{(a_A)^{Z_B}\,(\bar{a}_B)^{Z_A}} \quad (\mathbf{1a})$$

$$\Delta G°_{(A,B)} = -RT \ln K_{(A,B)} \quad (\mathbf{1b})$$

Ion-exchange studies on clinoptilolite (CEC = 1.5 to 2.2) revealed a high selectivity for the alkaline-earth elements $Ba^{2+} > Sr^{2+} > Ca^{2+} > Mg^{2+}$ and for alkali elements such as $Cs^+ > Rb^+ > K^+ > Na^+ > Li^+$, which generates the ability to extract ^{90}Sr and ^{137}Cs from radioactive wastes (Ames, 1960 and 1961). For the treatment of municipal wastewater streams and biogas production is the relatively high selectivity for NH_4^+ and heavy metal ions (Blanchard et al., 1984; Semmens and Seyfarth, 1978). At 333K clinoptilolite exhibits a high preference for NH_4^+ over Na^+ (Barrer et al., 1967) and even a complete exchange was observed at 298K (Townsend and Loizidou, 1984). At least partial exchange was also reported for K^+/NH_4^+ and Ca^{2+}/NH_4^+ (Vucinic, 1998) with different equilibrium constants and Gibbs free energies for a temperature of 298K (table 1-4). Thermodynamic value differences upon single ions and molecules were suggested to be due to the geological variability of the mineral samples, e.g. degree of impurity (Townsend and Loizidou 1984). Clinoptilolite used in studies presented in this work were originated in Eastern Europe. The second selectivity of importance is exhibited on heavy metal ions. The selectivity series for Na-clinoptilolite is as follows: $Pb^{2+} > Cd^{2+} > Cs^+ > Cu^{2+} > Co^{2+} > Cr^{3+} > Zn^{2+} > Ni^{2+} > Hg^{2+}$. In this context, good reversibilities for the exchange couples Na^+/Cd^{2+} and Na^+/Cu^{2+} were observed, but not for Na^+/Pb^{2+} and Na^+/Zn^+. These heavy metals are concentrated well by clinoptilolite, which leads to their effective removal from contaminated solutions. In summary, high selectivities for toxic or at least inhibiting elements and molecules makes clinoptilolite utmost suitable for the application in biogas production in order to maintain a healthy environment for microorganisms.

Tab. 1-4 Literature values of equilibrium constants and Gibbs free energies for some ion-exchange reactions of clinoptilolite regarding heavy metal ions and ammonium (after Pabalan and Bertetti 2001) at 25°C (exceptions noted in the remarks column, which also indicates zeolite sources).

ion-exchange reaction	ln $K_{(A,B)}$	$\Delta G°_{(A,B)}$ (kJ/mol)	Reference	origin/remarks
$Na^+ + KL \leftrightarrow K^+ + NaL$	-2.54	6.29	Ames (1964)	Hector, California
$K^+ + NaL \leftrightarrow Na^+ + KL$	3.22	-7.98	Pabalan (1994)	Death Valley Junction, California
$2K^+ + CaL_2 \leftrightarrow Ca^{2+} + 2KL$	2.22	-5.50	Vucinic (1998)	Serbia
$Ca^{2+} + 2NaL \leftrightarrow 2Na^+ + CaL_2$	-1,65	4.09	Pabalan (1994)	Death Valley Junction, California
$Ca^{2+} + 2KL \leftrightarrow 2K^+ + CaL_2$	-8.50	21.1	Pabalan and Bertetti (1999)	Death Valley Junction, California
$NH_4^+ + NaL \leftrightarrow Na^+ + NH_4L$	1.63	-4.04	Townsend and Loizidou (1984)	Hector, California
$NH_4^+ + NaL \leftrightarrow Na^+ + NH_4L$	1.65	-4.09	Jama and Yucel (1990)	Western Anatolia
$NH_4^+ + NaL \leftrightarrow Na^+ + NH_4L$	2.14	-5.40	Howery and Thomas (1965)	T = 30°C
$NH_4^+ + NaL \leftrightarrow Na^+ + NH_4L$	2.07	-5.73	Barrer et al. (1967)	Hector, California T = 60°C
$NH_4^+ + KL \leftrightarrow K^+ + NH_4L$	-0.163	0.403	Jama and Yucel (1990)	Western Anatolia clinoptilolite
$2NH_4^+ + CaL_2 \leftrightarrow Ca^{2+} + 2NH_4L$	4.98	-12.3	Jama and Yucel (1990)	Western Anatolia
$2NH_4^+ + CaL_2 \leftrightarrow Ca^{2+} + 2NH_4L$	4.868	-12.07	Vucinic (1998)	Serbia
$Cs^+ + NaL \leftrightarrow Na^+ + CsL$	3.86	-9,56	Ames (1964)	Hector, California
$Cs^+ + NaL \leftrightarrow Na^+ + CsL$	4.02	-10.1	Howery and Thomas (1965)	T = 30°C
$Cs^+ + KL \leftrightarrow K^+ + CsL$	1.30	-3.22	Ames (1964)	Hector, California
$Cd^{2+} + 2NaL \leftrightarrow 2Na^+ + CdL_2$	-2.23	5.53	Loizidou and Townsend (1987)	Hector, California
$Cd^{2+} + 2NaL \leftrightarrow 2Na^+ + CdL_2$	0.388	-0.962	Torres (1999)	
$Pb^{2+} + 2NaL \leftrightarrow 2Na^+ + PbL_2$	3.085	-7.64	Loizidou and Townsend (1987)	Hector, California

1.5.3 Application of natural zeolites

Most wastewater treatment technologies using natural zeolites for water purification depend on the unique cation-exchange behaviour through which harmful cations can be removed from liquids by exchanging them with cations on the zeolites exchange sites (Kalló 2001). The most common cation in waters affecting animal and human health is NH_4^+ (> 1mg l^{-1}). Many zeolites, e.g. clinoptilolite, mordenite, phillipsite or chabazite are able to exchange NH_4^+ even in the presence of larger amounts of competing cations. In return, biological acceptable cations such as Na^+, K^+, Mg^{2+}, Ca^{2+} or H^+ residing on the exchange sites of the zeolites are released. Effective NH_4^+ exchange capacitites of untreated zeolite-rich materials range from 0.4 to 0.9 meq g^{-1}, which can be increased to 1.7 meq g^{-1} by regeneration of Na-forms of the zeolite with NaCl solution (Passaglia and Azzolini, 1994). Besides NH_4^+, H_2S, NO^{3-} and PO_4^{3-} can also be removed efficiently from water (Galindo et al. 2000). Clinoptilolite and mordenite are also selective for transition metals (Cu^{2+}, Ag^+, Zn^{2+}, Cd^{2+}, Hg^{2+}, Pb^{2+}, Cr^{3+}, Mo^{2+}, Mn^{2+}, Co^{2+}, Ni^{2+} etc.), which are often present in industrial wastewaters and must not be released into the environment. Reasonably, natural zeolites are attractive for removing undesirable heavy-metal ions from wastewaters (Kesraoui-Ouiki et al., 1994). The multivalent metal ion exchange can be achieved over a pH range between 3 and 6, to keep cationic metal-forms in solution and competing H^+ exchange minimised at the same time. As observed for NH_4^+, clinoptilolite's CECs for Ba^{2+}, Cu^{2+}, Cd^{2+}, Pb^{2+} and Zn^{2+} can be increased to 2.23 meq g^{-1} when clinoptilolite-rich tuff is conditioned by two sequential treatments with NH_4Cl and NaCl solutions (Semmens and Seyfarth, 1978). Interestingly, CECs for Zn^{2+}, Mn^{2+}, Cu^{2+} and Ag^+ are drastically reduced in the presence of NH_4^+ (Otterstedt et al., 1989, Kang, 1989). Hydrated cation-forms might be preferred in the ion-exchange process, which is especially advantageous for wastewater treatment when the reduction of the chemical oxygen demand (COD) is required. Another aspect mentioned before is the very high selectiveness for Cs^+ and Sr^{2+} which is exploited for the removal of radioactive material from nuclear process wastewater or contaminated drinking water. Here, the advantage of natural zeolites over e.g. organic ion-exchange resins is to be found in their resistance to degradation through ionising radiation and low solubility. Thus zeolites can be used for long-term storage of exchanged long-lived radioisotopes by drying and sealing the loaded zeolite material in steel containers (lacking a final deposition strategy) as reported by

Ames (1960). Adsorption of organics in dissolved or colloidal form as hydrocarbons, halogenated derivatives, amines humic acids, proteins or lipids can only take place on the surfaces of zeolites, since most organic molecules or particles are too large to penetrate the channels and cages of the framework. External crystal surface areas can be as large as several 10 $m^2 g^{-1}$. Zeolites of sedimentary origin often have intercrystalline pore sizes of 10 nm up to 1 µm in diameter. Thus colloids, enzymes and microorganisms as large as bacteria can enter these intraparticle pores. As a result of this large accessible surface for bacteria, natural zeolites are more effective biofilters than e.g. quartz sand beds having an approx. 100-fold smaller total surface area (Tarasevich, 1994, Baykal and Guven, 1997). Zeolites can therefore be used particularly in cases when too much chemical (e.g. organic coagulatns) are added to waters and biological oxygen demand (BOD) increases to hazardous levels. Bacteria become adherent and can thus be removed from e.g. drinking water as reported for *Escherichia coli*, poliovirus, coxackie virus and bacteriophages using clinoptilolite-rich materials (Grigorieva et al., 1988). Adherence of bacteria can also be used *vice versa* by using clinoptilolite as a support medium for microorganisms as suggested for the simultaneous nitrification and denitrification for the removal of nitrogen from municipal wasterwater (Halling-Soerensen and Hjuler, 1992). The porous structure of the clinoptilolite rock provides alternating aerobic and anoxic conditions. Aerobic zones deliver oxygen for an enhanced nitrification process, until oxygen consumption results in anaerobic conditions and denitrification begins. Furthermore, a variety of applications in agronomy as soil conditioners, slow-release fertilizers, soilless substrates, carriers for remediation agents in contaminated soils have been described (Ming and Allen, 2001). The addition of zeolites to soils increases both, the soil's CEC and pH, which can lead to intensified plant growth and yielding as observed for potato, barley and wheat using clinoptilolite-rich tuff (Mazur et al., 1984). Zeolites improve physical properties of soils, such as their water availability, holding capacity, infiltration and reduce nutrient leaching, but also support the aeration. The beneficial effect of the zeolite's CEC is e.g. the reduction of the volatilisation of gaseous nitrogen (NH_3, N_2), because ammonium is selectively exchanged and N thus remains available in the soil. As fertilizers, clinoptilolites exchange plant-essential element nutrients, which are slowly released into the soil for the plant uptake. Zeolites can also be additionally loaded with nutrients (e.g. K, P) or trace metals (e.g. Cu^{2+}, Co^{2+}, Mn^{2+} or Zn^{2+}).

Such zeoponic material (foremost clinoptilolites) can be used as soilless substrate, where the zeolite's CEC and slow-release fertilisations by mineral dissolution are combined, leading to the complete replacement of soil-material wherever it's needed (Ming and Allen, 1999; Parham, 1984).

1.6 Analytical challenges

1.6.1 Enzyme screening

Hydrolytic enzymes must accommodate heterogeneous polymers with various degrees of polymerisation, side chain branching patterns and several altering substitutes. Because of this inhomogeneity of natural complex polymers, specific substrates and corresponding enzymes that act upon them are generally difficult to isolate and characterise. The quantitative determination of enzymatic activities is commonly based on accumulated products after hydrolysis including reducing sugars, total sugars and chromophores. Other assays measure the reduction in substrate quantity or the change in the physical properties of substrates. However, the production of reducing sugars is assayed using alkaline dinitrosalicylic acid (DNS), Cu-arsenomolybdate following Nelson and Somogyi, using the 4-hydroxybenzoylhydrazine (PAHBAH) method, the 2,2'-bicinhroninate (BCA) method or the ferricyanide methods (table 5). Total sugars can be measured directly using Anthrone- or Phenol-H_2SO_4. Focusing post-hydrolysis products, i.e. glucose as major product, enzymatic glucose kits using coupled hexokinase and glucose-6-phosphat dehydrogenase are available. Cellulase and hemicellulase activities are commonly assayed by measuring the rate of reducing group formation under optimum conditions, i.e. substrates are suspended in buffer for optimum pH and the enzyme-substrate mixes are incubated at enzyme specific temperatures (which can be adapted to approach specific conditions) for a minimum of time. The enzyme titre is then calculated according to product specific standard regression of several successive dilutions. The DNS method appears to be suitable for the detection of glucose and cellodextrin reducing sugars over a broad detection range (table 1-5) without requiring the removal of proteins since any interference from cellulase occur. However, the method's main drawback is the poor stoicheometric relationship between produced cellodextrins and pure D-glucose standards (Zhang and Lynd, 2005), which may result in an underestimation of cellulase activity (Schwarz et al., 1988).

Tab. 1-5 Common colorimetric assays based on the accumulation of sugars after hydrolysis, small sample volumes are covered over a range of 0.01 to 3.0 ml (summarised by Zhang et al., 2006).

Reducing sugar assay	Sugar amount [µg mg^{-1}]	Sugar concentration [µg ml^{-1}]	Reference
DNS	20-2500	6.7-5000	Ghose (1987), Miller (1959)
Nelson-Somogyi	1-600	0.2-300	Somogyi (1952)
Nelson	5-100	2.5-50	Nelson (1944)
Ferricyanide-1/2	0.18-9	0.18-9	Kidby and Davidson (1973), Park and Johnson (1949)
PAHBAH	0.5-50	1-5000	Lever (1972)
BCA	0.2-9	0.4-9	Zhang and Lynd (2005), Waffenschmidt and Janeicke (1987)
*Phenol-H_2SO_4	5-100	10-100	Zhang and Lynd (2005), Dubois et al. (1967)
Glucose-HK/PGHD kit	2-50	200-5000	Sigma Aldrich, St. Louis, USA

*total sugar assay

An underestimation of cellulase activities can be overcome by total carbohydrate assays, which show a strict stoicheometric relationship between glucose equivalents and the glucose standard, but are limited to pure cellulose substrates, because any carbohydrates and their derivates can cause strong interference readings. Nonspecific readings from other sugars can be avoided by using glucose assay kits or high pressure liquid chromatography (HPLC), where the conversion of longer cellodextrins to glucose is required. Regarding hemicelluloses, DNS, malto- or xylodextrin reducing sugars are detected, which accumulation is usually due to endoxylanase activities. Here, the DNS assay tends to overestimate the enzymatic acitivity (three-fold or more), because not only xylotriose, but also higher oligosaccharides are produced and co-measured (Khan et al., 1986). The ferricyanide, BCA and PAHBAH methods possess comparably higher sensitivities to reducing sugars, but suffer from non-specific interference from protein. The most exact methods for evaluating hemicellulase activities are product separation techniques, such as paper chromatography (Biely et al., 1980) or thin layer chromatography (Morosoli et al., 1986), but for quantitative analysis HPLC must be applied. Some columns of Bio-Rad (HPX-42A) or Dionex (Carbopac PA1) are

capable of separating and quantifying oligosaccharides with DPs up to 15 or more. The difficulty with this approach is that such high DP oligosaccharide standards are hard to obtain. However, many hemicellulases can only be distinguished by their action patterns or characteristic product profiles. Dyed substrates such as carboxy-methylcellulose/ –xylan (CMC/CMX) or lichenan are particularly useful in developing zymograms from electrophoresis gels (Schwarz et al., 1987). Assays based on dyed substrates are very sensitive, but the results are more difficult to interpret when quantitative data according to enzyme kinetics is needed (Schmidt and Kebernik, 1988). Furthermore, the degradation of natural and defined substrates such as CMC or CMX differentiates and thus manipulates the activity assay. One example is the discrepancy between complexity and simplicity of the substrates nature. When complex native cellulose polymers are degraded, several physical properties represent the cellulase activity including the swelling factor (alkali uptake), fibre strength, structure collapse, turbidity or viscosity (Oksanen et al., 2000; Wood, 1975), which also depend on whether the cellulose polymer part affected is crystalline or amorphous. This cannot be resembled by using CMC as model substrate for example. Even though CMC has a high DP comparable with natural sources, CMC is water-soluble and has a low fraction ratio of reducing ends to β-glucosidic bonds accessible to cellulases, which stands for a much higher cellulase adsorption capacity then to be usually found in natural insoluble substrates. As a result exo- and endoglucanases act differently upon CMC, which is due to their different modes of action. While endoglucanases are decreasing the viscosity of CMC significantly with little hydrolysis rates, exoglucanases increase the number of reducing sugars (Zhang and Lynd, 2004), which would not be detected by viscosimetric determinations, but only by product accumulation assays with short incubation periods. The longer the incubation time during the assay is the more likely is an enzyme inhibition caused by certain hydrolysis products, e.g. cellobiose. This glucose-dimer acts strongly suppressing on the cellobiohydrolase activity (Claeyssens and Aerts, 1992). However, substrates used for hydrolysis studies should therefore always be as similar to native polymer structures as possible regarding solubility, crystallinity and degree of polymerisation (table 1-6).

Tab. 1-6 Summary of typical values for insoluble (and soluble*) cellulose models regarding crystallinity index (CrI), the fraction of β-glucosidic bonds accessible to cellulases (F_a) estimated by maximum cellulase adsorption capacity (Zhang and Lynd 2004), the average degree of polymerisation (DP_N), the fraction of reducing ends (F_{RE}) and relative ratio of F_{RE} to F_a (summarised by Zhang et al., 2006).

Substrates	CrI	F_a	DP_N	F_{RE} [%]	F_{RE}:F_a ratio
Whatman No.1 filter paper	~0.45	1.8	750-2800	0.036-0.133	0.0198-0.0741
Microcrystalline cellulose	0.5-0.6	0.6	150-500	0.2-0.667	0.333-1.11
Pretreated cellulosic substrates	0.4-0.7	0.6	400-1000	0.1-0.25	0.167-0.417
Cotton	0.8-0.95	0.2	1000-3000	0.033-0.1	0.167-0.5
Pulp	0.4-0.7	1.8	750-1500	0.067-0.133	0.0370-0.0741
*CMC	-	100	100-2000	0.05-1	0.0005-0.01
*Cellodextrins	-	100	2-6	16.67-50	0.167-0.5

1.6.2 Community screening

An ideal method for microbial community analysis should allow the detection of different groups and enumerate all microbial species present in a sample from an ecosystem or habitat. Basically two approaches are used for community analyses: (1) cultivation-dependent analysis (CDA) aiming at the detection of selected groups and species of microorganisms and (2) cultivation-independent analysis (CIA), which are DNA-based and are used to assess the complexity and dynamics of microbial communities. CDA relies on several selective and non-selective culture media that supply different growth conditions for specific or non-specific microbial population targeting. Traditional methods require a vast knowledge of phenotypic features to characterise microorganisms, which is often inaccurate and also leads to an underestimation of the diversity of species. Thus CDA is nowadays complemented by molecular methods such as polymerase chain reaction (PCR) and fingerprinting techniques. However, the main drawback of conventional cultivation methods to recover less than 1% of the total species of microbes present in environmental samples remains (Amann et al., 1995). CIA is principally based on molecular techniques (table 1-7), applying PCR and hybridisation in order to identify microbes

directly from a sample material. Therefore, total genomic DNA or RNA must be extracted from collected microbial cells. Cell lysis is accomplished by several methods: mechanically using bead-beating, freeze-boil cycles or heating; chemically based on detergents or enzymatically using cell wall degrading enzymes, e.g. lysozyme, lyticase or proteinase (Candrian 2005; Roose-Amsaleg et al. 2001). Many types of sample matrices contain factors and compounds that can totally inhibit the next step of the CIA approach – the PCR.

Tab. 1-7 Molecular screening techniques for microbial community detection, fingerprinting and identification (summarised by Maukonen et al., 2003).

Method	Based on	Application	Reference
AFLP	Restriction of total microbial DNA	Strain-level identification	Vos et al. (1995)
ARDRA	Restriction of rRNA genes	Strain-level identification	Vaneechoutte et al. (1993)
RAPD	Random amplified polymorphic DNA	Strain-level identification	Power (1996), Welsh and McClelland (1990)
rep-PCR	Repetitive element sequence-based PCR (short sequence repeats [SSR])	Strain-level identification	Versalovic et al. (1991)
PFGE	Genomic restriction fragments in pulsed-field gel electrophoresis	Strain-level identification	Schwartz and Cantor (1984)
RFLP	Restriction fragment length of rRNA genes	Strain-level identification	Saiki et al. (1985)
DGGE	Mobility of partially melted dsDNA in linear gradient of DNA denaturants	Community analysis	Fischer and Lerman (1983)
TGGE	Mobility of partially melted dsDNA in linear temperature gradient	Community analysis	Rosenbaum and Riesner (1987)
SSCP	Mobility of conformed ssDNA in non-denaturing gels	Community analysis	Orita et al. (1989), Rolfs et al. (1992)
RT-PCR	Real-time measurement of PCR-product amounts	Activity analysis / Quantification	Reischl and Kochanowski (1995)
Microarray	Hybridisation of oligonucleotides or PCR-products for gene expression profiles / signatures	Activity analysis	Lockhart et al. (1996), Schena et al. (1995), Fodor et al. (1993)

Environmental microbiological studies are often based on ribosomal DNA or RNA sequences, because these sequences are functionally and evolutionary conserved and present in all organisms. Here, 16S rDNA and 23S rDNA sequence regions have already been determined for a large number of reasonably described bacterial, archaeal and fungal species. Thus 16S rDNA sequences can be used to investigate phylogenetic relationships and for the identification of unknown microbes via comparisons with database collection entries (Olsen et al., 1986). In contrast to rDNA, rRNA-targeted techniques rely on high-copy numbers per cell and are specifically used to assess changes in metabolically active microbial populations (Wagner, 1994), although extraction and handling procedures are much more complicated due to rRNA's instability (von Wintzingerode et al., 1997). The intergenic spacer region (ISR) between 16S and 23S rDNA often shows species-specific sequence variations and is therefore used alternatively foremost in diagnostic PCR-amplifications (Gürtler and Stanisich, 1996). However, in all cases PCR amplifies the target sequence, defined by two oligonucleotide primers, exponentially and in a highly sensitive (Mullis et al., 1986; Saiki et al., 1985) what generates defined PCR amplicons that can be separated by gel electrophoresis. Drawbacks are false-positive amplicons resulting from contaminating DNA, differential amplification or the formation of PCR artefacts, e.g. chimeric molecules that are not describing any species. It was also reported that the *rrn* operon heterogeneity leads to interferences with 16S rDNA sequence variations during the PCR procedure (von Wintzingerode et al., 1997). However, there are several broad-range and group-specific primers available, targeting many bacterial and archaeal species of interest including fermentative and methanogenic representatives. Genetic fingerprinting techniques are used to further characterise microbial communities or single isolates, providing pattern profiles of the community diversity (Stahl and Capman, 1994). This allows simultaneous analysis of multiple samples enabling the comparison of the genetic diversity of microbial communities from different habitats or sample sites. Techniques involve e.g. denaturing-gradient gel electrophoresis (DGGE), temperature-gradient gel electrophoresis (TGGE) or single-strand conformation polymorphism analysis (SSCP). SSCP detects sequence variations between different DNA fragments on the basis of single base modifications, which can change the conformation of a single-strand DNA molecule, altering its migration speed in non-denaturing gels (Orita et al.,

1989; Rolfs et al., 1992). Thus DNA fragments of same sizes (e.g. 16S rDNA) but possessing different base compositions can be separated (Hayashi, 1991). Limitations of the SSCP analysis are reproducibility problems when fragments analysed are built of more than 400bp (Vaneechoutte, 1996) and a high rate of DNA strand-annealing after initial denaturation during electrophoresis creating artefacts (Selvakumar et al., 1997). However, PCR-SSCP detection covers all populations that make up more than 1% of the total microbial community, depending on the primers used and positions of sequence variations in the gene focussed (Lee et al., 1996). Many communities are far too diverse, to be counted exhaustively, which makes statistical approaches necessary. The development of automated techniques as offered by Next/Next generation sequencing approaches (Pyro-, Deep-Sequencing etc.) allow high-throughput analysis of large numbers of samples that can be analysed simultaneously.

Besides PCR-based fingerprinting techniques, hybridisation can be used in combination with microarrays or fluorescence microscopy to detect selected groups or species in the course of community analysis. In hybridisation, a labelled probe, i.e. radioactive signal or fluorochrome joined denatured DNA fragment is annealed to a sequence homologous to a certain target DNA (genomic DNA or PCR-amplicons). Fluorescence-based microscopy is widely used in microbial ecology and allows the visualisation of spatial distribution of cells in a sample. Using group- or species-specific staining, the differentiation between distinct groups or populations is permitted, leading to deep insides into the organisation of biofilms for example. This strongly depends on the microscopy technique applied. Whereas epifluorescence microscopy just gives optical information from one layer that can only be analysed two-dimensional (Ploem, 1967; Wirtanen et al., 2000), confocal scanning laser microscopy (CLSM) is capable of scanning a specimen via successive expositions of thin sections that can be reconstructed by computational assistance. This allows the determination of three-dimensional relationships of cells and their surroundings (Caldwell et al., 1992; Lawrence et al., 1991). The specimen is focused with a laser beam and pinhole selected fluorescent signals are detected by a photomultiplier, which results in high sensitive, high detailed and non-destructive image aquisitaion (Taylor and Salmon, 1989). The image also allows the rapid quantification of fluorescence signals counted, e.g. percentage of area covered by biofilms or number of cells. On this score flow cytometry (FCM) combines the advantages of microscopy

and biochemical analysis for the measurement of biochemical and physical characteristics of individual cells moving in a fluid stream passing a optical sensors (Diaper et al., 1992; Crosland-Taylor, 1953). However, besides fluorochromes, numerous fluorescent dyes are available for DNA or RNA specific staining, such as acridine orange or 4',6-diamidino-2-phenylindole (DAPI) to detect the total number of bacteria (Stugger 1948; Kepner and Pratt 1994) or specific kits for the discrimination between viable and non-viable cells, e.g. the Live/Dead BacLight viability kit (Molecular Probes®). There are some drawbacks using hybridisation-based fluorescence microscopy that include fading or photo-bleaching of the fluorochrome, fluorescence quenching, the loss of fluorescence due to sample derived molecules that interact with the fluorochromes and inefficient or incorrect hybridisation. An approach to biofilm characterisation studies apart from molecular techniques is the application of scanning electron microscopy (SEM). Advantageous high resolution observations of sample surface can generate detailed images with magnifications of up to 500,000-fold (Zeiss Ultra 55, Carl Zeiss Micro Imaging). Even though biological structures can be maintained by critical point drying or lyophilisation, sample preparation is destructive.

2. Experiments and Results

2.1 Enhancement of biogas production by addition of hemi-cellulolytic bacteria immobilised on activated zeolite

Weiß, S.[1], Tauber, M.[2], Somitsch, W.[3], Meincke, R.[1†], Müller, H.[1], Berg, G.[1] and Guebitz, G.M.[1]

[1]Institute of Environmental Biotechnology, Graz University of Technology, Petersgasse 12, 8010 Graz, Austria; [2]IPUS GmbH, Werksgasse 281, 8786 Rottenmann, Austria; [3]Engineering Consultant, Wiedner Hauptstrasse 90/2/19, 1050 Vienna, Austria.

(Water Research, Volume 44, Issue 6, March 2010, Pages 1970-1980)

2.1.1 Abstract

Biogas from agricultural biomass and residues is a valuable source of renewable energy. However, recalcitrant plant cell structures represent a barrier in the fermentative biodegradation process in single- and two-stage reactors. Therefore, approaches concerning a more efficient de-polymerisation of cellulose and hemicellulose to monomeric sugars are required amongst others in order to optimise the fermentation efficiency and to increase methane yields. Here we show a new strategy for the enhancement of biogas production from hemicellulose-rich substrates. Hemicellulolytic populations from a common biogas fermenter consortium were successively enriched in batch-cultures using a synthetic medium containing xylan powder as single carbon source under anaerobic mesophilic conditions. Enriched hemicellulolytic bacteria were immobilised on trace metal activated zeolite to ensure a stable storage and easy application. Xylanase activity increased continuously during subsequent enrichment cycles by up to 162%. In batch-culture experiments we were able to observe an increase of methane by 53% compared to controls without additionally introduced microorganisms immobilised on zeolite. Specific enrichment of hemicellulolytic bacteria during the process was confirmed by using single strand conformation polymorphism (SSCP) analysis based on amplification of the eubacterial 16S rDNA fragments. Using sequence analysis conspicuous bands from SSCP patterns could be identified as belonging to the groups *Bacteroides* sp., *Azospira oryzae* (*Dechlorosoma* sp.) as well as to a wide spectrum of diverse species within the order of Clostridiales (Firmicutes).

2.1.2 Introduction

Previous studies have shown the assessment of various substrates ranging from organic household waste to more defined lignocellulosic substrates for biogas production (Held et al., 2002; Staubmann et al., 1997). Naturally occurring lignocellulosic plant biomass consists of 20-30% hemicellulosic materials which are heterogeneous polysaccharides with xylan as major constituent found in association with cellulose. Xylans are heteropolysaccharides with a homopolymeric backbone chain of β-1,4-linked D-xylopyranose units. Common substituents found on the backbone are *O*-acetyl, α-L-arabinofuranosyl, α-1,2-linked glucuronic or 4-*O*-methylglucuronic acid. Especially *O*-acetyl groups at the positions C-2 and C-3 of xylosyl residues hinder xylanases from completely degrading acetyl xylan (Kulkarni et al., 1999). Therefore, a synergistic activity of several enzymes such as endo-1,4-β-xylanase, β-xylosidase, α-glucoronidase, α-L-arabinofuranosidase and acetylesterase is essential for the complete breakdown of branched xylans. An universal obstacle for the anaerobic digestion of plant biomass is the structural heterogeneity and complexity of cell-wall constituents such as microfibrils and matrix polymers (Iiyama et al., 1994). At a molecular level, the crystalline cellulose core of cell-wall microfibrils is composed of precisely arranged cellodextrines with strong interchain hydrogen bonding between adjacent chains. The hydrophobic face provokes crystalline cellulose to be highly resistant to enzymatic hydrolysis (Matthews et al., 2006; Nishiyama et al., 2002). Additionally, hemicellulose restricts the access to crystalline cellulose cores of microfibrils by coating them (Ding and Himmel, 2006). Since it is known that the removal of hemicellulose increases the mean pore size of cell-wall structures which in turn enhances the enzymatic hydrolysis of cellulose in plant biomass substrates (Grethlein, 1985), we focused on hemicellulolytic bacteria producing xylan-degrading enzymes in this study.

Whereas mechanical and chemical pre-treatment methods are well studied and commonly used in practice to increase methane yields from recalcitrant biomass, little is known about the prospects of a biological pre-treatment for anaerobic digestion processes (Hendriks and Zeeman, 2009). However, enzymatic pre-treatment is quite expensive and demands strict control of reaction conditions (Zhang and Lynd, 2006), but the use of vital microorganisms is probably more dynamic and efficient due to their ability of regeneration and concomitant production of diverse enzymes responding to the given substrate. Bagi et al. (2007) demonstrated an increase of

biogas formation by about 60-70% due to inoculation of biogas reactors up to 5 m³ size with external hydrogen-producing bacteria with cellulolytic activity (e.g. *Caldicellulosyruptor saccharolyticus*) in long-term experiments. In the present study, inocula of mixed bacteria were obtained from natural occurring consortia present in biogas plant second-stage sludge in order to enhance the hydrolytic activity by re-introduction of selectively enriched xylanolytic bacteria to the fermentation process. Expectable hydrolytic species resulting from the cultivation on xylan as mono-substrate belong to the genera *Clostridium*, *Bacillus*, *Bacteroides* and *Pseudomonas* sp. (Klocke et al., 2007). The use of second-stage sludge as inoculum for the fermentation of organic materials and cultivation of specific bacterial fractions delivers several major advantages compared to artificial inocula (Friedmann et al., 2004), i.e. (i) providing a biocenosis accommodated to several organic substrates, (ii) vital bacteria cells held under starvation, responding sensitively to newly introduced substrates by metabolistic adjustments and specific enzyme expression.

Zeolites are aluminosilicates with well-defined crystalline structures that contain aluminium, silicium and oxygen in their regulatory framework. The nanoporous crystal structure retains cations, water and has shown a great capacity for ammonia nitrogen (NH_4-N) and heavy metal adsorption (e.g. Cu, Cd, Pb and Zn), thus removing molecules toxic to microorganisms in anaerobic and aerobic digestion processes (Tada et al., 2005; Green et al., 1996). Moreover, zeolites can be purposefully modified by loading trace metal elements (Fe, Mg, Ni and Co) in variable concentrations on their surface which favours methanogenic and acidogenic bacteria to be grouped in small micro-colonies, supplying co-factors for enzyme biosynthesis (Fernández et al., 2007). Consequently, zeolites are used for the immobilisation of microorganisms in anaerobic reactors to stabilise and optimise the process efficiency (Milán et al., 2003). Here we describe how immobilising hemicellulolytic bacteria populations on zeolite leads to an increase of methane yields in batch-culture experiments.

2.1.3 Material and Methods

2.1.3.1 Cultivation and enrichment

As inoculum for the enrichment of hemicellulolytic microorganisms, second-stage sludge from a biogas plant (Fürstenfeld, Austria) primarily digesting maize silage was chosen. The sludge was composed of dry matter (DM), 2.31%; organic dry matter (ODM), 1.7% and the ODM fraction of DM (ODM/DM) was 73.64%. Cultivation was carried out using a minimal medium for the determination of total anaerobic degradability of organic compounds in wastewater and digestion slurry (DIN EN ISO 11734 L47, 1998) containing the following compounds in g l^{-1}: $CaCl_2$ • 2 H_2O, 0.075; $FeCl_2$ • 4 H_2O, 0.02; KH_2PO_4, 0.27; $MgCl_2$ • 6 H_2O, 0.1; Na_2HPO_4 • 2 H_2O, 0.56; Na_2S • 1 H_2O, 0.04; NH_4Cl, 0.53; Resazurin, 0.001. After autoclaving, 10 ml of a mineral base (DIN EN ISO 11734, 1998) with the following composition in g l^{-1} was added: $CuCl_2$, 0.003; H_3BO_3, 0.005; $MnCl_2$ • 4 H_2O, 0.05; Na_2MoO_4 • 2 H_2O, 0.001; $ZnCl_2$, 0.005. Before use, the medium was flushed with oxygen-free nitrogen gas for 20 min l^{-1} to obtain anaerobic conditions. The cultivation experiment was carried out under mesophilic conditions at 35°C in 1000 ml ground flasks with a maximum loading volume of 800 ml wherein 10% inoculum (v/v) were introduced. Insoluble powder of xylan from birchwood (Roth, Karlsruhe, Germany) was then added in a concentration of 0.1% (w/v) as sole carbon source. As blank pure second stage sludge without any addition of xylan was used to estimate enzymatic auto-activity. To establish steady anaerobic conditions, an anaerobic system was used, following Louis Pasteur's bottle "en col de cygne" (around 1862), which allows gases to pass off whilst external air is prevented from entering via a water sealing. After 5 days of cultivation 10% (v/v) were transferred into fresh L47 medium. These cycles of cultivation and re-inoculation were repeated for an overall period of 13 times. Analysis data were obtained from the average of triplicate experiments. Samples were collected at 3- to 5-day intervals.

2.1.3.2 Immobilisation

For immobilisation of enriched xylanolytic bacteria, the zeolite product IPUS meth-max® was used and kindly provided by IPUS GmbH (Rottenmann, Austria). It consists of a natural zeolitic tuff containing > 85% clinoptilolite, which was milled to a grain size below 100 µm. Loaded with several trace metal elements in variable concentrations it is able to enhance microbial activity (Holper et al., 2005) and was

therefore used as operational environment for xylanolytic bacteria. Subsequent to the cultivation in L47 medium, vital cells were collected by centrifugation for 10 min at 16,000 g for cell mass determination. 10% of dry cell mass was loaded on 5 g of zeolite by resuspension in 100 ml of L47 medium (thoroughly mixed) followed by another centrifugation step. Thereafter immobilised material was air dried for 2 days at room temperature.

2.1.3.3 Batch-culture

Laboratory batch experiments were carried out following the guidelines for "Fermentation of organic materials" (Friedmann et al., 2004) and modified according to DIN DEV 38414 S8 (1985). 1000 ml ground flasks were used as reaction vessels with a total volume of 600 ml. The fermentation mixture contained 30% (v/v) of seeding sludge from an anaerobic treatment plant (origin and characteristics as described above) adjusted to 1.5% ODM with deionised H_2O and 0.7% (w/v) of insoluble powder of xylan from birchwood as substrate. Then 0.2% (w/v) of immobilised material was added introducing 0.02% DM of xylanolytic bacteria to the total volume. Controls were charged with 0.2% (w/v) of pure activated zeolite. To estimate the auto-activity of pure seeding sludge, blanks had no addition of substrate or zeolite. Resulting methane yields were used for blank subtraction. Before starting the incubation under mesophilic conditions at 35°C, the flasks were flushed with oxygen-free nitrogen gas for 20 min. To remove CO_2, generated biogas was washed with 2 M NaOH solution. NH_4^+ and H_2S were eliminated using an acidic solution containing $Na_2SO_4 \cdot 10\ H_2O$, 200 g l^{-1} and 98% H_2SO_4, 30 ml l^{-1}. However, trace gases cause an error ratio of round about 1%. Parameter of measurement is the amount of CH_4 in litre per kg of ODM at standard ambient temperature and pressure (STP), calculated from displaced acidic solution volumes following VDI 4630 (Friedmann et al., 2004). Analysis data were obtained from the average of triplicate samples collected daily over a total fermentation period of 34 days whereupon methane production was measured cumulatively.

2.1.3.4 Enzyme activity assay

Xylanase activity was measured using a 3-amino,5-nitrosalicylic acid (DNS) assay which is based on the quantification of reducing sugars released with DNS as described previously by Bailey et al. (1992). The DNS reagent contained (in g l^{-1}): 3,5-dinitrosalicylic acid ($C_7H_4N_2O_7$), 7.48; NaOH, 13.98; sodium potassium tartrate

($C_4H_4KNaO_6$ • 4 H_2O), 216.1; phenol (C_6H_6O), 5.155; sodium metabisulfite ($Na_2O_5S_2$), 5.86. D-(+)-xylose standards in mg ml^{-1}: 2.5, 1.25, 0.625, 0.313, 0.156. Composition of samples and sample blanks in µl: 1% xyan solution, 180; sample, 20; DNS solution, 300. Before adding the DNS solution, samples were incubated at 35°C for 30 min. The photometric absorption was determined at 540 nm in 96 well plates (Greiner, Frickenhausen, Germany) using a plate reader (Tecan Infinite 200M, Männedorf, Switzerland). Xylanase activity is stated as units of enzyme activity per litre (U l^{-1}). An enzyme unit is defined as the conversion of 1 µmol D-(+)-xylose per minute under the given conditions above. 1 U corresponds to 16.67 nanokatals.

2.1.3.5 Cell counting

Bacterial growth was estimated by microscopic determination of cell numbers using a counting chamber (Neubauer improved: 16 x 0.0025 mm^2, 0.01 mm depth; LO Laboroptik, Friedrichsdorf, Germany). Cell counts were determined fourfold from 8 squares for each sample and sample dilution. A pre-treatment step was necessary to separate cell clusters and cells from other organic and inorganic particles: Samples were washed in 1 ml phosphate buffered saline (PBS, pH 7.0) twice and centrifuged for 5 min at 16,750 g. The pellet was resuspended in 1 ml PBS and then treated in an ultrasonic bath for 10 min at 100% intensity (Elma Transsonic Digital S, Schalltec, Mörfelden-Walldorf, Germany).

2.1.3.6 High performance liquid chromatography (HPLC) analysis

An HP 1100 HPLC system (Hewlett Packard, Palo Alto, California) equipped with an ICSep ION-300 column (7.8 x 300 mm) (Transgenomic, Omaha, USA) and an ICSep GC-801/C guard cartridge (4 x 20 mm) (Transgenomic, Omaha, USA) was used for quantification of organic acids. 5 mM sulphuric acid was used as mobile phase. Sample injection volumes were 40 µl; flow rate of 0.5 ml min^{-1}; at a temperature of 42°C. Compounds were detected with an HP 1047A refractive index detector (Hewlett Packard, Palo Alto, California). Standards of acetic acid, butyric acid, citric acid, isobutyric acid, isovaleric acid, lactic acid, propionic acid and valeric acid were injected for identification. Samples were prepared as follows: Carrez protein precipitation was carried out using $K_4[Fe(CN)_6]$ • 3 H_2O and $ZnSO_4$ • 3 H_2O as previously described by Carrez (1912). Subsequently, samples were diluted with double deionised H_2O to a final dilution of 1:40.

2.1.3.7 DNA extraction

The total bacterial community DNA was extracted as described by Martin-Laurent et al. (2001). To collect microorganisms, 1 g of sample material was centrifuged for 15 min at 16,750 g. The pellet was then resuspended in 1 ml of extraction buffer containing (in g l^{-1}): ethylenediaminetetraacetic acid (EDTA), 37.25; NaCl, 5.85; polyvinylpyrrolidone (PVP), 10; Tris-HCl, 12 and 20% (v/v) sodium dodecyl sulphate (SDS), 100 ml l^{-1}. To ensure complete cell lysis, glass beads from 0.15 to 2.00 µm in diameter were added to crush cell structures using FastPrep Instrument (Qbiogene, Heidelberg, Germany) for 2 x 30 s including cooling steps on ice in between for 2 min. After centrifugation for 1 min at 16,750 g, the supernatant was mixed with 5 M sodium acetate, 100 µl and incubated on ice for 15 min for protein precipitation. Succeeding another centrifugation step for 5 min, an equal volume of chloroform-phenol-isoamylalcohol mixture (15:24:1) was added to the supernatant. Subsequently, the genomic DNA was precipitated by adding an equal volume of isopropanol to the upper phase. The precipitated DNA was recovered by centrifugation for 10 min, washed once with 70% (v/v) ethanol and resuspended in a total volume of 50 µl of 10 mM Tris-HCl buffer (pH 8.0).

2.1.3.8 Polymerase chain reaction (PCR) amplification

Amplification of bacterial 16S rRNA gene fragments was carried out using the eubacterial primer pair Unibac-II-515f (5'-GTG CCA GCA GCC GC-3') and Unibac-II-927rP (5'-CCC GTC AAT TYM TTT GAG TT-3') according to Lieber et al. (2002), using a Biometra T personal/ gradient system (Biometra, Göttingen, Germany). The reaction mixture was set up on ice and contained: 1x Taq & Go (Qbiogene, Heidelberg, Germany); 3.0 mM $MgCl_2$ (Finnzyme, Espoo, Finland); 0.5 mM forward primer; 0.5 mM reverse primer; 20 ng template DNA (1 µl) and double deionised H_2O to fill up to a final volume of 20 µl for template DNA extracted from SSCP-Gels and 60 µl for template DNA extracted from second-stage sludge and L47 culture samples respectively. Negative control PCR contained no template DNA. The cycling conditions were as follows: (1) denaturation at 94°C for 4 min, (2) denaturation at 94°C for 20 sec, (3) annealing at 53°C for 30 sec, (4) extension at 72°C for 60 sec, (5) final extension at 72°C for 10 min, (6) hold at 4°C. Steps (2) till (4) were repeated 35 times. For the purification of PCR generated DNA products, Gene Clean Turbo Kit

(Qbiogene, Heidelberg, Germany) was used following the manufacturer's recommendations.

2.1.3.9 Single strand conformation polymorphism (SSCP) analysis

SSCP analysis of amplified bacterial 16S rRNA gene fragments was carried out according to Schwieger and Tebbe (1998). For single strand formation 10 µl of purified PCR products, adjusted to 50 ng dsDNA-content were used. Exonuclease digestion was performed with a λ-Exonuclease, 12 U (New England Biolabs, Frankfurt, Germany) at 37°C for 1 h, followed by an addition of 50% (v/v) loading buffer (95% deionised formamide, 10 mM NaOH, 0.025% (w/v) bromophenol blue), a denaturation step at 98°C for 3 min and a re-folding step on ice for 5 min. Separation of folded ssDNA was achieved by electrophoresis in 5x Tris-borate-EDTA buffer (TBE) at 26°C for 26 h using a TGGE MAXI system (Biometra). After silver-staining according to Bassam et al. (1992), gels were digitalised using a transillumination scanner. For further characterisation of microbial communities, i.e. sequence analysis, constantly dominant or variably emerging SSCP bands were excised with a scalpel. DNA was eluted from gel slices through incubation in sterile elution buffer (5 M ammonium acetate, 10 mM magnesium acetate, 1 mM EDTA, 0.1% sodium dodecyl sulphate [SDS], pH 8.0) at 37°C for 5 h following Sambrook et al. (1989). Afterwards, eluted DNA was re-amplified using the same primer pairs as for the SSCP analysis as described above.

2.1.3.10 Computer-assisted cluster analysis

In order to compare SSCP fingerprints of microbial communities, a computer-assisted cluster analysis was carried out using the GelCompar® software (Applied Math, Kortrijk, Belgium). DNA standards were loaded onto each gel allowing a post-run correction of gel-specific differences between several gel runs using the normalisation function of the GelCompar® software. After background subtraction and normalisation of digitalised images of the SSCP gels, similarities between the SSCP fingerprints were calculated using the band-based Dice similarity coefficient according to Dice (1945). Afterwards, the fingerprints were grouped according to their similarity using the hierarchical cluster method: *unweighted pairwise grouping method using arithmetic means* (UPGMA). Differences between clusters within software generated dendrograms were statistically verified by permutation significance tests according to Kropf et al. (2004).

2.1.3.11 Sequence analysis

About 60 ng of each PCR product from bands excised from PA gels were used for sequencing reactions, which were performed by the ZMF laboratory of the Medical University of Graz (Graz, Austria). To identify similar sequences that are available in the NCBI Genbank, sequences were used in BLASTn searches (Altschul et al., 1997; http://www.ncbi.nlm.nih.gov/blast/).

2.1.4 Results and Discussion

2.1.4.1 Cultivation and enrichment

In a first stage, the effect of xylan as single carbon source on xylanase production by anaerobic populations was studied. Xylanase activity in cultures containing xylan was significantly higher ($P < 0.05$) at day 3 to day 6 and day 10 of cultivation compared to reference cultures (figure 2-1). A maximum activity of 335 U l^{-1} in the mean was measured around day 5 representing a rise of 260 U l^{-1} compared to reference cultures (following figure I-1, standard deviations are indicated as error bars). The subsequent decrease of xylanase activity could be due to lower activity of xylanolytic organisms because of a complete consumption of all xylan followed by proteolytic degradation of xylanases. It is known that anaerobic cellulolytic species (e.g. those of the genera *Fibrobacter* and *Clostridium*) are limited in their carbohydrate range, growing well on cellulose and its hydrolytic products but often not on corresponding mono-, oligo- and polysaccharides (Lynd et al., 2002). Furthermore, increasing xylanase activities were accompanied by decreasing pH values, starting with pH 7.00 ± 0.01 (adjusted through L47 medium) at day 1, decreasing to a minimum pH of 4.95 in average with a standard deviation of 0.07 at day 4 (data not shown). At day 5, where a maximum xylanase activity was observed, a pH of 5.03 ± 0.08 appeared. Optimum pH conditions for xylanases have been previously reported to be at a pH of 5.2 for e.g. *Clostridium acetobutylicum* (Lee et al., 1985). In general, xylanases from different organisms show stabilities over a wide pH range with optima between pH 4 and 7 (Kulkarni et al., 1999).

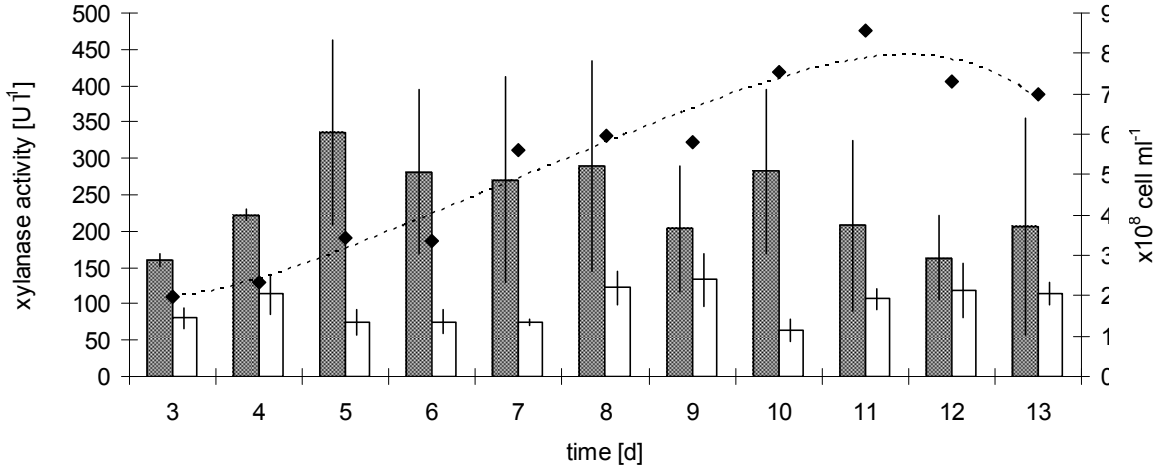

Fig. I-1 Xylanase activity in [U l^{-1}] determined during anaerobic cultivation of xylanolytic populations in L47 medium on xylan as mono-substrate (grey columns) and in second-stage sludge without xylan as blank (white columns) over 13 days. Significant differences are defined as $P < 0.05$ and marked with [*] in the diagram. Cell counts ml^{-1} (line) represent the bacterial growth during a single cultivation cycle over 13 days in L47 medium on xylan.

Characteristics of enzymatic activity levels related to bacterial growth determined by cell counts simultaneously during the cultivation in minimal medium (figure I-1). Focusing day 3 of cultivation $2.0 \cdot 10^8$ ml^{-1} ± 0.2 cell counts were observable. Followed by an exponential growth phase, increasing cell counts were accompanied by an increase of pH values and decreasing xylanase activities. At day 7 a pH of 5.40 ± 0.20 in average and 5.6 (± 1.3) • 10^8 ml^{-1} cell counts were observed. Both parameters increased from this point on, reaching a pH value of 6.39 ± 0.09 and a maximum cell number of 8.6 (± 1.5) • 10^8 ml^{-1} at day 11, representing the end of the exponential growth phase. These observations for xylanolytic bacteria, where pH values were not controlled, match with former findings concerning the degradation of cellulose. Cellulolytic bacteria are known not to grow at pH below 6.0, but at the same time cellulose removal in some anaerobic mixed cultures is observed at pH as low as 4.5, having an optimum around pH 5 (Chyi and Dague, 1994). Most fermentative microbes grow within a fairly narrow pH range, but in some habitats pH fluctuations permit cellulose degradation to occur at pH values below those actually supporting bacterial growth (Lynd et al., 2002). Ruminal bacteria for example, once being adhered to cellulose, having synthesised a glycocalyx, pH drops below 6.0 where substantial cellulose hydrolysis occurs, but growth has already stopped

(Mourino et al., 2002). However, as maximum enzymatic activities were measured around day 5 during the exponential bacterial growth phase, cultures at day 4 to 6 were then considered as inoculum for subsequent cultivation steps depending on actual enzyme activity levels.

With respect to increasing bacteria cell counts resulting from co-cultivated non-xylanolytic populations, xylanase activity of successive enrichment cycles was related to total cell numbers to obtain a factor specific for xylanolytic populations. Cellulose and hemicellulose degradation in anaerobic processes have been primarily ascribed to the activity of multi-enzyme complexes, namely cellulosomes and xylanosomes as well as to extracellular enzymes such as endoglucanase (carboxymethycellulase), cellulase, xylanase and aryl-β-xylosidase produced constitutively (Schwarz, 2002; Thomson, 1993). Thus, a higher specific xylanase activity in culture liquids should indicate an enrichment of hemicellulolytic organisms within the mixed microbial community. However, this specific xylanase activity of successive cultivation cycles increased significantly until the fourth cultivation cycle and varied later with only a slight increase up to the thirteenth cultivation cycle (figure I-2).

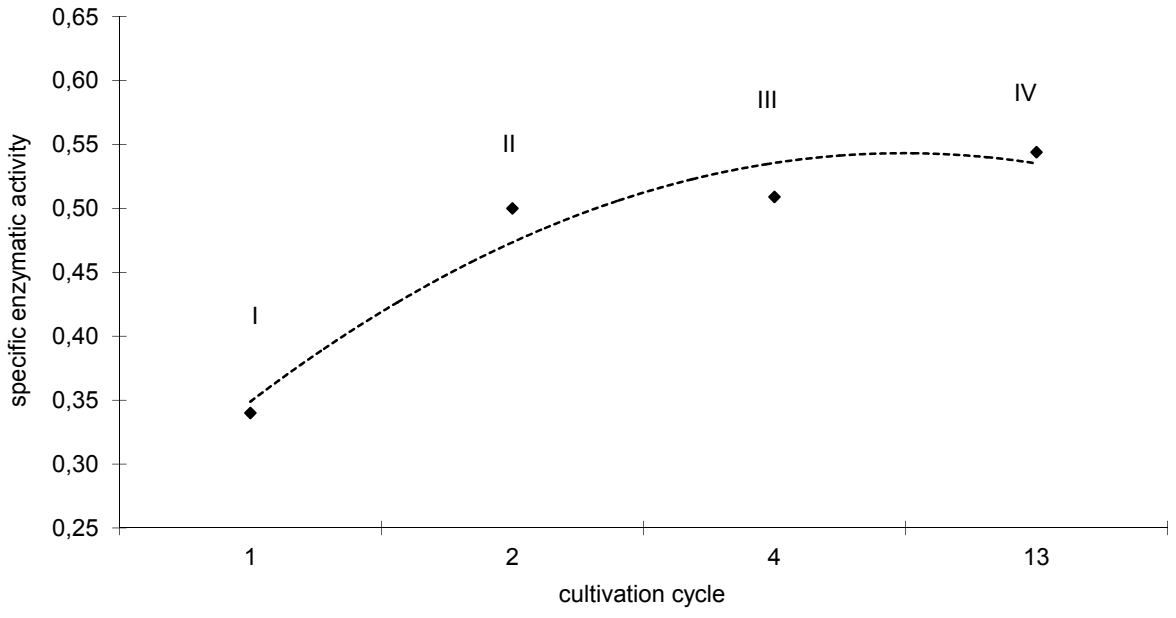

Fig. I-2 Enzymatic activity of xylanase (U l^{-1}) related to the bacterial growth (cell counts ml^{-1}) generates a community specific enzyme activity shown for the first [I], second [II], fourth [III] and thirteenth [IV] cultivation cycle in L47 medium on xylan as mono-substrate. Data were collected at day 5 in respect to maximum enzymatic activity levels within exponential growth phase periods of each cultivation cycle.

Correspondingly to the second [II], fourth [III] and thirteenth [IV] cultivation cycle, the following maximum values were stated at day 5 respectively: 495 (± 150) U l^{-1} to 3.8 (± 0.2) • 10^8, 509 (± 18) U l^{-1} to 8.6 (± 1.7) • 10^8 and 544 (± 56) U l^{-1} to 1.4 (± 0.4) • 10^8 cell counts ml^{-1}. Comparatively to the values obtained from the first cultivation cycle, a maximum increase of + 60% in xylanase activity was measured after thirteen cultivation cycles due to high enzymatic activity corresponding to relatively low cell counts at a pH of 4.53 ± 0.02, while a value of 50% was almost reached after the fourth enrichment cycle at a pH of 5.72 ± 0.09 showing mildly lower enzymatic activity (- 35 U l^{-1} in average) related to even more cells counted (+ 7.2 • 10^8 in average) compared to cultivation cycle thirteen.

Overall, the increase in specific xylanase activity in successive enrichment cycles was limited and indicates that the anaerobic community from maize silage digestion was already well adapted to xylan as substrate, since whole maize plants show high contents of cellulose and hemicelluloses of about 29% and 32% in average respectively (Amon et al., 2003). Also obligate synthrophic relationships between hemicellulolytic bacteria and acidogenic or acetogenic bacteria in further converting mono- and oligomeric metabolites (e.g. xylose, xylobiose) might contribute to this effect by affecting the measurement of reducing sugars. In general particular enrichment of xylanolytic bacteria in synthetic medium L47 on xylan as carbon source was successful and is in agreement with previous reports (Poutanen et al., 1987; Lee et al., 1985). Even though *Bacillus* sp. strains show comparatively higher xylanase activities in pure cultures (Subramaniyan and Prema, 2002), enzymatic activities in this study represent a cumulative effect derived from different species contributing to a mixed culture, where e.g. interspecific stress must be considered. On the other hand, selective enrichment of certain species from naturally balanced communities, e.g. biogas-producing community, entails the risk of interfering vital syntrophic relationships of hydrolytic, acidogenic, acetogenic and methanogenic partners (Schink, 2006). Moreover, enrichment in continuous batch or fed-batch reactors under controlled pH conditions might lead to even more specialised populations. However, as the specific xylanase activity has reached three paramount maxima (figure 2-2: II, III, IV), SSCP and sequencing analysis was carried out to identify responsible species.

2.1.4.2 Community profile

The identification of changes within bacterial community organisation during the cultivation on xylan as mono-substrate was achieved by SSCP-analysis using 16S rDNA as bacteria-specific target for the PCR amplification. Figure I-3 shows an exemplary SSCP gel from samples of the cultivation in L47 medium compared to the bacterial community naturally occurring in second-stage sludge of a biogas plant mainly operated with mono-maize silage revealing distinguishable band patterns.

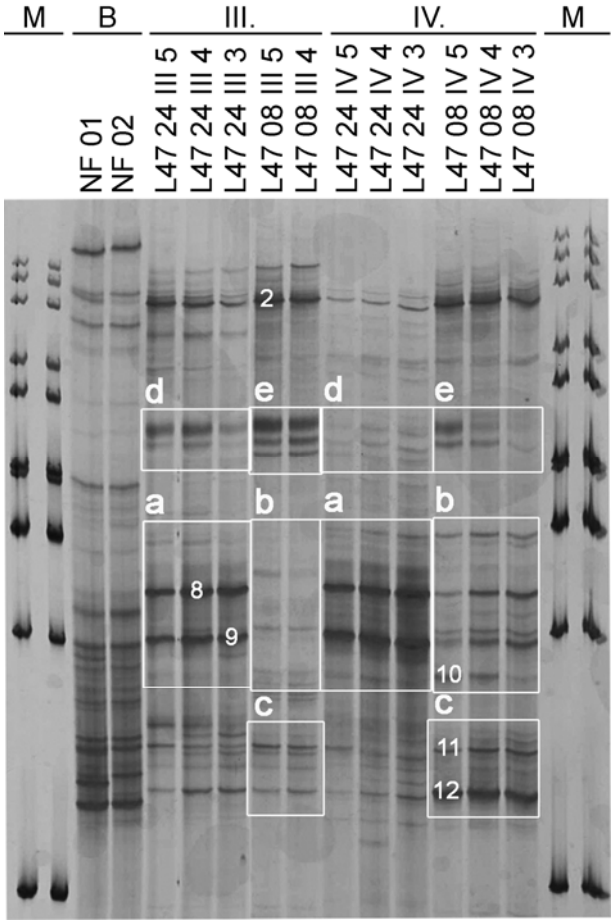

Fig. I-3 Exemplary non-denaturating polyacrylamide gel from the SSCP-analysis based on 16S rDNA fragments focusing the bacterial community cultured in L47 medium and from second-stage sludge: [M] represents 1 kb DNA-ladder marker lanes; [B] represents the blank, i.e. pure second-stage sludge [NF 01/02]; [III.] and [IV.] represent corresponding cultivation periods in L47 medium on xylan as mono-substrate. Sample-Code: L47 = medium, 08/24 = replicate number, III/IV = cultivation cycle, 3/4/5 = day of current cultivation. Boxes [a], [b] and [c] show the intensification, boxes [d] and [e] the weakening of specific band patterns indicating shifts in bacterial community organisation during the cultivation in L47 medium. Boxes [2], [8], [9], [10], [11] and [12] represent specific bands selected for DNA extraction and sequencing analysis.

In summary, 29 bands for the total bacterial community in second-stage sludge were detected. In view of the total bacterial community in L47 medium at the third and forth enrichment cycle, 19-24 bands with variations in dominance appeared. Boxes [a], [b] and [c] demonstrate intensifications of specific band patterns of certain replicates, whereas box [d] and [e] reveal a weakening over the periods of cultivation. Enforcing a certain catabolic pathway constitutes a breach in syntrophic association of methane producing bacteria and can therefore be assumed as causal reason for the vanishing of species.

Hence cultivation-dependant formation of specific band patterns indicates shifts within bacterial community structure, SSCP patterns were taken as operational taxonomic units (OTU). The cultivation in synthetic medium led to OTUs distinguishable from that ones found in second-stage sludge. To analyse the shifts in bacterial community composition, Pearson's correlation coefficients were compared by UPGMA. All cultivation cycles in L47 medium analysed corporately formed one cluster significantly discriminable ($P < 0.05$) from another one formed by pure second-stage sludge samples (blank) corroborating an assumed shift, potentially towards a distinctive enriched hydrolytic bacterial community (figure I-4). The corresponding similarity between OTUs of blank samples (NF 03 to NF 12) and the OTUs that have arisen from the cultivation on xylan (cycle four, eight and nine) was under 57%, whereas similarities between OTUs within one cluster were up to 67 % for pure second stage-sludge samples and > 69% for samples from the cultivation on xylan in L47 medium respectively.

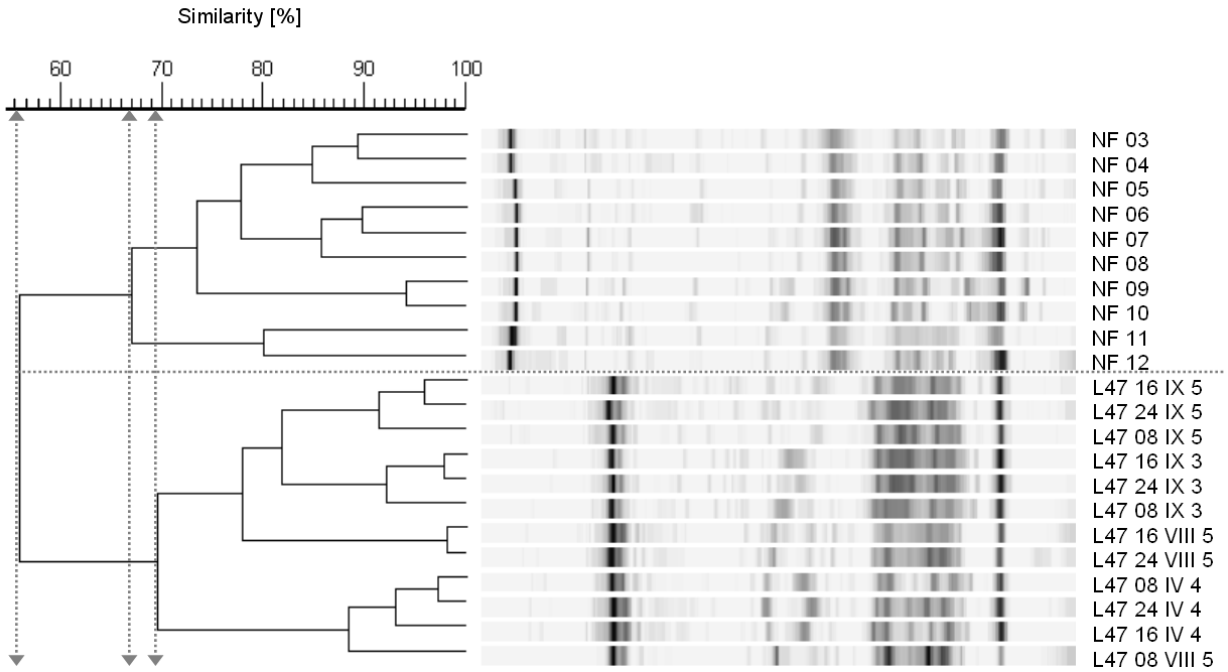

Fig. I-4 Dendrogram based on amplified 16S rDNA fragments of bacterial cultures in L47 medium and pure second-stage sludge [NF 03-12] respectively obtained by using eubacterial primers and separated by SSCP. Band patterns were grouped by UPGMA. Double-headed vertical arrows indicate the similarity for the groupings. Sample-Code: L47 = medium, 08/16/24 = replicate number, IV/VIII/IX = cultivation cycle, 3/4/5 = day of cultivation and sample collection.

Furthermore, a change of the eubacterial community structure was observed during the cultivation in L47 medium. Derived patterns differentiate significantly ($P < 0.05$) from cultivation cycle three to four, forming separated OTUs at a similarity of < 67-68% depending on triplicates observed. Triplicates participating cultivation cycle three form one distinct OTU at a similarity of > 74% (figure 2-5). Thus, increasing xylanase activity in successive enrichment cycles correlated with the observation of correspondingly differentiated community profiles.

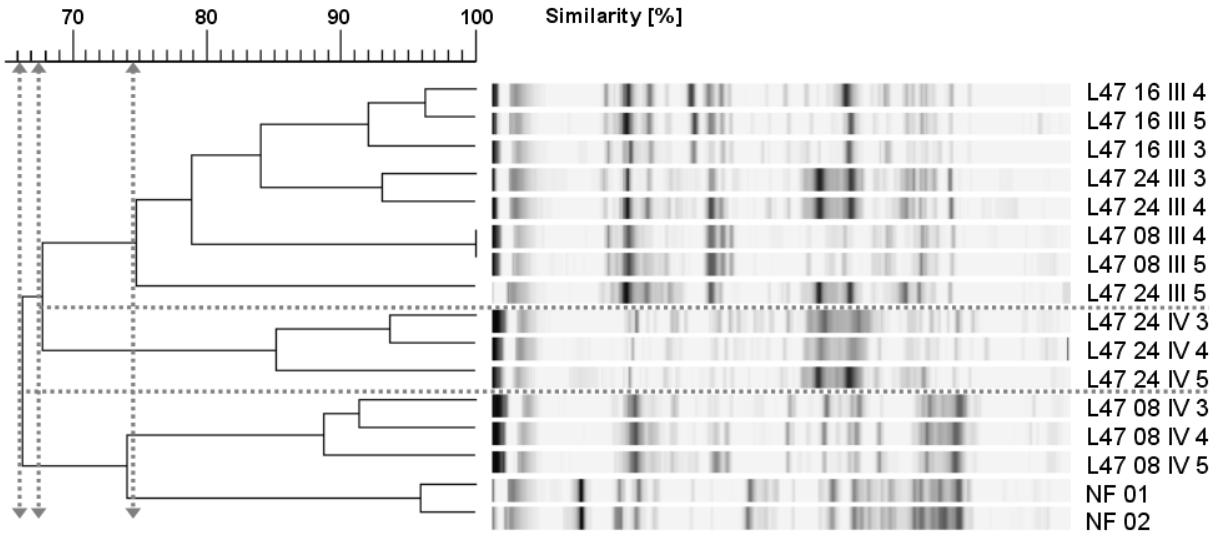

Fig. I-5 Dendrogram based on amplified 16S rDNA fragments of bacterial cultures in L47 medium and pure second-stage sludge [NF 01/02] respectively obtained by using eubacterial primers and separated by SSCP. Band patterns were grouped by UPGMA. Double-headed vertical arrows indicate the similarity for the groupings. Sample-Code: L47 = medium, 08/16/24 = replicate number, III/IV = cultivation cycle, 3/4/5 = day of cultivation and sample collection.

Sequence analysis of DNA extracted from single bands representing specific species was then used as a holistic approach for further community characterisation (Schwieger and Tebbe, 1998). Sequence analyses of bands exposed in boxes [8] and [9] shown in Fig. 3 reveal three affiliations within the phylum Bacteroidetes (i.e. *Bacteroides* sp.) and one with the class Betaproteobacteria (i.e. *Azospira oryzae*), each with an identity value of 98%. *Bacteroides* sp. are well known plant cell structure degraders, while e.g. *B. succinogenes* together with *B. ruminicola* are among the most important cellulolytic bacteria in the rumen environment with endoglucanase (carboxymethylcellulase), cellulase, xylanase and aryl-β-xylosidase activities (Forsberg et al., 1981). Heylen et al. (2006) isolated species from the genus *Azospira* sp. from activated sludge samples derived from municipal wastewater treatment plants, characterising a denitrifying potential. Since ammonia has potential inhibitory effects on the anerobic-digestion microbial consortia (Heinrichs et al., 1990; Sprott and Patel, 1986), e.g. inhibition of methanogenic growth and acetate uptake (Poggi-Varaldo et al., 1991), the elimination of dissolved nitrogen by members of the microbial community would also have a positive effect on the poduction of biogas.

DNA extraction from bands represented in figure 2-3, i.e. [11] and [12] reveal a wide spectrum of diverse species related to the phylum Firmicutes with a close relationship to different members of the order Clostridiales, i.e. *Clostridium beijerinckii*, *C. butyricum*, *C. chromoreductans*, *C. corinoforum*, *C. diolis*, *C. favososporum*, *C. puniceum*, *C. roseum*, *C. saccacharoperbutylacetonicum* with identity values of 97-98%. *Clostridium beijerinckii* for example is an exceptional bacterium for studies on crucial hemicellulose and cellulose degradation (Schwarz, 2002). Besides having a major hydrolysing activity, Clostridia are distinct hydrogen-producing bacteria, especially *C. butyricum* and *C. diolis* have shown specifically high hydrogenase activities in activated sludge samples (Wang et al., 2007). Though biogas formation only takes place below a certain threshold hydrogen concentration, the biological activity of methanogens requires hydrogen to carry out redox-reactions, e.g. acetate reduction to methan and is therefore syntrophically related to acetogenic species via an interspecies hydrogen transfer (Fang et al., 2002; Wolin, 1975; Zeikus et al., 1975). Intermittent dominant bands marked with [10] reveal sequences corresponding to *Bacteroides* sp. with an identity value of 98%, whereas bands marked with [2], which were dominant throughout all cultivation cycles, represent uncultured bacteria of unknown origin. Members of *Bacteroides* and *Clostridium* are known to be principally responsible for the bioconversion of renewable raw material to biogas, i.e. the degradation of major plant structural polysaccharides forming acetate, formiate, lactate amongst other fatty acids (Klocke et al., 2007).

A favourable change towards a more specialised and xylanolytically active community structure could be confirmed by sequence analyses. Thus, our findings emphasise a hydrolytic potential of xylan-grown populations, which impact on the methanogenic biogas-producing process was studied as follows.

2.1.4.3 Influence of zeolite-immobilised hemicellulolytic microorganisms on biogas process

To investigate the effect of hemicellulolytic microorganisms on biogas formation, enriched xylanolytic cultures were immobilised on trace metal activated zeolite and then introduced in a comparative batch-culture experiment under mesophilic temperature conditions (i.e. 35°C). Figure 2-6 shows a comparison of batch-cultures with and without addition of immobilised bacteria on activated zeolite, i.e. their effects on corresponding methane yields cumulatively measured over a total fermentation period of 34 days (standard deviations are indicated as error bars in the diagram).

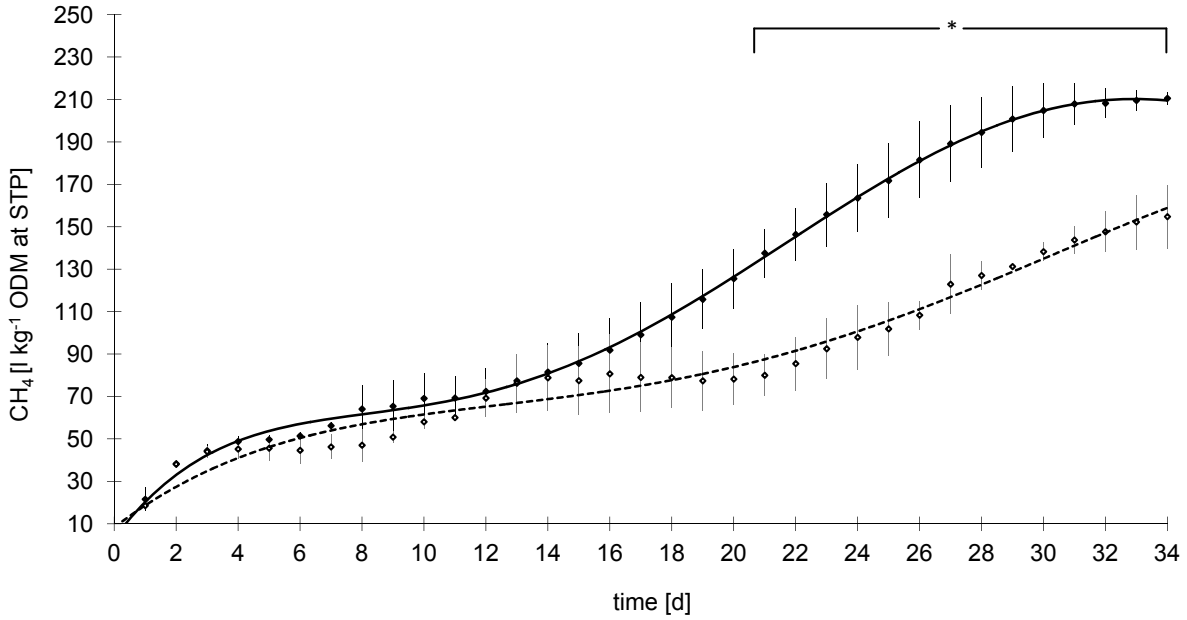

Fig. I-6 Cumulative biogas production, i.e. CH_4 in [l kg^{-1} ODM at STP] during discontinuous fermentation in the presence of xylanolytic bacteria immobilised on activated zeolite (black line ●) and control with activated zeolite but without immobilised microorganisms (dotted line ○) at 35 °C over a total period of 34 days. From day 21 of the fermentation on differences in biogas amounts were significant. Significant differences are defined as $P < 0.05$ and are marked with [*] in the diagram.

Small differences in measured methane amounts of about Δ 13.9 l CH_4 kg^{-1} ODM at STP in average were already observed around day 9 of the fermentation, indicating a slightly better initiation of the fermentation process by introducing immobilised material. These first minor differences expanded from day 21 on, revealing a much higher biogas production rate in the presence of hemicellulolytic bacteria immobilised on activated zeolite when compared to controls supported with trace metal activated zeolite only. Methane yields were increased by about 64.1 l CH_4 kg^{-1} ODM at STP in average which equals an increase of 53% in the mean. At day 26 of the fermentation a maximum discrepancy of Δ 73.2 l CH_4 kg^{-1} ODM at STP was noticed which is equivalent to an increase of 121%.

Furthermore, HPLC-analysis revealed a correlation between increased biogas productivity upon addition of xylanolytic bacteria immobilised on activated zeolite and an increase of acetic acid in corresponding replicates (figure I-7).

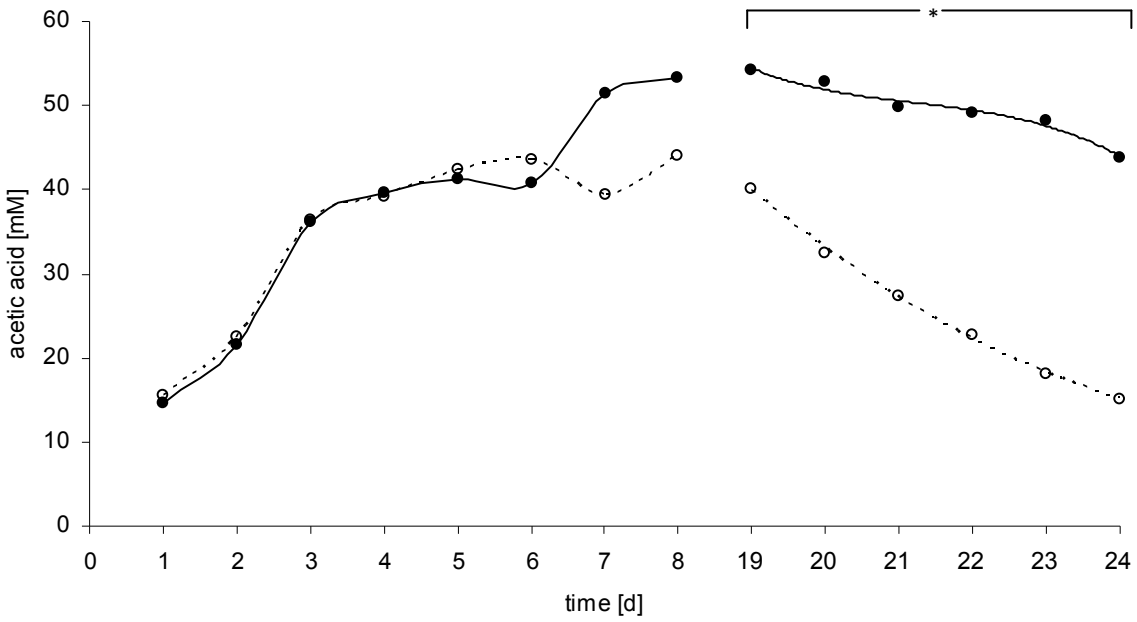

Fig. I-7 Acetic acid concentrations obtained from single measurements during discontinuous fermentation at 35 °C in the presence of xylanolytic bacteria immobilised on activated zeolite (black line ●), control with activated zeolite but without immobilised microorganisms (white line ○). From day 19 on, acetic acid concentrations differ significantly. Significant differences are defined as $P < 0.05$ and marked with [*] in the diagram.

With day 7 of the fermentation process the concentration of acetic acid was starting to increase by 9.11 mM in comparison to control replicates without zeolite-immobilised hemicellulolytic microorganisms, correlating with initially risen amounts of methane around day 9 (figure I-6). However, from day 19 on a significant increase of 14.03 mM acetic acid (+35%) was observed, reaching a maximum at day 24 with 28.62 mM which is equivalent to an increase of 189%. Overall, acetic acid concentrations increased by 20.4 mM in average which equals 88% in the mean, correlating with simultaneously risen methane amounts observed between day 21 and day 26 of the total fermentation time (figure I-6). Thus, it is assumable that aceticlastic methanogenic species, producing a major part of the total methane yield during the methanogenesis, were favoured due to the increased availability of their exclusive substrate acetate (Jetten et al., 1992; Zeikus et al., 1975). A clarification could be achieved by DNA microarrays, which have been used for bacterial detection, as well as for microbial community analysis, while further functional gene

arrays are able to verify the expression of specific enzymes in processes such as methanogenesis (Saleh-Lakha et al., 2005).

2.1.5 Conclusion

In summary we have shown that hemicellulolytic populations within mixed fermentative microbial communities can be enforced by substrate determination. Since the interaction of bacteria cells with certain substrates predisposes their growth and regulates the biosynthesis of their enzymes, xylan powder proved to be a capable carbon source for the induction of xylanase activity in mixed fermentative populations. As exposed by SSCP and sequence analyses, higher enzymatic activities were due to the development of a hemicellulolytic population, significantly distinctive from the natural bacteria community composition, revealing participations of *Bacteroides* sp., *Azospira* sp. among a wide spectrum of diverse Clostridia species in xylan degradation. In laboratory batch experiments methane yields in discontinuous fermentation of xylan powder were increased significantly upon the addition of hemicellulolytic microorganisms when immobilised on trace metal activated zeolite. Increased methane production correlated with simultaneously risen concentrations of acetic acid, suggesting the acetogenic fermentation phase to be enhanced through higher hydrolytical activity derived from pre-cultured xylanolytical bacteria providing an enforced conversion of xylan. This strategy demonstrates a scheme principally easy to apply to biogas processes. Though further studies in semi-continuous and continuous laboratory and large scale experiments are required, including considerations to the degradation of crystalline cellulose and lignocellulose, the use of supplemental introduced immobilised bacteria might either reduce the need for e.g. chemical pre-treatment approaches or make recalcitrant agricultural biomass and residues more economic substrates for the production of biogas. The understanding of cell adhesion to the surface of zeolites and its influence on growth and enzyme synthesis as operational environment during subsequent fermentation stages are part of future studies.

2.1.6 Acknowledgment

This work has been kindly supported by IPUS GmbH, Department of Research and Development. The authors would also like to send many thanks to the Center for Medical Research at the Medical University of Graz.

In memory of

***

Remo Meincke

*(*13th July 1978 – †01st October 2008)*

***

A keen and utmost promising scientist

and adorable friend.

2.1.7 References

Altschul, S.F., Madden, T.L., Schaffer, A.A., Zhang, J.H., Zhang, Z., Miller, W. and Lipman, D.J. (1997) Gapped BLAST and PSI-BLAST: a new generation of protein database search programs. Nucleic *Acids Research* **25** (17), 3389-3402.

Amon, T., Kryvoruchko, V., Amon, B., Moitzi, G., Lyson, D., Hackl, E., Jeremic, D., Zollitsch, D. and Pötsch, E. (2003) Optimierung der Biogaserzeugung aus den Energiepflanzen Mais und Kleegras. *Bundesministeriums für Land- und Forstwirtschaft, Umwelt- und Wasserwirtschaft* **77**, 1-10.

Bagi, Z., Acs, N., Balint, B., Horvath, L., Dobo, K., Perei, K.R., Rakhely, G. and Kovacs, K.L. (2007) Biotechnological intensification of biogas production. *Applied Microbiology and Biotechnology* **76** (2), 473-482.

Bailey, M.J., Biely, P. and Poutanen, K. (1992) Interlaboratory testing of methods for assay of xylanase activity. *Journal of Biotechnology* **23**, 257-270.

Bassam, B.J., Caetanoanolles, G. and Gresshoff, P.M. (1991) Fast and sensitive silver staining of DNA in polyacrylamide gels. *Analytical Biochemistry* **196** (1), 80-83.

Carrez, C. (1912) Die Kupferreagenzien und die Bestimmung der Zuckerarten. *Zeitschrift für Analytische Chemie* **51** (6), 394-395.

Chyi, Y.T. and Dague, R.R. (1994) Effects of particulate size in anaerobic acidogenesis using cellulose as a sole carbon source. *Water Environment Research* **66** (5), 670-678.

Dice, L.R. (1945) Measures of the amount of ecologic association between species. *Ecology* **26** (3), 297-302.

Fang, H.H.P., Zhang, T. and Liu, H. (2002) Microbial diversity of a mesophilic hydrogen-producing sludge. *Applied Microbiology and Biotechnology* **58** (1), 112-118.

Fernández, N., Montalvo, S., Fernández-Polanco, F., Guerrero, L., Cortés, I., Borja, R., Sánchez, E. and Travieso, L. (2007) Real evidence about zeolite as microorganisms immobilizer in anaerobic fluidized bed reactors. *Process Biochemistry* **42** (4), 721-728.

Forsberg, C.W., Beveridge, T.J., and Hellstrom, A. (1981) Cellulase andxylanase release from *Bacteroides succinogenes* and its importance in the rumen environment. *Applied and Environmental Microbiology* **42** (5), 886-896.

Green, M., Mels, A., Lahav, O. and Tarre, S. (1996) Biological ion-exchange process for ammonium removal from secondary effluent. *Water Science and Technology* **34** (1-2), 449-458.

Grethlein, H.E. (1985) The Effect of pore-size distribution on the rate of enzymatic hydrolysis of cellulosic substrates. *Bio/Technology* **3** (2), 155-160.

Held, C., Wellacher, M., Robra, K.H. and Gübitz,G.M. (2002) Two-stage anaerobic fermentation of organic waste in CSTR and UFAF-reactors. *Bioresource Technology* **81** (1), 19-24.

Hendriks, A.T.W.M. and Zeeman, G. (2009) Pretreatments to enhance the digestibility of lignocellulosic biomass. *Bioresource Technology* **100** (1), 10-18.

Heylen, K., Vanparys, B., Wittebolle, L., Verstraete, W., Boon, N. and De Vos, P. (2006) Cultivation of denitrifying bacteria: optimization of isolation conditions and diversity study. *Applied and Environmental Microbiology* **72** (4), 2637-2643.

Holper, J., Lesjak, M., Heinzel, U., Boos, B., (2005) Zeolith in der Biogasgewinnung. Sonn. 05450052.5 [EP 1 577 269 A1], Patent Styria, Austria.

Iiyama, K., Lam, T.B.T. and Stone, B.A. (1994) Covalent cross-links in the cell-wall. *Plant Physiology* **104** (2), 315-320.

Jetten, M.S.M., Stams, A.J.M. and Zehnder, A.J.B. (1992) Methanogenesis from acetate - a comparison of the acetate metabolism in *Methanothrix soehngenii* and *Methanosarcina* spp.. *FEMS Microbiology Reviews* **88** (3-4), 181-197.

Klocke, M., Mähnert, P., Mundt, K., Souidi, K. and Linke, B. (2007) Microbial community analysis of a biogasproducing completely stirred tank reactor fed continuously with fodder beet silage as mono-substrate. *Systematic and Applied Microbiology* **30** (2), 139-151.

Kropf, S., Heuer, H., Ning, M. and Smalla, K. (2004) Significance test for comparing complex microbial community fingerprints using pairwise similarity measures. *Journal of Microbiological Methods* **57** (2), 187-195.

Kulkarni, N., Shendye, A. and Rao, M. (1999) Molecular and biotechnological aspects of xylanases. *FEMS Microbiology Reviews* **23** (4), 411-456.

Lee, S.F., Forsberg, C.W. and Gibbins, L.N. (1985) Xylanolytic activity of *Clostridium acetobutylicum*. *Applied and Environmental Microbiology* **50** (4), 1068-1076.

Lieber, A., Kiesel, B. and Babel, W. (2002) Microbial diversity analysis of soil by SSCP fingerprinting technique using TGGE Maxi System. In: Merbach, W., Hütsch, B.W. and Augustin, J. (eds.), Teubner, Stuttgart. *Ökophysiologie des Wurzelraumes*, 61-65.

Lynd, L.R., Weimer, P.J., Van Zyl, W.H. and Pretorius, I.S. (2002) Microbial cellulose utilisation: fundamentals and biotechnology. *Microbiology and Molecular Biology Reviews* **66** (3), 506-577.

Martin-Laurent, F., Philippot, L., Hallet, S., Chaussod, R., Germon, J.C., Soulas, G. and Catroux, G. (2001) DNA extraction from soils: old bias for new microbial diversity analysis methods. *Applied and Environmental Microbiology* **67** (5), 2354-2359.

Matthews, J.F., Skopec, C.E., Mason, P.E., Zuccato, P., Torget, R.W., Sugiyama, J., Himmel, M.E. and Brady, J.W. (2006) Computer simulation studies of microcrystalline cellulose I beta. *Carbohydrate Research* **341** (1), 138-152.

Milán, Z., Villa, P., Sánchez, S., Montalvo, S., Borja, R., Ilangovan, K., and Briones, R. (2003) Effect of natural and modified zeolite addition on anaerobic digestion of piggery waste. *Water Science Technology* **48** (6), 263-269.

Mourino, F., Akkarawongsa, R. and Weimer, P.J. (2001) Initial pH as a determinant of cellulose digestion rate by mixed ruminal microorganisms in vitro. *Journal of Dairy Science* **84** (4), 848-859.

Nishiyama, Y., Langan, P. and Chanzy, H. (2002) Crystal structure and hydrogen-bonding system in cellulose I beta from synchrotron x-ray and neutron fiber diffraction. *Journal of the American Chemical Society* **124** (31), 9074-9082.

Poutanen, K., Ratto, M., Puls, J. and Viikari,L. (1987) Evaluation of different microbial xylanolytic systems. *Journal of Biotechnology* **6**, 49-60.

Saleh-Lakha, S., Miller, M., Campbell, R.G., Schneider, K., Elahimanesh, P., Hart, M.M. and Trevors, J.T. (2005) Microbial gene expression in soil: methods, applications and challenges. *Journal of Microbiological Methods* **63** (1), 1-19.

Sambrook, J.E., Fritsch, E.F. and Maniatis,T. (1989) Gel electrophoresis of DNA and pulsed-field agarose gel electrophoresis – isolation of DNA fragments from polyacrylamide gels. In: Sambrook, J.E., Fritsch, E.F. and Maniatis,T. (eds.), Cold Spring Harbor, New York. *Molecular cloning: a laboratory manual* **2**, 551-555.

Schink, B. (2006) Syntrophic associations in methanogenic degradation. *Progress in Molecular and Subcellular Biology* **41**, 1-19.

Schwarz, W.H. (2002) The cellulosome and cellulose degradation by anaerobic bacteria. *Applied Microbiology and Biotechnology* **56**, 634-649.

Schwieger, F. and Tebbe, C.C. (1998) A new approach to utilise PCR-single-strand-conformation polymorphism for 16S rRNA gene-based microbial community analysis. *Applied and Environmental Microbiology* **64** (12), 4870-4876.

Staubmann, R., Foidl, G., Foidl, N., Gübitz, G.M., Lafferty, R.M., Arbizu, V.M.V. and Steiner, W. (1997) Biogas production from Jatropha curcas press-cake. *Applied Biochemistry and Biotechnology* **63** (5), 457-467.

Subramaniyan, S. and Prema, P. (2002) Biotechnology of microbial xylanases: Enzymology, molecular biology and application. *Critical Reviews in Biotechnology* **22** (1), 33-64.

Tada, C., Yang, Y., Hanaoka, T., Sonoda, A., Ooi, K. and Sawayama, S. (2005) Effect of natural zeolite on methane production for anaerobic digestion of ammonium rich organic sludge. *Bioresource Technology* **96** (4), 459-464.

Thomson, J.A. (1993) Molecular-biology of xylan degradation. *FEMS Microbiology Reviews* **104** (1-2), 65-82.

Wang, X., Hoefel, D., Saint, C.P., Monis, P.T. and Jin, B. (2007) The isolation and microbial community analysis of hydrogen producing bacteria from activated sludge. *Journal of Applied Microbiology* **103** (5), 1415-1423.

Wolin, M.J. (1975) Interspecies hydrogen transfer between hydrogen-producing and methane-producing species. In: Schlegel, H.G., Gottschalk, G. and Pfenning, N. (eds), Acadamy of Sciences, Göttingen. *Allgemeine Mikrobiologie*, 141-150.

Zhang, Y.H.P. and Lynd, L.R. (2004) Toward an aggregated understanding of enzymatic hydrolysis of cellulose: Noncomplexed cellulase systems. *Biotechnology and Bioengineering* **88** (7), 797-824.

2.2 Investigation of microorganisms colonising activated zeolites during anaerobic biogas production from grass silage

Weiß, S.[1], Zankel, A.[2], Lebuhn, M.[3], Petrak, S.[4], Somitsch, W.[5] and Guebitz, G.M.[1]

[1]Institute of Environmental Biotechnology, Graz University of Technology, Petersgasse 12, 8010 Graz, Austria; [2]Institute for Electron Microscopy, Graz University of Technology, Steyrergasse 17, 8010 Graz, Austria; [3]Bavarian State Research Center for Agriculture, Vöttinger Straße 38, 85354 Freising, Germany; [4]IPUS GmbH, Werksgasse 281, 8786 Rottenmann, Austria; [5]Engineering Consultant, Wiedner Hauptstrasse 90/2/19, 1050 Vienna, Austria

(Bioresource Technology, Volume 102, Issue 6, March 2011, Pages 4353-4359)

2.2.1 Abstract

The colonisation of activated zeolites (i.e. clinoptilolites) as carriers for microorganisms involved in the biogas process was investigated. Zeolite particle sizes of 1.0-2.5 mm were introduced to anaerobic laboratory batch-cultures and to continuously operated bioreactors during biogas production from grass silage. Incubation over 5-84 days led to the colonisation of zeolite surfaces in small batch-cultures (500 ml) and even in larger scaled and flow-through disturbed bioreactors (28 l). Morphological insights were obtained by using scanning electron microscopy (SEM). Single strand conformation polymorphism (SSCP) analysis based on amplification of bacterial and archaeal 16S rRNA fragments demonstrated structurally distinct populations preferring zeolite as operational environment. Via sequence analysis conspicuous bands from SSCP patterns were identified. Populations immobilised on zeolite (e.g. *Ruminofilibacter xylanolyticum*) showed pronounced hydrolytic enzyme activity (xylanase) shortly after re-incubation in sterilised sludge on model substrate. In addition, the presence of methanogenic archaea on zeolite particles was demonstrated.

2.2.2 Introduction

In numerous studies grass silage has been recommended as an excellent substrate for biomethane production resulting from high energy yields and low energy input demand (Prochnow et al., 2009). The high potential of methane production from grass silage was confirmed both in batch and semi-continuous experiments and batch leach bed processes (Lehtomäki et al., 2008). In practice, grass silage is the most important substrate for agricultural biogas production following maize silage in Germany (Rösch et al., 2007). Though grass silage may be less energetically productive compared to maize silage, it still offers a good energy balance and environmental advantages (Gerin et al., 2008). The formation of inhibitory NH_3 and high chemical oxygen demand (COD) values in the course of grass biomethane production are drawbacks, which may be counteracted by the high ammonia binding capacity of zeolites as reported by Montalvo et al. (2005).

The addition of support materials like magnesium or aluminium silicates to anaerobic digestion processes has been reported to lead to higher methane yields or better gas quality (Pande and Fabiani, 1989). Furthermore, the immobilisation of micro-organisms on various zeolite types was claimed to be beneficial, expanding the possibilities to support the process (Murray and van den Berg, 1981). Among natural and synthetic zeolites, clinoptilolite has a superior CO_2 adsorption capacity, regenerability and stability through several adsorption-desorption cycles, upgrading the quality of biogas by adjusting the CO_2/CH_4 ratio (Alonso-Vicario et al., 2010). Moreover, clinoptilolite has been shown to be suitable as operational environment for microorganisms in biogas production processes (Milán et al., 2003). Recently, we have demonstrated that the degradation of recalcitrant cell wall components can be enhanced by addition of hydrolytic bacterial populations immobilised on activated zeolite to the biogas process (Weiß et al., 2010). However, our understanding of the specificity of zeolites regarding the immobilisation of certain microbial populations is still poor. Therefore, we characterised the microbial populations colonising trace metal activated clinoptilolite during anaerobic digestion of grass silage and of a model substrate in this study.

2.2.3 Materials and Methods

2.2.3.1 Batch-culture and continuously operated bioreactor experiments

The zeolite used (IPUS GmbH, Rottenmann, Austria) consisted of a natural zeolitic tuff containing > 85% clinoptilolite, which was milled to a grain size below 2.5 mm. The material was loaded with Fe, Ni, Co, Mo, Se, Cu and Zn as trace metal elements to enhance microbial activity (Holper et al., 2005). To investigate the capability of zeolite surfaces as a functional colonisation area, particles of 1.0 to 2.5 mm were introduced to batch experiments (0.01 g ml^{-1}) carried out in 1000 ml ground flasks with a total volume of 500 ml of seeding sludge with the following properties: dry matter content (DM) of 9.50%; organic dry matter content (ODM) of 6.45% and an ODM fraction of DM (ODM/DM) of 67.39%. The seeding sludge was obtained from fermenters long-term mono-digesting grass silage (360 d) at increasing organic loading rates of 0.5-3.0 kg ODM m^{-3} d^{-1} and mesophilic conditions (Andrade et al., 2009). Before use, the sludge was flushed with oxygen-free nitrogen gas for 20 min l^{-1} to obtain anaerobic conditions. Two different substrates were used: (i) Grass silage (DM content of 56.13%), grained to fibrous wool with a blender and (ii) a model substrate which properties resemble natural grass silage in principle (DM ratio adapted from Wiselogel et al. (1996): Carboxymethyl cellulose sodium salt (Fluka, St. Gallen, Schweiz), 16.7%; xylan from Birchwood (Roth, Karlsruhe, Germany), 25.8%; lignin with low sulfonate content (Sigma-Aldrich, St. Louis, Missouri, USA) 7.2% and amylopectin (Roth), 0.5%. 1% DM (w/v) of substrate (i) or (ii) were alternatively introduced to the total reaction volume, which was then digested under mesophilic conditions at 35°C for community and enzymatic analyses or at 45°C for morphological studies using scanning electron microscopy. Batch-cultivation was carried out over a total time period of 6 weeks. Alternatively, 6 fractions á 0.4 g zeolite were introduced to previously described single-stage flow-through reactors of 28 l operating volume (Lebuhn et al., 2008), continuously mono-digesting grass silage at an organic loading rate of 1-2 kg ODM m^{-3} d^{-1} during gradual adjustment of the temperature (1°C d^{-1}) from 37°C to 45°C. The seeding sludge was obtained from fermenters mono-digesting grass silage at mesophilic conditions (Andrade et al., 2009). The zeolite was entrapped in 0.5 mm mesh size polyamide bags (“*in sacco*”).

2.2.3.2 Enzyme activity assay

Xylanase activity was measured after re-incubation of zeolite particles exposed to batch-culture experiments before, using in-activated inoculum sludge as full medium or synthetic medium as control (DIN EN ISO 11734 L47, “Evaluation of the ultimate anaerobic biodegradability of organic compounds in digested sludge”, 1998). Inoculum sludge was in-activated by autoclaving at 121°C for 20 min, heating to 95°C for 5 min, followed by another autoclaving cycle. Re-incubation was carried out at 35°C for up to 62 h. Zeolite particles were rinsed thrice with 1x PBS (phosphate-buffered saline; pH 7.4) before activities were determined. The 3-amino, 5-nitrosalicylic acid (DNS) assay which is based on the quantification of reducing sugars released with DNS was used as described previously by Bailey et al. (1992). The DNS reagent contained (in g l^{-1}): 3,5-dinitrosalicylic acid ($C_7H_4N_2O_7$), 7.48; NaOH, 13.98; sodium potassium tartrate ($C_4H_4KNaO_6 \cdot 4\ H_2O$), 216.1; phenol ($C_6H_6O$), 5.155; sodium metabisulfite ($Na_2O_5S_2$), 5.86. For the determination of xylanase activity, D-(+)-xylose standards were prepared (in mg ml^{-1}): 2.50, 1.25, 0.63, 0.31 and 0.16. Samples and sample blanks contained (in µl): 1% xylan solution, 180; sample, 20; DNS solution, 300. Before adding the DNS solution, samples were incubated at 35°C for 30 min. Sample blanks were not incubated before addition of DNS solution to suppress enzymatic reactions. The photometric absorption was determined at 540 nm in 96 well plates (Greiner, Frickenhausen, Germany) using a plate reader (Tecan Infinite 200M, Männedorf, Switzerland). An enzyme unit is defined as the conversion of 1 µmol substrate per minute, in which 1 U corresponds to 16.67 nanokatals.

2.2.3.3 DNA extraction

The total bacterial community DNA was extracted as described by Martin-Laurent et al. (2001). To collect microorganisms, 1 g of sample material was centrifuged for 15 min at 16,750 g. The pellet was then resuspended in 1 ml of extraction buffer containing (in g l^{-1}): ethylenediaminetetraacetic acid (EDTA), 37.25; NaCl, 5.85; polyvinylpyrrolidone (PVP), 10; Tris-HCl, 12 and 20% (v/v) sodium dodecyl sulphate (SDS), 100 ml l^{-1}. To ensure complete cell lysis, glass beads from 0.15 to 2.00 µm in diameter were added to crush cell structures using FastPrep Instrument (Qbiogene, Heidelberg, Germany) for 2 x 30 s including a cooling step on ice in between for 2 min. After centrifugation for 1 min at 16,750 g, the supernatant was mixed with 5 M

sodium acetate, 100 µl and incubated on ice for 15 min for protein precipitation. Succeeding another centrifugation step for 5 min, an equal volume of chloroform-phenol-isoamylalcohol mixture (15:24:1) was added to the supernatant. Subsequently, the genomic DNA was precipitated by adding an equal volume of ice-cold isopropanol to the upper phase. The precipitated DNA was recovered by centrifugation for 10 min, washed once with 70% (v/v) ethanol and resuspended in a total volume of 50 µl of 10 mM Tris-HCl buffer (pH 8.0). Alternatively a DNA extraction kit for soil samples was used (FastDNA® Spin Kit for Soil, MP Biomedicals, Solon, Ohio, USA) following the manufacturer's recommendations.

2.2.3.4 Polymerase chain reaction (PCR) amplification

Amplification of bacterial 16S rRNA gene fragments was carried out using the eubacterial primer pair Unibac-II-515f (5'-GTG CCA GCA GCC GC-3') and Unibac-II-927rP (5'-CCC GTC AAT TYM TTT GAG TT-3') for an amplicon size of 412 bp according to Lieber et al. (2002). Amplification of archaeal 16S rRNA gene fragments was performed using the primer pair ARC-787f (5'-ATTAG ATACC CSBGT AGTCC-3') and ARC-1059r (5'-GCCAT GCACC WCCTC T-3') for an amplicon size of 273 following Yu et al. (2005), using a Biometra T personal/ gradient system (Biometra, Göttingen, Germany). The reaction mixture was set up on ice and contained: 1x Taq & Go (Qbiogene, Heidelberg, Germany); 3.0 mM $MgCl_2$ (Finnzyme, Espoo, Finland); 0.5 mM forward primer; 0.5 mM reverse primer; 20 ng template DNA (1 to 2 µl) and double deionised H_2O to fill up to a final volume of 20 or 60 µl for template DNA extracted from polyacrylamide SSCP-Gels and template DNA extracted from digestion sludge samples respectively. Negative control PCR contained no template DNA. The cycling conditions for eubacterial templates were as follows: (1) denaturation at 94°C for 4 min, (2) denaturation at 94°C for 20 sec, (3) annealing at 53°C for 30 sec, (4) extension at 72°C for 60 sec, (5) final extension at 72°C for 10 min, (6) hold at 4 °C. Steps (2) till (4) were repeated 30 times. For archaeal templates the annealing temperature was set to 55-50°C (touch down: 0.6°C per cycle). For the purification of PCR generated DNA products, Gene Clean Turbo Kit (Qbiogene, Heidelberg, Germany) was used following the manufacturer's recommendations. For DNA-content determination 1 µl of purified PCR-products were analysed using a micro-volume spectrophotometer for nucleic acid and protein quantitation (NanoDrop 2000, Thermo Fisher Scientific, Wilmington, Delaware, USA).

2.2.3.5 Single strand conformation polymorphism (SSCP) analysis and DNA elution from gel slices

SSCP analysis of amplified bacterial and archaeal *rrs* (16S rRNA gene) fragments was carried out according to Schwieger and Tebbe (1998). For single strand formation 10 µl of purified PCR products, adjusted to 150 ng dsDNA-content were used. Exonuclease digestion was performed with a λ-Exonuclease of 12 U initial concentration (New England Biolabs, Frankfurt, Germany) at 37°C for 1 h, followed by the addition of 50% (v/v) loading buffer (95% deionised formamide, 10 mM NaOH, 0.025% (w/v) bromophenol blue), a denaturation step at 98°C for 3 min and a re-folding step on ice for 5 min. Separation of folded ssDNA was achieved by electrophoresis in 5x Tris-borate-EDTA buffer (TBE) using a polyacrylamide gel (8% for eubacterial DNA, 9% for archaeal DNA) at 26°C for 17 h (archaeal DNA) and 26 h (eubacterial DNA) respectively using a TGGE MAXI system (Biometra). After silver-staining according to Bassam et al. (1991), gels were digitalised using a transillumination scanner. For further characterisation of microbial communities, i.e. sequence analysis, constantly dominant or variably emerging SSCP bands were excised with a scalpel and transferred into 1.5 ml reaction tubes for an incubation time of 12 h at -70°C. For DNA elution from gel slices, a method previously described by Sambrook et al. (1989) was modified. 150 µl sterile elution buffer (0.5 M ammonium acetate, 10 mM magnesium acetate, 1 mM EDTA, 0.1% sodium dodecyl sulphate [SDS], pH 8.0) were added to each gel slice sample and subsequently incubated for 15 min at -70°C, 5 min at 50°C, 5 min at 90°C and finally at 37°C for 3 h with 500 rpm shaking speed (Thermomixer, Eppendorf, Hamburg, Germany). After 3 days of incubation at -20°C, a centrifugation step at 14,500 g and 4°C for 15 min was used to eliminate gel slice debris. 120 µl of the supernatant were taken and mixed with 300 µl 70% ethanol for protein precipitation at -20°C for 3 h. DNA was pelletized by a final centrifugation step at 14,500 g for 30 min, then air dried and dissolved in 20 µl 10 mM Tris-HCl (pH 8.0). Afterwards, eluted DNA was re-amplified using the same primer pairs as for the PCR (2.2.3.4).

2.2.3.6 Computer-assisted cluster analysis

In order to compare SSCP fingerprints of microbial communities, a computer-assisted cluster analysis was carried out using the GelCompar® II software (Applied Math, Kortrijk, Belgium). DNA standards were loaded onto each gel allowing a post-run correction of gel-specific differences between several gel runs using the normalisation function of the GelCompar® II software. After background subtraction and normalisation of digitalised images of the SSCP gels, similarities between the SSCP fingerprints were calculated using the band-based Dice similarity coefficient. Afterwards, the fingerprints were grouped according to their similarity using the hierarchical cluster method: unweighted pairwise grouping method using arithmetic means (UPGMA). Differences between clusters within software generated dendrograms were statistically verified by permutation significance tests.

2.2.3.7 Sequence analysis

About 60 ng of each PCR product from bands excised from PA gels were used for sequencing reactions, which were performed by the ZMF laboratory of the Medical University of Graz (Graz, Austria). To identify similar sequences that are available in the NCBI Genbank, sequences were used in BLASTn searches (Altschul et al., 1997; http://www.ncbi.nlm.nih.gov/blast/).

2.2.3.8 Scanning electron microscopy

The scanning electron microscope (SEM) Zeiss ULTRA 55 was used to investigate zeolite particles with 1.0 to 2.5 mm in diameter. The biological material was imaged with the high efficiency “In-lens SE detector” using secondary electrons (SE), which deliver topographic contrast (Goldstein et al., 2003). Additionally imaging with an angle selective backscattered electron (AsB) detector was performed. It detects backscattered electrons (BSE) and delivers compositional contrast, which is determined by the differences in the local chemical composition of an investigated specimen (Goldstein et al., 2003).. In the case of SE imaging 5 kV acceleration voltage of the primary electrons was applied with the exception of one micrograph which was imaged simultaneously with the AsB detector at an acceleration voltage of 15 kV. Before application fresh samples were fixed in glutaraldehyde (2.5% in 0.1 M phosphate puffer, pH 7.2), dehydrated in a graded ethanol series with a final step in propylene oxide and ultimately dried by lyophilisation (Labconco Freeze Dry System FreeZone 4.5, Kansas City, Missouri, USA) or critical point drying (CO_2; Bal-Tec

CPD, Balzers, Fürstentum Liechtenstein). For observation, prepared samples were mounted on aluminum stubs using double-sided carbon tape and moreover a carbon film was applied onto the specimens' surfaces by high-vacuum evaporation.

2.2.4 Results and Discussion

2.2.4.1 Scanning electron microscopy imaging

For morphological studies, zeolite particles were introduced to batch-cultures fed with model substrate at 45°C in order to allow the colonisation. Scanning electron microscopy (SEM) was chosen to visualise how the surface of zeolite particles is colonised as micro-geographical relief. During batch-wise cultivation over 5 days, rod-shaped microorganisms with dimensions of approximately 0.4 µm in diameter and ranging from 1.6 to > 5.0 µm in length were seen on zeolite particles (figure II-1A-D). For colonisation, cragged and pitted areas where preferred. Coccoid organisms were not seen which is in contrast to previous studies reporting large accumulation of coccoid type microorganisms besides bacillary, filamentous shaped bacteria in the interior of ruggedness and superficial zones of zeolite particles (Fernández et al., 2007). However, these authors investigated digestion of distillery wastewater with pig sludge inoculation in contrast to the model substrate used in this study mimicking the cell wall composition of grass silage. Furthermore, the inoculum used in the present study was well adapted to grass silage as substrate. As a novel aspect, bacteria/archaea-borne fibrous structures could be seen. Two drying methods, i.e. critical point drying (CPD) and lyophilisation were compared regarding the stability of biological structures as cell morphology. There were no significant differences, but fibrous structures were conserved slightly better using CPD. Pilus-like appendages (figure II-1B, D) appeared to reach out from bacterial/archaeal cells directly either to the zeolite's surface or to neighbouring cells. The pili-dimensions were around 45 nm in width and ranging from 300 nm up to 3 µm in length. This would be within the interspecies distance for both, syntrophic oxidation of propionate, ethanol and iso-propanol between methanogenic consortia members (Ishii et al., 2005) and for elongated polycellulosomal protuberance fibres between substrate and the cell surface as described for *Clostridium thermocellum* (Shoham et al., 1999). However, these structures could have different functions: (i) adhesion fibres for attachment, supporting growth and nutrition for substrate-cellulosome-bacteria interactions (Shoham et al., 1999), (ii) conductive nanowires for interspecies

hydrogen or electron transfer like demonstrated for syntrophic co-cultures of hydrogen-consuming methanogenic *Methanothermobacter thermautotrophicus* and propionate-oxidizing *Pelotomaculum thermopropionicum* (Gorby et al., 2006; Ishii et al., 2006; Reguera et al., 2005). (iii) non-conductive nanowires as a foremost structural factor for cell aggregation and biofilm formation as described for pili of metal-reducing bacteria, e.g. *Geobacter sulfurreducens* (Reguera et al., 2007).

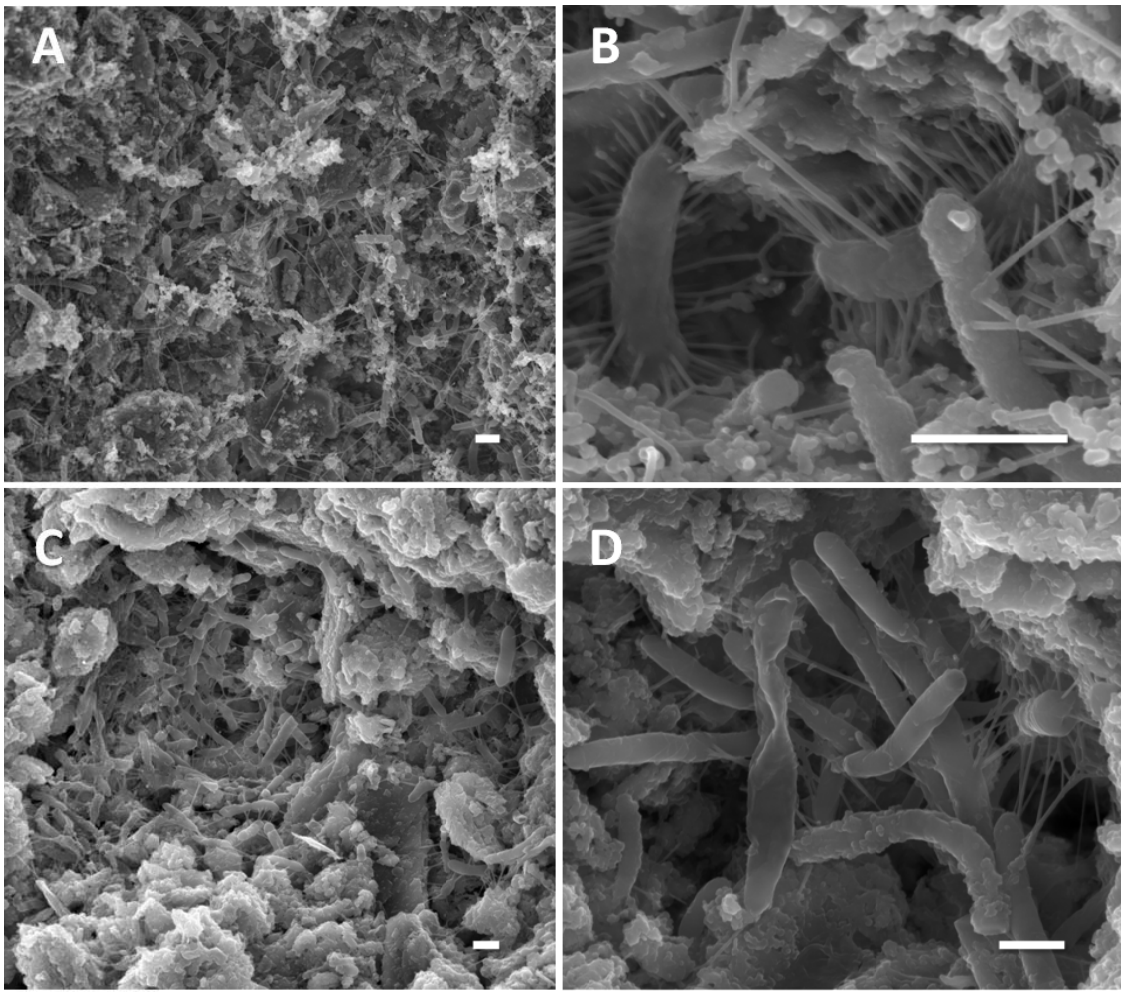

Fig. II-1 SEM images (SE, In-lens detector) of colonised zeolite particles (< 2.5 mm in diameter) after 5 d batch-wise cultivation on a model substrate for grass silage at 45°C. **A** CPD dried zeolite with area-wide biofilm formation. **B** CPD dried zeolite, cells forming fibrous structures. **C** Lyophilised zeolite with biofilm formation mainly in a pit. **D** Lyophilised zeolite, microorganisms colonising a pit. (Bar length: 1 µm).

In a second approach zeolite particles from a continuously operated 28 l single-stage flow-through reactor fed on grass silage were depicted (figure II-2a-d). After a total incubation time of 12 weeks, microorganisms similar in morphology and dimensions

as for batch-wise operated reactors had colonised the surface of zeolite particles. This finding confirms the capability of zeolites to act as a carrier both in batch and in larger scale flow-through disturbed fermentation processes. Micrographs imaged simultaneously using In-lens and AsB detectors at an acceleration voltage of 15 kV showed topographic and compositional contrasts from one sample site in comparison (figure II-2c, d). The compositional contrast gives the opportunity to distinguish between carbon-based biological material (i.e. bacteria/archaea cells) and inorganic matter and thus clearly confirms the biological origin of bacillary and fibrous structures as they disappeared in comparison to the inorganic zeolite background.

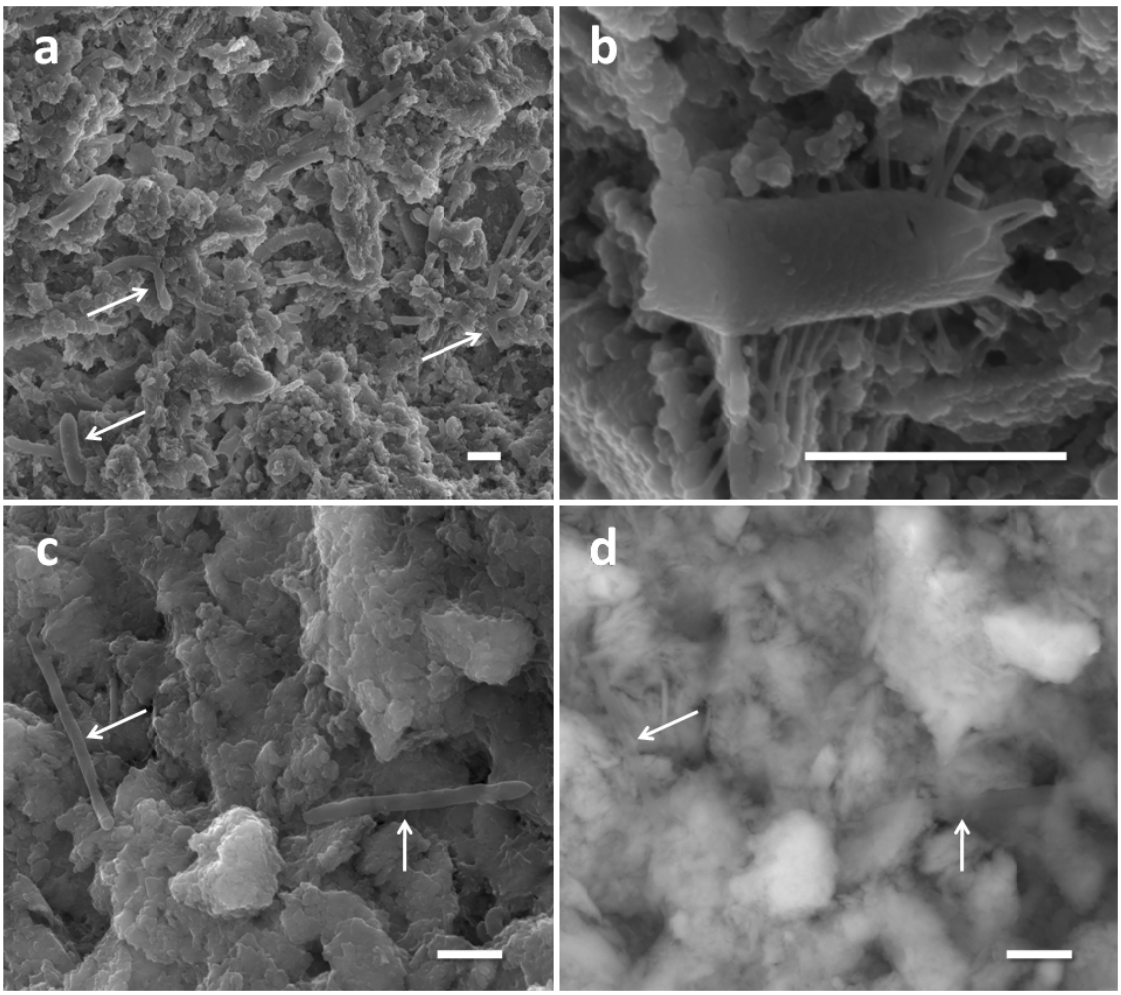

Fig. II-2 SEM images (a, b, c: SE, In-lens detector; d: BSE, AsB detector) of colonised and lyophilised zeolite particles (< 2.5 mm in diameter) after 84 d *in sacco* incubation in continuously operated bioreactors (28 l) fed with grass silage at 45 °C. **a** Zeolite with biofilm formation. **b** Microorganism with fibrous structures on the surface of a zeolite. **c**, **d** Two rod-shaped cells, vanishing when AsB detector is used. (Bar length: 1 µm).

2.2.4.2 Enzymatic activity from colonised zeolites

To investigate functionality of bacterial populations immobilised on zeolite surfaces, the activity of xylanase was determined in zeolite particles taken from batch-cultures fed with model substrate at 35°C. This enzyme is responsible for the hydrolysis of xylan as a major cell wall component of grass silage (Nizami et al., 2009). Furthermore, solubilisation of xylan triggers the accessibility of cellulose (Hendriks and Zeeman, 2009). Plant cell wall polymer degradation should naturally depend on the presence of grass silage fibres. Even so, xylanase activity was detected on zeolite fractions obtained from batch-cultivation on model substrate at 35 °C over 14 d. The pH value was decreasing from 8.7 to 7.6 during this fermentation time. Colonised zeolite particles were then re-incubated in autoclaved fermentation broth as well as in synthetic minimal medium as a control (figure II-3). After 38 h of re-incubation of washed zeolite a maximum xylanase activity of 116 ± 57 U l^{-1} was measured. When washing before re-incubation was omitted, a higher activity of 190 ± 26 U l^{-1} was seen which is most likely due to the release of adsorbed enzymes. In both cases, enzyme activity decreased after 62 h. A considerably lower activity was determined after re-incubation of washed zeolite in minimal medium (25 ± 4 U l^{-1} after 38 h) indicating that xylanase production was related to growth of immobilised microorganisms and probably is induced by medium components (e.g. xylo-oligosaccharides). However, a slight increase in activity over re-incubation time still demonstrates that microbes slowly grew in minimal medium probably utilizing adsorbed biomass as carbon source. In contrast, when zeolite particles were autoclaved too, no significant enzyme activity was observed during re-incubation at 35°C over 62 hours. These findings clearly indicate that hydrolytic microorganisms were adherent to zeolite particles.

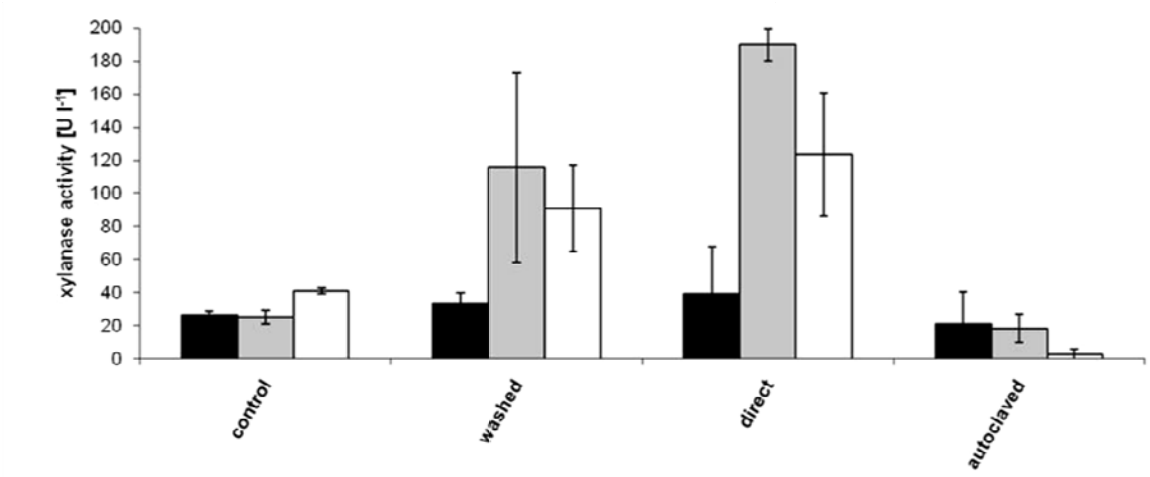

Fig. II-3 Xylanase activity determined after re-incubation of zeolite particles in synthetic minimal medium (control), full medium (washed: carefully rinsed with 1x PBS; direct: not rinsed; autoclaved: inactivated zeolite fraction) for 14 h (black columns), 38 h (grey columns) and 62 h (white columns) at 35°C. Zeolite samples were taken from anaerobic batch-cultivation on model substrate after 14 d at 35°C.

2.2.4.3 Bacteria screening

For further characterisation of microbial populations immobilised on zeolite, PCR-based SSCP-analysis of amplified bacterial *rrs* (16S rRNA gene) fragments was carried out with samples from batch-cultivation on grass silage or model substrate at 35 °C for comparison. Banding profiles from the batch-fermentations clearly formed three major clusters (figure II-4). Bacteria attached to the surface of grass silage fibres formed one cluster with band patterns of > 60% similarity. Bacteria attached to the surface of zeolite particles formed a second cluster with a similarity of > 66%, combining samples from incubation upon model substrate and grass silage. This cluster was separated distinctively ($P < 0.01$) from grass silage surfaces, as indicated by a similarity value of only 7%. A third cluster was formed by the supernatant samples regardless of the substrates used. Here the homologous band patterns were forming an exclusive cluster at a similarity of > 82%, which is significantly differing ($P < 0.01$) from both surface generated clusters. These findings suggest that different sample sites are colonised by distinct bacterial populations. Functional populations developed on zeolites, producing the hemicelluloses degrading enzyme xylanase, were different from populations in the liquid phase and from those present on grass silage fibres. Thus, zeolites are not only providing more surface as support, but

obviously allow the development of specific functional populations which are essential in the biogas process (e.g. hemicellulase producers).

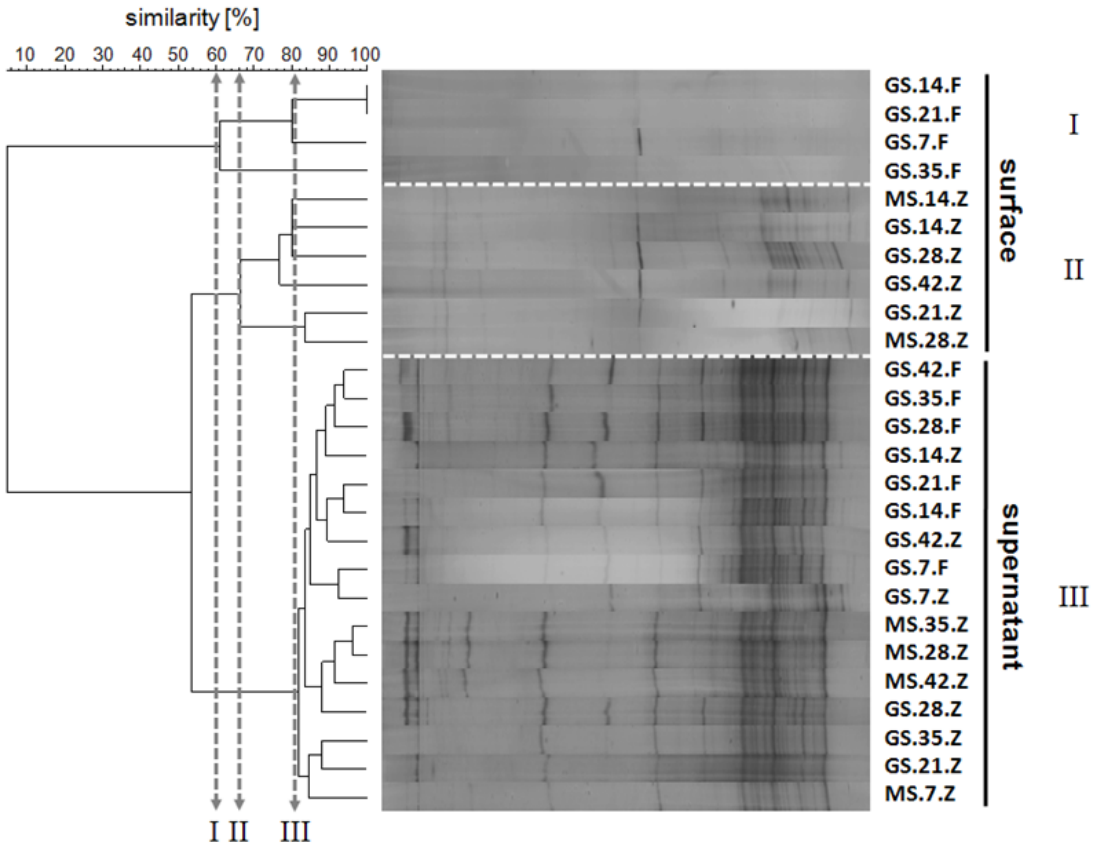

Fig. II-4 Dendrogram based on SSCP separated *rrs* (16S rRNA) amplicons of batch-cultures fed with grass silage or model substrate for comparison. Band patterns were grouped by UPGMA. Double-headed vertical arrows indicate the similarity for the groupings. The dendrogram reveals three major clusters depending on the sample site: (I) surface of grass silage fibres, (II) surface of zeolite particles and (III) supernatant samples forming one cluster. Sample code: sample site; batch-identity (MS = model substrate, GS = grass silage, 7-42 = fermentation time in days, F = grass silage fibres, Z = zeolite).

Sequence analysis of DNA extracted from single bands representing specific species was then used for further analysis of community members (Schwieger and Tebbe, 1998). Databank searches with obtained sequences (in total 44 reads) foremost led to entries for uncultured bacteria. Bands chosen for sequencing analyses are labelled in figure II-5. Top hits found for surface sample sequences (bands 9, 13 and 13b) were typical for fermentation processes (FN436026, CU919914, FN436026). Amongst them were bacteria sequences from thermophilic methanogenic sludge

(AB530683) that match ours with 98% identity (band 2) and sequences from uncultured bacteria of the class Thermotogae (CU924654). After 28 d of fermentation, the populations on zeolite surfaces where affiliated with the phylum Bacteroidetes, i.e. *Ruminofilibacter xylanolyticum* (DQ141183, EU551120) within the family Rikenellaceae with 98% identity (band 7). This band also appeared from surface samples of grass silage fibres (band 7b). After 42 d of fermentation, the close relationship to *Ruminofilibacter xylanolyticum* was confirmed with an identity value of 99%. This species has been isolated from the rumen in other studies where growth of *Ruminococcus* spp. and other bacteria with cellulolytic, pectinolytic and hemicellulolytic activities (*Bacteroides* spp. and *Clostridium* spp.) was increased by high levels of dietary fibre (Metzler and Mosenthin, 2008). In addition, *R. xylanolyticum* was also found in a production-scale biogas plant fed with maize silage, green rye and liquid manure (Kröber et al., 2009).

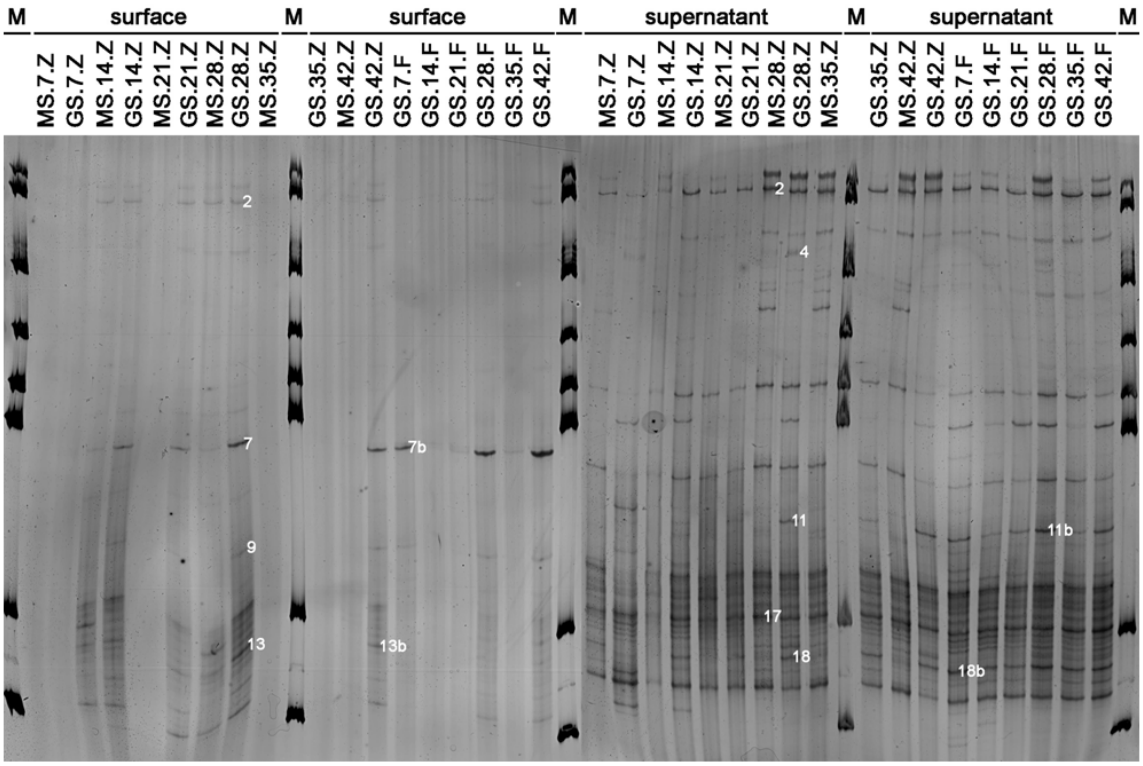

Fig. II-5 Non-denaturating polyacrylamide gel from the SSCP analysis of batch-cultures fed with grass silage or model substrate for comparison based on bacterial *rrs* (16S rRNA gene) fragments. Sample code: M, 1 kb DNA-ladder marker lanes; sample site; batch-identity (MS = model substrate, GS = grass silage, 7-42 = fermentation time in days, F = grass silage fibres, Z = zeolite).

In the present study, there were multiple hits for two bands (2 and 17) of supernatant samples from batch-cultures fed with model substrate. These were similar to a sequence from an uncultured bacterium found in a large-scale thermophilic municipal biogas plant (EU878320) and to sequences from thermophilic anaerobic solid biowaste digestors (AM947527, EF558972) with identity values of 97%. Furthermore, there were again affiliations to Thermotogae (CU918433) and to an uncultured member of the class Bacteroidetes (CU919517) with 98% identity. In contrast, sequence of band 4 from grass silage batch-culture supernatant after 28 days of fermentation revealed a relationship to the phylum Firmicutes, i.e. *Bacillus* sp. (AF548884) with 97% identity. Sequences obtained from bands 11, 11b, 18 and 18b were moderately similar (92% identity) to uncultured *rrs* (16S rRNA gene) sequences from bacterial community analyses of mesophilic bioreactors (FJ825461), cassava pulp and pig manure co-digestion (GQ458213) and bacteria associated with the leachate of a closed municipal solid waste landfill (AJ853654).

2.2.4.4 Archaea screening

The second important taxonomic group investigated was the domain of archaea. Members of this domain are responsible for methanogenesis. PCR-based SSCP-analysis of amplified archaeal *rrs* (16S rRNA) fragments was carried out with samples from batch-cultivation on grass silage or model substrate at 35°C for comparison. Amplicons were obtained for supernatants and zeolite surfaces, but not for grass silage fibres surfaces. SSCP analysis revealed two foremost double-banded pattern fields (figure 4), in which the upper one was intense in samples from zeolite surfaces over the total fermentation time (7 to 42 days), utilising model substrate. Here, bands 1 and 2 were excised for sequencing analysis. In contrast, supernatants from the same batch-cultures showed less intense bands in this field, but slightly stronger double-bands in the lower area. Supernatants from batch-cultures fed with grass silage (right side in figure II-6) showed a weakening of bands in the upper field from day 21 on (bands 1b and 2b were excised). Possibly the corresponding archaea were diminished, eventually outcompeted by the archaea corresponding to the lower bands which apparently increased (see below), or they moved from the supernatant to the zeolite's surface. However, zeolite surfaces appeared to be suitable for colonisation by methanogenic archaea (see below).

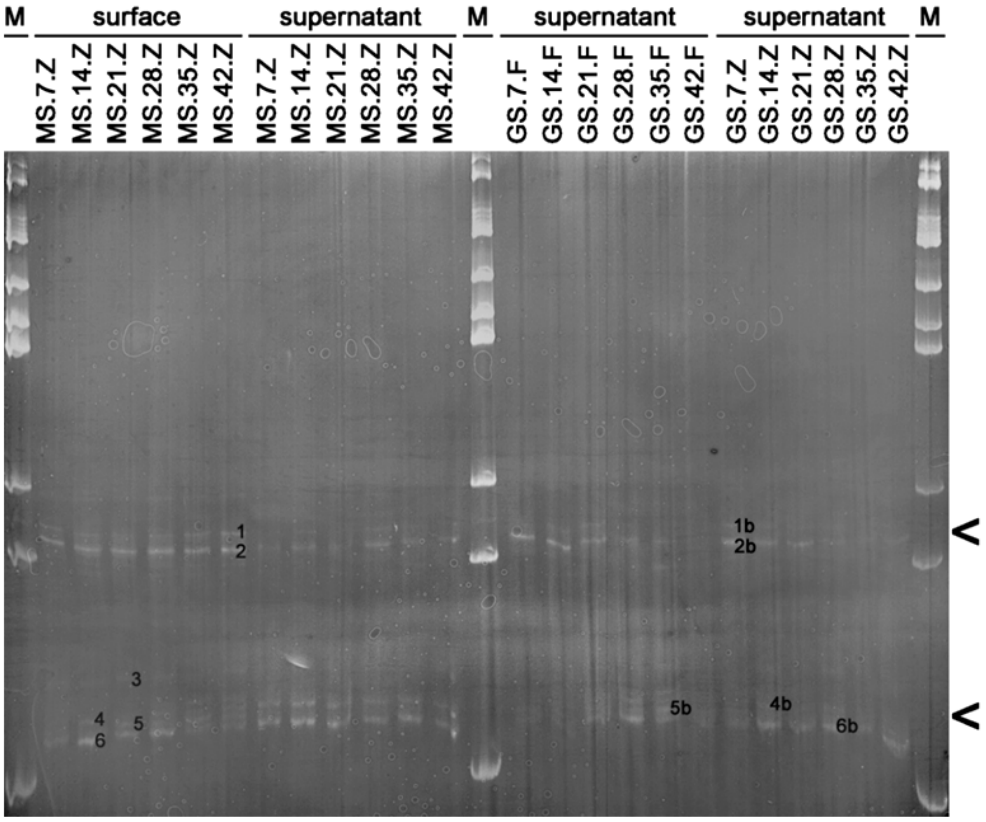

Fig. II-6 Non-denaturating polyacrylamide gel from the SSCP analysis of batch-cultures fed with grass silage or model substrate for comparison based on archaeal *rrs* (16S rRNA gene) fragments. Sample code: M, 1 kb DNA-ladder marker lanes; sample site; batch-identity (MS = model substrate, GS = grass silage, 7-42 = fermentation time in days, F = grass silage fibres, Z = zeolite).

Bands appearing from samples of zeolite surfaces incubated at 35°C in batch-cultures fed with model-substrate (bands 1 to 6 in figure II-6) were most similar to uncultured *rrs* (16S rRNA gene) sequences from archaeal community analyses of anaerobic digestion in biogas digesters (AB479397, DQ262609, FJ205782, HM066950) with 89% to 99% identity. Bands marked with 1 and 2 were present in all batch-cultures regardless of the substrate used. Sequences of band 1 affiliated with Methanomicrobiales (AB479397) with 94% identity. The amplicon of band 2 was moderately similar (89% identity) to *Methanosarcina barkeri* (AF028692) within the order Methanosarcinales. *M. barkeri*, known for its metabolic diversity, is able to use methanol, H_2/CO_2 and acetate for methanogenesis (Meurer et al., 2002). Furthermore, *Methanosarcina* spp. were previously identified to be part of the predominant genera on zeolite surfaces (Fernández et al., 2007). Band 5 appeared at day 21 of cultivation on model substrate and grass silage. Sequences were most similar to *Methanoculleus* sp. (AF107105, AJ550158) and *M. bourgensis* (AY196674, DQ150254) with moderate identity values of 91% indicating the presence of the order

Methanomicrobiales. However, members of the genus *Methanoculleus* spp. were to be found the dominant archaea in the methanogenic microbial community of an agricultural biogas plant (Kröber et al., 2009). Certain representatives of the order Methanomicrobiales (obligatory hydrogenotrophic), were recently proposed to be useful as bio-indicators for process disturbance through acidification in methanogenesis (Lebuhn et al., 2009). Sequences from supernatant samples of batch-cultures fed with grass silage (bands 1b to 6b in figure II-6) were most related to databank entries originating from biogas production (AB494258, FJ205785, HM066955) and included origins such as landfill sites and composting processes (AB541745, AJ576208, AY062220) with identity values of 94% to 99%. Amplicons of bands 4b to 6b which appeared later (at day 14, 28 and 35) were most similar to *Methanoculleus* spp. (AF107103, AF107106, AJ550158) with identity values of 97% and 94%, respectively.

2.2.5 Conclusion

Colonisation of clinoptilolite particles by microorganisms was demonstrated, revealing spontaneous adhesion to preferentially sheltered areas as pits. The microbial abundance ranged from single cells to dense biofilm-like aggregations on the cratered zeolite's surface. Two dominant cell morphologies were observed, i.e. long rod-shaped and shorter bacillus-like types. Colonies adherent to zeolite surfaces were composed of bacterial representatives with confirmed hemicellulolytical activity and methanogenic archaea known to be predominant in biogas-producing communities. This neighbouring existence argues for a syntrophic relationship between members of both domains, naturally co-cultured and spontaneously co-aggregated on zeolite as an exclusive operational environment in the biogas production process.

2.2.6 Acknowledgement

This work has been founded by the Austrian Research Promotion Agency (FFG) and IPUS GmbH. The authors would like to send many thanks to contributors of the Bavarian State Research Center for Agriculture and the Center for Medical Research at the Medical University of Graz. Special thanks go to Ph.D Elisabeth Ingolic and Claudia Mayerhofer (Institute for Electron Microscopy, Graz University) for kindly providing technical assistance.

2.2.7 References

Alonso-Vicario, A., Ochoa-Gómez, J. R., Gil-Río, S., Gómez-Jiménez-Aberasturi, O., Ramírez-López, C. A., Torrecilla-Soria, J. and Domínguez, A. (2010) Purification and upgrading of biogas by pressure swing adsorption on synthetic and natural zeolites. *Microporous and Mesoporous Materials* **134** (1-3), 100-107.

Altschul, S.F., Madden, T.L., Schaffer, A.A., Zhang, J.H., Zhang, Z., Miller, W. and Lipman, D.J. (1997) Gapped BLAST and PSI-BLAST: a new generation of protein database search programs. *Nucleic Acids Research* **25** (17), 3389-3402.

Andrade, D., Marin-Perez, C., Heuwinkel, H., Lebuhn, M. and Gronauer, A. (2009) Biogasgewinnung aus Grassilage: Untersuchungen zur Prozessstabilität. *1st International Congress on Biogas Science*. Erding, *LfL-Schriftenreihe, Proceedings* **16** (3), 529-538.

Bailey, M.J., Biely, P. and Poutanen, K. (1992) Interlaboratory testing of methods for assay of xylanase activity. *Journal of Biotechnology* **23** (3), 257-270.

Bassam, B.J., Caetanoanolles, G. and Gresshoff, P.M. (1991) Fast and sensitive silver staining of DNA in polyacrylamide gels. *Analytical Biochemistry* **196** (1), 80-83.

Fernández, N., Montalvo, S., Fernández-Polanco, F., Guerrero, L., Cortés, I., Borja, R., Sánchez, E. and Travieso, L. (2007) Real evidence about zeolite as microorganisms immobilizer in anaerobic fluidized bed reactors. *Process Biochemistry* **42** (4), 721-728.

Gerin, P.A., Vliegen, F. and Jossart, J.M. (2008) Energy and CO_2 balance of maize and grass as energy crops for anaerobic digestion. *Bioresource Technology* **99** (7), 2620-2627.

Goldstein, J.I., Newbury, D.E., Echlin, P., Joy, D.C., Lyman, C.E., Lifshin, E., Sawyer, L. and Michael, J.R. (2003) Electron Beam-Specimen Interactions – imaging signals from the interaction volume. In: Goldstein, J.I. and Newbury, D.E. (eds.) Kluwer Academic/Plenum, New York. *Scanning Electron Microscopy and X-Ray Microanalysis 3. Edition*, 75-97.

Gorby, Y.A., Yanina, S., Mclean, J.S., Rosso, K.M., Moyles, D., Dohnalkova, A., Beveridge, T.J., Chang, I.S., Kim, B.H., Kim, K.S., Culley, D.E., Reed, S.B., Romine, M.F., Saffarini, D.A., Hill, E.A., Shi, L., Elias, D.A., Kennedy, D.W., Pinchuk, G., Watanabe, K., Ishii, S., Logan, B., Nealson, K.H. and Fredrickson, J.K. (2006) Electrically conductive bacterial nanowires produced by *Shewanella oneidensis* strain MR-1 and other microorganisms. *Proceedings of the National Academy of Sciences*, USA **103** (30), 11358-11363.

Hendriks, A.T.W.M. and Zeeman, G. (2009) Pretreatments to enhance the digestibility of lignocellulosic biomass. *Bioresource Technology* **100** (1), 10-18.

Holper, J., Lesjak, M., Heinzel, U., Boos, B., (2005) Zeolith in der Biogasgewinnung. Sonn. 05450052.5 [EP 1 577 269 A1], Patent Styria, Austria.

Ishii, S., Kosaka, T., Hori, K., Hotta, Y. and Watanabe, K, (2005) Coaggregation facilitates interspecies hydrogen transfer between *Pelotomaculum thermopropionicum* and *Methanothermobacter thermautotrophicus*. *Applied Environmental Microbiology* **71** (12), 7838-7845.

Ishii, S., Kosaka, T., Hotta, Y. and Watanabe, K. (2006) Simulating the contribution of coaggregation to interspecies hydrogen fluxes in syntrophic methanogenic consortia. *Applied Environmental Microbiology* **72** (7), 5093-5096.

Kröber, M., Bekel, T., Diaz, N.N., Goesmann, A., Jaenicke, S., Krause, L., Miller, D., Runte, K.J., Viehöver, P., Pühler, A. and Schlüter, A. (2009) Phylogenetic characterization of a biogas plant microbial community integrating clone library 16S-rRNA sequences and metagenome sequence data obtained by 454-pyrosequencing. *Journal of Biotechnology* **142** (1), 38-49.

Lebuhn, M., Bauer, C., Munk, B. and Gronauer, A. (2009) Methanogenic population dynamics during acidification. *1st International Congress on Biogas Science*. Erding, *LfL-Schriftenreihe, Proceedings* **16** (2), 319-332.

Lebuhn, M., Liu, F., Heuwinkel, H. and Gronauer, A. (2008) Biogas production from mono-digestion of maize silage-long-term process stability and requirements. *Water Science Technology* **58** (8), 1645-1651.

Lehtomäki, A., Huttunen, S., Lehtinen, T.M. and Rintala, J.A. (2008) Anaerobic digestion of grass silage in batch leach bed processes for methane production. *Bioresource Technology* **99** (8), 3267-3278.

Lieber, A., Kiesel, B. and Babel, W. (2002) Microbial diversity analysis of soil by SSCP fingerprinting technique using TGGE Maxi System. In: Merbach, W., Hütsch, B.W. and Augustin, J. (eds.), Teubner, Stuttgart. *Ökophysiologie des Wurzelraumes*, 61-65.

Martin-Laurent, F., Philippot, L., Hallet, S., Chaussod, R., Germon, J.C., Soulas, G. and Catroux, G. (2001) DNA extraction from soils: old bias for new microbial diversity analysis methods. *Applied and Environmental Microbiology* **67** (5), 2354-2359.

Metzler, B.U. and Mosenthin, R. (2008) A review of interactions between dietary fiber and the gastrointestinal microbiota and their consequences on intestinal phosphorus metabolism in growing pigs. *Asian-Australasian Journal of Animal Sciences* **21** (4), 603-615.

Milán, Z., Villa, P., Sánchez, S., Montalvo, S., Borja, R., Ilangovan, K. and Briones, R. (2003) Effect of natural and modified zeolite addition on anaerobic digestion of piggery waste. *Water Science Technology* **48** (6), 263-269.

Montalvo, S., Díaz, F., Guerrero, L., Sánchez, E. and Borja, R. (2005) Effect of particle size and doses of zeolite addition on anaerobic digestion processes of synthetic and piggery wastes. *Process Biochemistry* **40** (3-4), 1475-1481.

Murray, W.D. and van den Berg, L. (1981) Effect of support material on the development of microbial fixed films converting acetic acid to methane. *Journal of Applied Bacteriology* **51** (2), 257-265.

Pande, D.R. and Fabiani, C. (1989) Feasibility studies on the use of a naturally occurring molecular sieve for methane enrichment from biogas. *Gas Separation and Purification* **3** (3), 143-147.

Prochnow, A., Heiermann, M., Plöchl, M., Linke, B., Idler, C., Amon, T. and Hobbs, P.J. (2009) Bioenergy from permanent grassland – a review: 1. Biogas. *Bioresource Technology* **100** (21), 4931-4944.

Reguera, G., McCarthy, K.D., Mehta, T., Nicoll, J.S., Tuominen, M.T. and Lovley, D.R. (2005) Extracellular electron transfer via microbial nanowires. *Nature* **435** (7045), 1098-1101.

Reguera, G., Pollina, R.B., Nicoll, J.S. and Lovley, D.R. (2007) Possible nonconductive role of *Geobacter sulfurreducens* pilus nanowires in biofilm formation. *Journal of Bacteriology* **189** (5), 2125-2127.

Rösch, C., Raab, K., Sharka, J. and Stelzer, V. (2007) Sustainability of bioenergy production from grassland concept - indicators and results. *15th European Biomass Conference and Exhibition*, Berlin, *European Travel Commission, Renewable Energies, Proceedings*, 2658-62.

Sambrook, J.E., Fritsch, E.F. and Maniatis,T. (1989) Gel electrophoresis of DNA and pulsed-field agarose gel electrophoresis – isolation of DNA fragments from polyacrylamide gels. In: Sambrook, J.E., Fritsch, E.F. and Maniatis,T. (eds.), Cold Spring Harbor, New York. *Molecular cloning: a laboratory manual 2. Edition*, 551-555.

Schwieger, F. and Tebbe, C.C. (1998) A new approach to utilise PCR-single-strand-conformation polymorphism for 16S rRNA gene-based microbial community analysis. *Applied and Environmental Microbiology* **64** (12), 4870-4876.

Shoham, Y., Lamed, R. and Bayer, E.A. (1999) The cellulosome concept as an efficient microbial strategy for the degradation of insoluble polysaccharides. *Trends in Microbiology* **7** (7), 275-281.

Turan, M., Gulsen, H. and Çelik, M.S. (2005) Treatment of landfill leachate by a combined anaerobic fluidized bed and zeolite column system. *Journal of Environmental Engineering* **131** (5), 818-819.

Weiß, S., Tauber, M., Somitsch, W., Meincke, R., Müller, H., Berg, G. and Guebitz,G.M. (2010) Enhancement of biogas production by addition of hemicellulolytic bacteria immobilised on activated zeolite. *Water Research* **44** (6), 1970-1980.

Wiselogel, A., Tyson, S. and Johnson, D. (1996) Biomass feedstock resources and composition. In: Wyman, C.E. (ed.), *Handbook on Bioethanol: Production and Utilization*. Taylor and Francis, Washington, DC, 105-118.

Yu, Y., Lee, C., Kim, J. and Hwang, S. (2005) Group-specific primer and probe sets to detect methanogenic communities using quantitative real-time polymerase chain reaction. *Biotechnology and Bioengineering* **89** (6), 670-679.

2.3 Activated clinoptilolite migulators – bioresponsive carriers for microorganisms in anaerobic digestion processes?

Weiß, S.[1], Lebuhn, M.[2], Andrade, D.[2], Zankel, A.[3], Cardinale, M.[1], Birner-Gruenberger, R.[4], Somitsch, W.[5], Ueberbacher, B.J.[6] and Guebitz, G.M.[1]

[1]Institute of Environmental Biotechnology, Graz University of Technology, Petersgasse 12, 8010 Graz, Austria; [2]Bavarian State Research Center for Agriculture, Vöttinger Straße 38, 85354 Freising, Germany; [3]Institute for Electron Microscopy, Graz University of Technology, Steyrergasse 17, 8010 Graz, Austria; [4]Proteomics Core Facility, Center for Medical Research and Institute of Pathology, Medical University of Graz, Stiftingtalstrasse 24, A-8010 Graz, Austria; [5]Engineering Consultant, Wiedner Hauptstrasse 90/2/19, 1050 Vienna, Austria; [6]IPUS Mineral- & Umwelttechnologie GmbH, Werksgasse 281, 8786 Rottenmann, Austria

(Applied Microbiology and Biotechnology, *under review* 08.07.2012)

2.3.1 Abstract

Plant cell structures represent a barrier in the biodegradation process to produce biogas for combustion and energy production. Consequently, approaches concerning a more efficient de-polymerisation of cellulose and hemicellulose to monomeric sugars are required. Here we show that natural activated clinoptilolites (i.e. trace metal activated clinoptilolites) represent eminently suitable mineral microhabitats and potential carriers for immobilisation of microorganisms responsible for anaerobic hydrolysis of biopolymers stabilising related bacterial and methanogenic communities. A strategy for comprehensive analysis of immobilised anaerobic populations was developed, that includes the visualisation of biofilm formation via scanning electron microscopy (SEM) and confocal laser-scanning microscopy (CLSM), community and fingerprint analysis as well as enzyme activity and identification analyses. Using SDS polyacrylamide gel electrophoresis hydrolytical active protein bands were traced by congo red staining. Liquid chromatography/ mass spectroscopy (LC-MS) revealed cellulolytical endo- /exoglucanase (exocellobiohydrolase) and hemicellulolytical xylanase/mannase after proteolytic digestion. Relations to hydrolytic/fermentative clinoptilolite colonisers were obtained by using single strand conformation polymorphism analysis (SSCP) based on amplification of bacterial and archaeal 16S rRNA fragments. Thus, species of the genera *Clostridium*, *Pseudomonas*, *Bacillus*, *Dysgenomonas* were identified. Amongst methanogenic colonisers, *Methanoculleus* spp. was dominant.

The specific immobilisation on natural clinoptilolites with functional microbes already colonising naturally during the fermentation offers a strategy to systematically supply the biogas formation process responsive to population dynamics and process requirements through this mineral bioregulators, so called migulators.

2.3.2 Introduction

In order to stabilise and optimise biogas formation from energy plants several approaches were investigated to avoid unfavourable acidification, ammonia accumulation etc. decreasing the production of methane. Adequate availability of essential trace elements for the bacterial community was identified to be essential (Takashima and Speece 1989; Goodwin 1990). Pobeheim (2010a) showed that the addition of mixed trace elements increased methane yields by up to 30% in batch digestion of maize silage. Furthermore, effective removal of volatile solids (around 73%) has been reported for maize silage operated completely stirred tank reactors (CSTR), when higher concentrated solutions of trace metals were added (Bougrier 2011). Enhancement of methane production (up to 20%), was also observed for Co and Ni addition which was corroborated by risen cofactor F_{420} activities and dominance of hydrogenotrophic *Methanoculleus* sp. (Pobeheim 2010b). The importance of Co, Se and other trace metals was also observed for stable food waste digestion. Here, the accumulation of volatile fatty acids (VFAs) can only be avoided, when digesters are supplemented with a certain concentration of Se, Mo, Co and W (Banks 2012).

Activated clinoptilolite zeolites as used in this study combine trace metal activation on the surface with an high ion-exchange capacity for supplementation with cationic macro-elements such as Na^+, K^+, Mg^{2+} or Ca^{2+} and trace elements as well, that clinoptilolites can be loaded with. Consequently, these materials potentially provide an excellent operational environment for microorganisms participating either in the biomass hydrolysis or methane formation process (Holper 2005). They are available on the market under the name ‘migulator’, derived from ‘mineral bioregulator’. Recent studies demonstrated the capability of these clinoptilolites to be colonised by certain microbial populations during anaerobic batch-wise cultivation and laboratory-scaled mono-grass silage or vinasses operated bioreactors (Weiß 2011; Fernández 2007). Furthermore, it was shown that a certain functional microbial group, obtained by

selective cultivation, can be immobilised on clinoptilolite surfaces. Functional populations can provide a specific enzymatic activity as addition to the natural consortium activities, e.g. hydrolytic activity to increase recalcitrant biomass degradation (plant cell walls) and thus result in higher methane yields in batch-culture experiments as demonstrated before (Weiß 2010). This effect could not be seen with enzymatic treatment alone as reported by Bruni (2010) applying commercially available laccases or mixture of cellulases and hemicellulases to digested biofibres. Consequently, there is strong need to identify clinoptilolite immobilised organisms and their enzymes in order to exploit this unique system to improve biogas formation. Here, we show that a combination of sophisticated microscopic (CLSM-FISH, SEM), genetic (SSCP) and biochemical (LC-MS Protein identification) methods can lead to a comprehensive mechanistic understanding of the function of clinoptilolite immobilised anaerobic populations.

2.3.3 Materials and Methods

2.3.3.1 Semi-continuous and batch cultivation

The activated clinoptilolite migulator used (IPUS GmbH, Rottenmann, Austria) consisted of a natural zeolitic tuff containing > 85% clinoptilolite, which was crushed to a grain size below 2.5 mm. The material was loaded with Fe, Ni, Co, Mo, Se, Cu and Zn as trace metal elements to enhance microbial activity (Holper et al., 2005). Powderous particles of < 100 µm size provided by IPUS were introduced to batch experiments (0.01 g ml^{-1}) using *in situ* concentrate bags (6.75 cm x 12 cm; Ankom, Macedon, NY, USA) to apply an *in sacco* incubation during batch-cultivation. Activated clinoptilolite migulator particles of 1.0 to 2.5 mm size were entrapped in 0.5 mm mesh size polyamide bags in 6 fractions á 0.4 g in order to apply an *in sacco* incubation during single-stage flow-through mono-digestion of grass silage in bioreactors of 28 l operating volume (Lebuhn et al., 2008). Organic loading rates ranged from 1 to 2 kg ODM m^{-3} d^{-1} after slow adjustment of the temperature (1°C d^{-1}) to 45°C. Clinoptilolite sample fractions were collected after 7, 14, 21, 42 and 84 days.

Batch-cultivation was carried out in 1000 ml ground flasks with a total volume of 500 ml of seeding sludge, which was obtained from fermenters long-term mono-digesting grass silage (360 d) at increasing organic loading rates of 0.5-3.0 kg ODM m^{-3} d^{-1} and mesophilic conditions (Wichern et al., 2009). Before use, the

sludge was flushed with oxygen-free nitrogen gas for 20 min l^{-1} to obtain anaerobic conditions. Two different substrates were used for cultivation: (i) Grass silage (DM content of 56.13%), grained to fibrous wool with a blender and (ii) a soluble model substrate resembling natural grass silage (Weiß et al., 2011). Re-activation of collected clinoptilolites after batch-wise cultivation for 6 weeks and long-term storage at 4°C was then carried out in mineral salt medium, which had the following composition in [mg l^{-1}]: $MgSO_4 \cdot 7H_2O$, 9.4; $CaSO_4 \cdot 2H_2O$, 4.7; $Na_2HPO_4 \cdot 2H_2O$, 752; KH_2PO_4, 63.92; NH_4CL, 18.8. After mixing, 0.47 ml trace element solution was added and pH adjusted to 7.2 by using 1 M HCl. Trace element solution was composed of [mg l^{-1}]: $Na_2EDTA \cdot 2H_2O$, 2740; $ZnSO_4 \cdot 7H_2O$, 100; $MnCl_2 \cdot 4H_2O$, 25.6; H_3BO_3, 300; $CoCl_2 \cdot 6H_2O$, 200; $CuCl_2 \cdot 2H_2O$, 10; $NiCl_2 \cdot 2H_2O$, 20; $Na_2MO_4 \cdot 2H_2O$, 900; $Na_2SeO_3 \cdot 5H_2O$, 30.4; $FeSO_4 \cdot 7H_2O$, 1000. In order to induce production of hydrolytic enzymes,, the following model substrate was added fed-batch-wise to the mineral salt medium in a concentration of 1% DM (w/v): microcrystalline cellulose (in-house production), 30%; xylan from Birchwood (Roth, Karlsruhe, Germany), 50%; lignin with low sulfonate content (Sigma-Aldrich, St. Louis, Missouri, USA), 14.5%, pectin C (Roth), 0.5% and starch (Roth), 5%. The re-activation experiment was carried out over a total period of 55 days at temperatures according to the former batch-cultivation experiments, i.e. 35°C and 45°C respectively. Samples were taken as duplicates at regular intervals.

2.3.3.2 PCR-based SSCP and sequencing analysis

The total bacterial community DNA was extracted by using a DNA extraction kit for soil samples (FastDNA® Spin Kit for Soil, MP Biomedicals, Solon, Ohio, USA) following the manufacturer's recommendations. To collect free microorganisms, 1 ml of sample supernatant was centrifuged for 15 min at 16,750 g. To collect clinoptilolite-immobilised microorganisms, 0.1 g of clinoptilolite was rinsed three times with 500 µl of 1x PBS (pH 8.0) before applying the DNA extraction procedure. Amplification of bacterial 16S rRNA gene fragments was carried out using the eubacterial primer pair Unibac-II-515f (5'-GTG CCA GCA GCC GC-3') and Unibac-II-927rP (5'-CCC GTC AAT TYM TTT GAG TT-3') for an amplicon size of 412 bp according to Lieber et al. (2002). Amplification of archaeal 16S rRNA gene fragments was performed using the primer pair ARC-787f (5'-ATTAG ATACC CSBGT AGTCC-3') and ARC-1059r (5'-GCCAT GCACC WCCTC T-3') for an amplicon size of 273 following Yu et al. (2005),

using a Biometra T personal/ gradient system (Biometra, Göttingen, Germany). After purification of PCR generated DNA products using the Gene Clean Turbo Kit (Qbiogene, Heidelberg, Germany) following the manufacturer's recommendations, DNA-content was determined before SSCP analysis. Therefore, 1 µl of purified PCR-products were analysed using a micro-volume spectrophotometer for nucleic acid and protein quantitation (NanoDrop 2000, Thermo Fisher Scientific, Wilmington, Delaware, USA). SSCP analysis of amplified bacterial and archaeal *rrs* (16S rRNA gene) fragments was carried out according to Schwieger and Tebbe (1998). For single strand formation 10 µl of purified PCR products containing 150 ng of dsDNA were used to generate comparable bacterial and archaeal fingerprints after λ-Exonuclease digestion. Eluted DNA from PA gel bands was re-amplified using the same primer pairs as for the initial PCR using the same primers. PCR products from re-amplification of bands excised from PA gels were used for sequencing reactions after adjusting the total DNA concentration to 2 ng μl^{-1}. Sequencing analyses were performed by Eurofins MWG Operon (Ebersberg, Germany). To identify similar sequences that are available in the NCBI Genbank, sequences were used in BLASTn searches (Altschul et al., 1997; http://www.ncbi.nlm.nih.gov/blast/). Database hits with minimum 95% sequence identity were considered for discussion.

2.3.3.3 Enzyme activity assay

Enzyme activity, i.e. cellulase, pectinase and xylanase were measured using a 3-amino,5-nitrosalicylic acid (DNS) assay which is based on the quantification of reducing sugars released with DNS according to Bailey et al. (1992). Samples were collected at two different sample sites: (i) liquid phase, for determination of extracellular enzymes a sample volume of 1 ml was centrifuged (13,000 g for 5 min) and supernatants used; (ii) pellet, for determination of cell-bound enzymes of clinoptilolite-immobilised microorganisms a sample volume of 1 ml was centrifuged, the pellet collected and two times rinsed with 1x PBS, before it was resuspended in 500 µl of 1x PBS (pH 8.0). The resuspension was achieved by gently using the pipet tip (a) or treating the pellet with glass beads (0.15 to 2.00 µm) for 40 sec. using a FastPrep Instrument (Qbiogene, Heidelberg, Germany) to ensure complete detachment of clinoptilolite-immobilised bacteria cells (b). The different sample fractions were then incubated at 50°C for 10 min in the presence of a substrate solution containing 1% (w/v) carboxymethylcellulose (Fluka, St. Gallen, Switzerland),

polygalacturonic acid (Fluka) or xylan from birchwood (Roth) in an adjusted pH range of 6.0 to 6.5 by using potassium phosphate buffer. The photometric absorption was determined at 530/540 nm in 96 well plates (Greiner, Frickenhausen, Germany) using a plate reader (Tecan Infinite 200M, Männedorf, Switzerland). Enzyme activity is given as units of enzyme activity per litre ($U\ l^{-1}$). An enzyme unit is defined as conversion of 1 µmol reduced sugar (D-glucose, D-galacturonic acid or D-xylose) per minute under the given conditions above. 1 U corresponds to 16.67 nanokatals.

2.3.3.4 SDS-PA-Gel analysis

For protein separation SDS-PAGE was performed in 10% polyacrylamide slab gels according to Laemmli (1970). The separating gel composition [5 ml] contained: 1.25 ml acrylamide (40 %), 1.25 ml Tris (1.5 M, pH 8.8), 50 µl sodium dodecyl sulphate (SDS; 10%), 25 µl ammonium persulfate (APS; 10%), 6 µl N, N, N', N'-tetramethylethylenediamine (TEMED), 2.4 ml dH_2O. The stacking gel [5 ml] was composed of: 0.5 ml acrylamide (40%), 1.25 ml Tris (0.5 M, pH 6.8), 50 µl SDS (10%), 25 µl APS, 6 µl TEMED, 3.2 ml dH_2O. For activity staining, polymeric substrate, i.e. carboxymethylcellulose (Fluka, St. Gallen, Switzerland), lichenan (Megazyme, Wicklow, Ireland) or xylan (Roth, Karlsruhe, Germany) was incorporated into the separating gel in a concentration of 0.5% (w/v) prior to the addition of APS according to Zverlov et al. (2010). Protein samples were mixed with loading dye (1:1) containing 2.2% SDS and applied directly to the polymerised gel after determination of the protein concentration following Lowry et al. (1951) using the Roti®-Nanoquant protein quantitation assay (Roth, Karlsruhe, Germany). The running buffer contained the following components: 1 g SDS; 3 g Tris; 14 g glycine (Roth). Electrophoresis was performed on ice at a conduction current of 30 mA (~60 V) until the loading dye front reached the bottom of the slab gel (~2-3 h). Gels were then put between cellulosic filter papers (Schleicher & Schuell, Dassel, Germany) soaked with 0.1 M succinate buffer (pH 4.5) and incubated for 120 min at 50°C for renaturation. Protein bands were optionally detected by staining with Coomassie blue R-250 following Kang et al. (2002). After destaining with 10% ethanol solution containing 2% (v/v) o-phosphoric acid, Congo red (Sigma-Aldrich, St. Louis, Missouri, USA) was applied to detect enzymatically active bands by staining the polymeric gel matrix. Therefore gels were submersed in Congo red solution (0.02%) for 15 min at room temperature (~20°C). After destaining with 1 M NaCl, halo zones in the red stained background

revealed the degradation of the matrix incorporated biopolymer, which were therefore chosen for further characterisation via LC-MS/MS.

2.3.3.5 LC-MS/MS analysis

Protein identification and internal sequence information was received from LC-MS/MS. Protein bands were excised from gels and reduced, alkylated and digested with Promega modified trypsin according to the method of Shevchenko et al. (1996). Digests were separated by nano-HPLC (Agilent 1200 system, Vienna, Austria) equipped with a Zorbax 300SB-C18 enrichment column (5 µm, 5 x 0.3 mm) and a Zorbax 300SB-C18 nanocolumn (3.5 µm, 150 x 0.075 mm). 40 µl of sample were injected and concentrated on the enrichment column for 6 min using 0.1% formic acid as isocratic solvent at a flow rate of 20 µl min^{-1}. The column was then switched in the nanoflow circuit, and the sample was loaded on the nanocolumn at a flow rate of 300 nl min^{-1}. Separation was carried out using the following gradient, where solvent A is 0.3% formic acid in water and solvent B is a mixture of acetonitrile and water (4:1) containing 0.3% formic acid: 0-6 min: 13% B; 6-63 min: 13-28% B; 63-88 min: 28-50% B, 88-89 min: 50-100% B; 89-100 min: 100% B; 100-101 min: 100-13% B; 101-120 min: re-equilibration at 13% B. The sample was ionized in the nanospray source equipped with nanospray tips (PicoTipTM Stock# FS360-75-15-D-20, Coating: 1P-4P, 15+/- 1 µm Emitter, New Objective, Woburn, MA, USA). It was analyzed in a Thermo LTQ-FT mass spectrometer (Thermo Fisher Scientific, Waltham, MA, USA) operated in positive ion mode, applying alternating full scan MS (m/z 400 to 2000) in the ion cyclotron and MS/MS by collision induced dissociation of the 5 most intense peaks in the ion trap with dynamic exclusion enabled. The LC-MS/MS data were analyzed by searching the NCBI public database with Mascot 2.2 (MatrixScience, London, UK). A maximum false discovery rate of 5% using decoy database search, an ion score cut off of 20 and a minimum of 2 identified peptides was chosen as identification criteria.

2.3.3.6 Scanning electron microscopy (SEM)

For the investigation of morphological colonisation characteristics of activated clinoptilolite migulator particles scanning electron microscopy was used (Zeiss ULTRA 55, Carl Zeiss MicroImaging GmbH, Germany). Particles of 1.0 to 2.5 mm in diameter were analysed. The biological material was imaged with the high efficiency

“In-lens SE detector” using secondary electrons (SE), which deliver topographic contrast (Goldstein et al., 2003). Additionally, imaging with an angle selective backscattered electron (AsB) detector was performed. It detects backscattered electrons (BSE) and delivers compositional contrast, which is determined by the differences in the local chemical composition of an investigated specimen (Goldstein et al., 2003). In the case of SE imaging 5 kV acceleration voltage of the primary electrons was applied with the exception of one micrograph which was imaged simultaneously with the AsB detector at an acceleration voltage of 15 kV. Before application fresh samples were fixed in glutaraldehyde (2.5 % in 0.1 M phosphate puffer, pH 7.2), dehydrated in a graded ethanol series with a final step in propylene oxide and ultimately dried by lyophilisation (Labconco Freeze Dry System FreeZone 4.5, Kansas City, Missouri, USA) or critical point drying (CO_2; Bal-Tec CPD, Balzers, Fürstentum Liechtenstein). For observation, prepared samples were mounted on aluminum stubs using double-sided carbon tape and moreover a carbon film was applied onto the specimens’ surfaces by high-vacuum evaporation.

2.3.3.7 Confocal laser-scanning microscopy and fluorescence *in situ* - hybridisation (FISH)

To investigate taxonomic groups embedded in biofilms on grass silage fibres and activated clinoptilolite migulator particles < 100 µm in diameter, *in situ* hybridization using fluorescence-labelled nucleic acid probes that are complementary to target signature regions of rRNA was done. Before fixation, samples were washed three times with 1x phosphate-buffered saline (PBS), approximately 500 µl for 0.3 g fresh matter. For fixation 800 µl of a 4% paraformaldehyde/1x PBS solution (4:1) were mounted for an incubation time of 12 h at 4°C and then discarded. Then three washing steps in ice-cold 1x PBS (rinse/5 min/10 min) followed, before the storage at -20°C in 500 µl of a 96% ethanol/1x PBS solution (1:1). After another washing step with 200 µl of 1x PBS, 10 µl of 1 mg ml^{-1} lysozyme (Sigma-Aldrich, St. Louis, Missouri, USA) were added for permeabilisation over 10 min at room temperature on polysine slides (Menzel-Gläser, Braunschweig, Germany). The samples were then rinsed twice in ice-cold 1x PBS before an ethanolic dehydration series (50-80-96%) was applied. After quickly rinsing with PBS, another washing step for 3 min at room temperature followed before hybridizations were performed. The hybridization buffer contained 0.9 M NaCl, 0.02 M Tris-HCl (pH 8.0), 0.01% (w/v) SDS and 2.5-5.0 ng $µl^{-1}$

per probe. The concentration of formamide™ (Invitrogen, Karlsruhe, Deutschland) was 10% (w/v) for every probe. Probes used: EUB338Mix (5'-GCT GCC TCC CGT AGG AGT-3', 5'-GCA GCC ACC CGT AGG TGT-3', 5'-GCT GCC ACC CGT AGG TGT-3') adapted from Amann et al. (1990)and Daims et al. (1999) for most bacteria; ARCH915 (5'-GTG CTC CCC CGC CAA TTC CT-3') described by Stahl and Amann (1996) for Archaea and Univ-1390 (5'-GAC GGG CGG TGT GTA CAA-3') for counter-staining of all organisms (Zheng et al., 1996). All hybridizations were realised by incubation at 36°C in the dark for 90-180 min. To eliminate the hybridization buffer afterwards, samples were rinsed with 40 µl of pre-warmed (38°C) washing buffer before a further incubation step for 10-15 min at 38°C. The washing buffer contained: 0.45 M NaCl and 0.02 M Tris-HCl. Finally, samples were rinsed with 500 µl ice-cold double-distilled H_2O and mounted with Molecular Probes® ProLong Gold antifadent with or without DAPI (Invitrogen) over 30 min to 24 h at room temperature as recommended by the manufacturer. Sample stained with multiple probes were simultaneously observed using a Leica TCS SPE confocal laser-scanning microscope (Leica Microsystems, Heidelberg, Germany), taking advantage of the non-overlapping emission wavelengths of the fluorochromes used (maximum excitation/emission in [nm]: FITC 490/525; Cy3 548/562; Cy5 650/670).

2.3.3.8 Accession numbers

Accession numbers for primary nucleotide sequence data determined during 16S rRNA gene fragment based community analyses have been submitted to NCBI GenBank (BankIt1555395). Band numbers are represent SSCP-generated bands analysed and referred to in the results section.

band no.	sequence no.	accession no.
17	1	JX436453
9	2	JX436454
3	3	JX436455
1	4	JX436456
8	5	JX436457
7	6	JX436458
4	7	JX436459

2.3.4 Results

2.3.4.1 Community profile and characterisation of populations on clinoptilolite

In order to visualize anaerobic hydrolytic populations immobilized onclinoptilolite surfaces, SEM pictures were taken after critical point drying (figure III-1A) or lyophilisation (figure III-1B-D). Extensive colonisation during batch-wise cultivation was observed area-wide after 5 days of incubation at 45°C and 21 days when incubated at 35°C respectively (figure III-1A, B). Microbial cells observed ranged from 0.3 to 0.5 µm in width and 1.2 to 5.4 µm in length showing morphologies matching bacterial sequencing findings in this study (see PCR-based SSCP and sequencing analyses discussed below), revealing affiliations to the orders Clostridiales, Bacillales and Bacteroidales. In contrast, cells observed after *in sacco* incubation in semi-continuously operated bioreactors were more rod-shaped with lengths of 5.5 to 7.0 µm (figure III-1C, D). Pilus-like appendages (figure III-1B) were observed to reach out from microbial cells directly either to the clinoptilolite's surface or to neighbouring cells. Pili-dimensions ranged from 230 nm to 3 µm in length and 45 to 77 nm in width. The organic origin of bacillary and fibrous structures was confirmed by using In-lens and AsB detectors simultaneously (Figure III-1C, D) to expose topographic and compositional contrasts that allow the discrimination between carbon-based biological material (i.e. microbial cells) and inorganic matter.

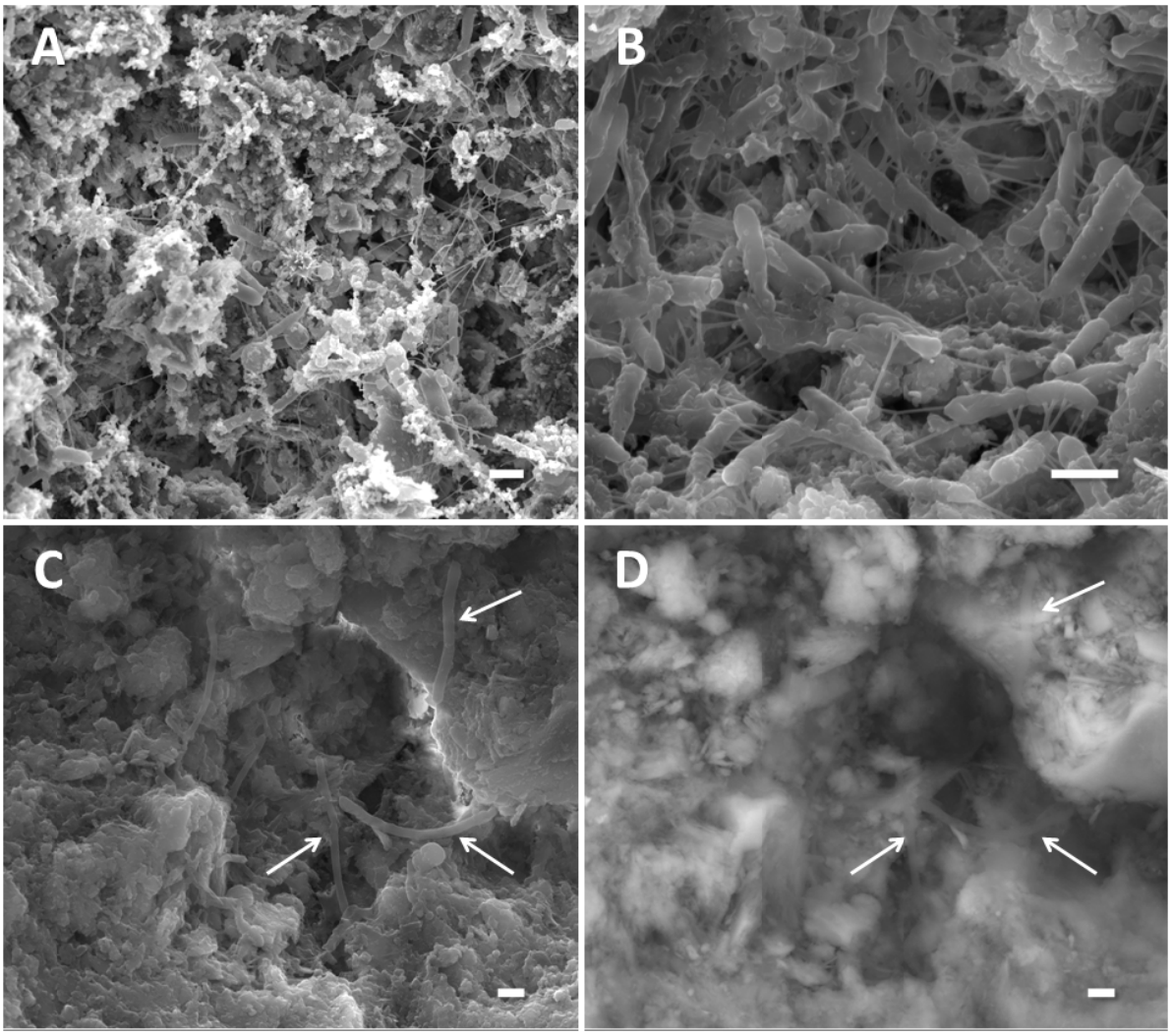

Fig. III-1 SEM images of activated clinoptilolite migulator particles (< 2.5 mm in diameter) colonised by anaerobic microbial populations during batch-wise (A, B) and *in sacco* incubation in continuously operated bioreactors (C, D). A, B (SE, In-lens detector) activated clinoptilolite migulator heavily colonized by microorganisms (biofilm formation). C, D rod-shaped cells, vanishing when inorganic matter is focused (AsB detector). (Bar length: 1 µm).

Rapid degradation of grass silage fibres was observed after 7 days of cultivation at 35°C as determined by confocal laser scanning microscopy (CLSM). Bacteria were present on grass fibres, forming degradation sites on leaves and stems (figure III-2 a-f). Approximately $4.02 \pm 7.79 \times 10^{11}$ cells cm^{-3} based on staining probes specific for eubacteria (yellow fluorescence signals) were counted. Epidermis layers were affected first, at which decomposition was beginning from the primary cell wall proceeding to the outer cuticula.

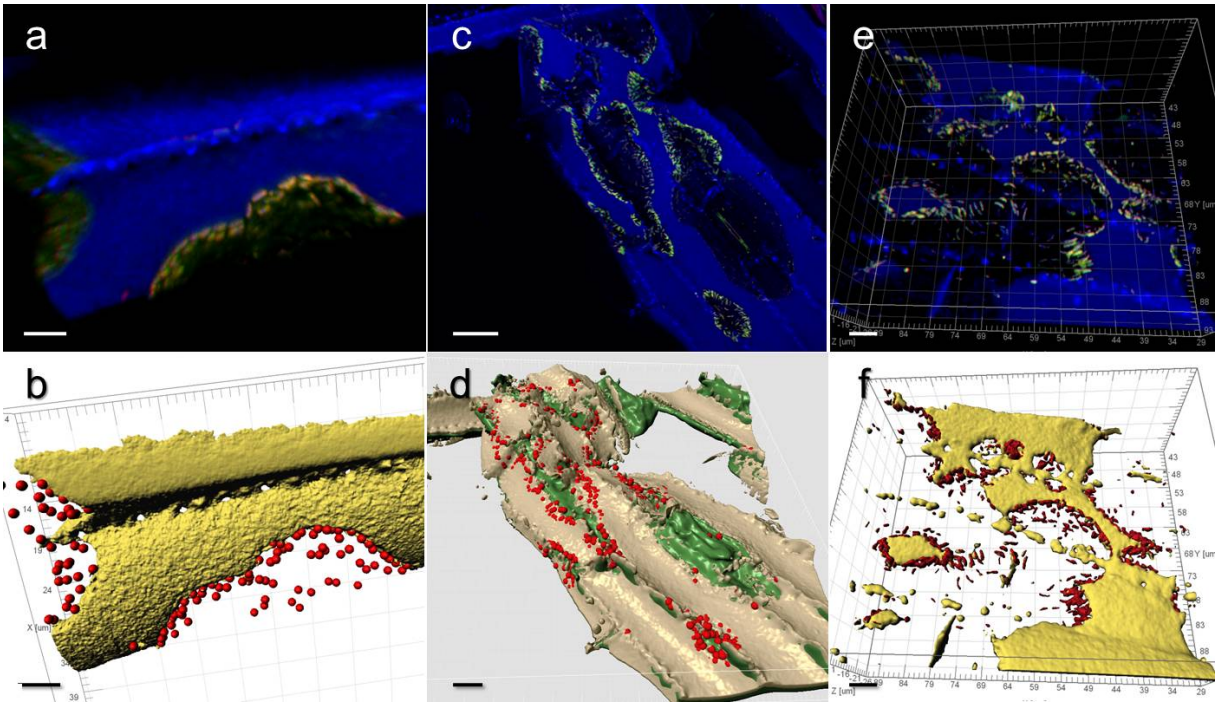

Fig. III-2 a, c, e confocal laser scanning micrographs of grass silage fibres with fluorescence labelled bacteria after 7 days of fermentation at 35°C. EUB338-Cy3 probe mix was used for the specific staining of bacteria. Negative controls with non-sense FISH probe (NON-EUB) showed no positive signals. b, d, f 3D reconstructions (formed by spots and isosurfaces) of images a, c and e. Red spots represent bacteria degrading outer layers of grass leave cell walls (yellow/beige). (Bar length: 5 µm).

Apart from grass silage fibres, bacteria were also detected on activated clinoptilolite migulator particles (< 100 µm in diameter) present in batch-digestion reactors of a model substrate for grass silage (figure III-3 C,D). Here, eubacteria were seen both on the surface and deep inside the clefts of clinoptilolites. Bacterial colonization was less pronounced when compared to grass silage, however, still approximately $7.22 \pm 3.92 \times 10^{10}$ cells cm^{-3} were counted. This finding confirms clinoptilolites to be quite suitable for microbial colonisation during anaerobic batch-wise cultivation. Contrary to the findings of the community analysis, where genera of archaea could be verified, the application of archaeal probes for FISH did not result in positive signals.

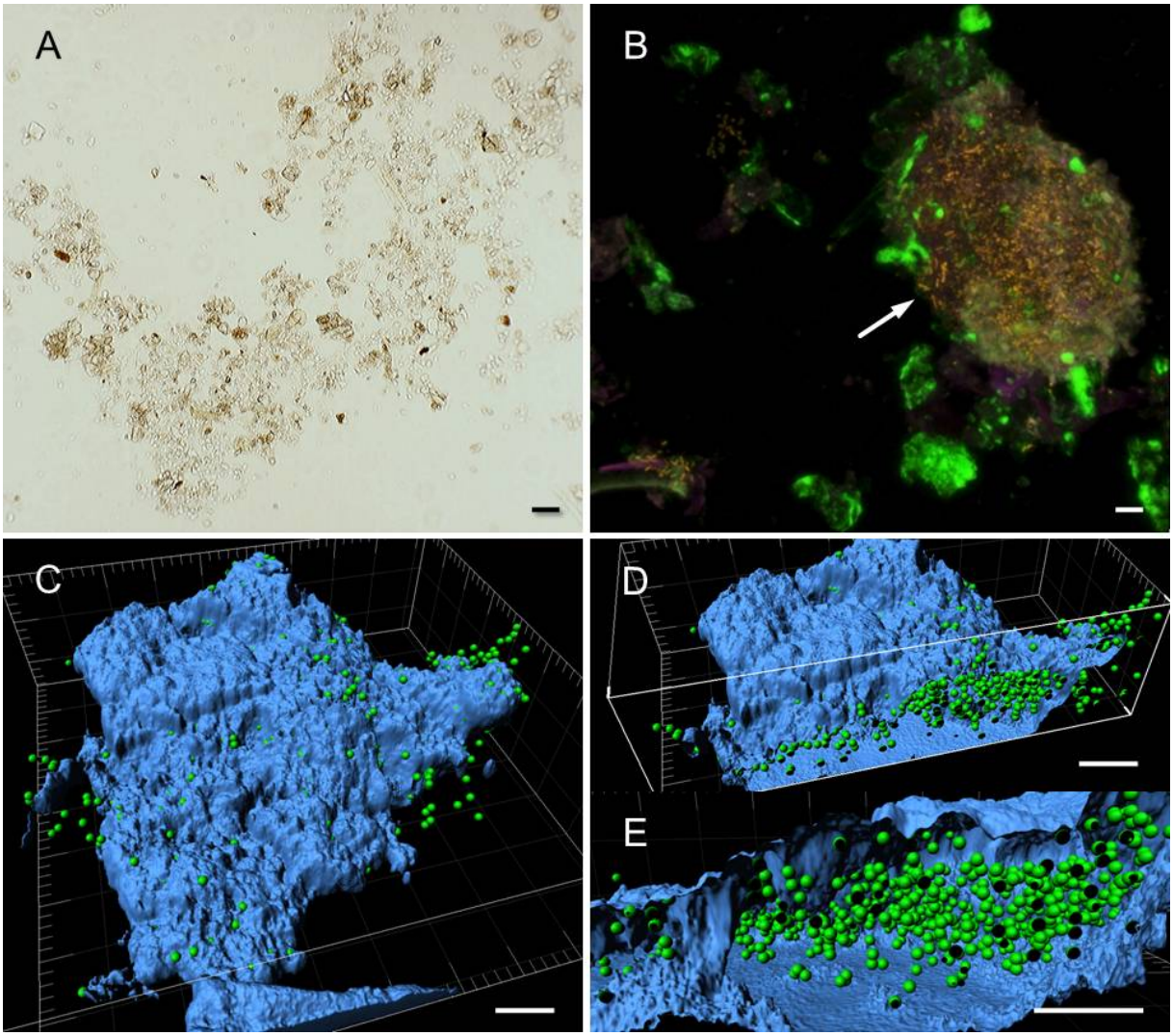

Fig. III-3 A bright filed total view of washed clinoptilolite particles < 100 µm in diameter; B confocal laser scanning micrograph of a clinoptilolite particle colonised by anaerobic bacteria. EUB338-Cy3 probe mix was used for the specific staining of bacteria. Negative controls with non-sense FISH probe (NON-EUB) showed no positive signals. C to E 3D reconstructions (formed by spots and isosurfaces) of image B. Green spots represent bacteria colonising the particle's surface and inside as well. (Bar length: 100 µm [A]; 5 µm [B-E]).

Fingerprints of microbial populations colonising clinoptilolite surfaces in large-scale bioreactors and batch-cultivation were performed by PCR-based SSCP analyses. Figure III-4 shows fingerprints of the archaeal community (A) and bacterial community (B) associated with activated clinoptilolite migulators during fermentation of grass silage and the model substrate in continuously operated mode and batch mode, respectively.

Regarding bacterial community analysis, total sludge (supernatant) of continuously operated bioreactors was analysed to compare fingerprints of activated clinoptilolite migulators and liquid phase associated populations.

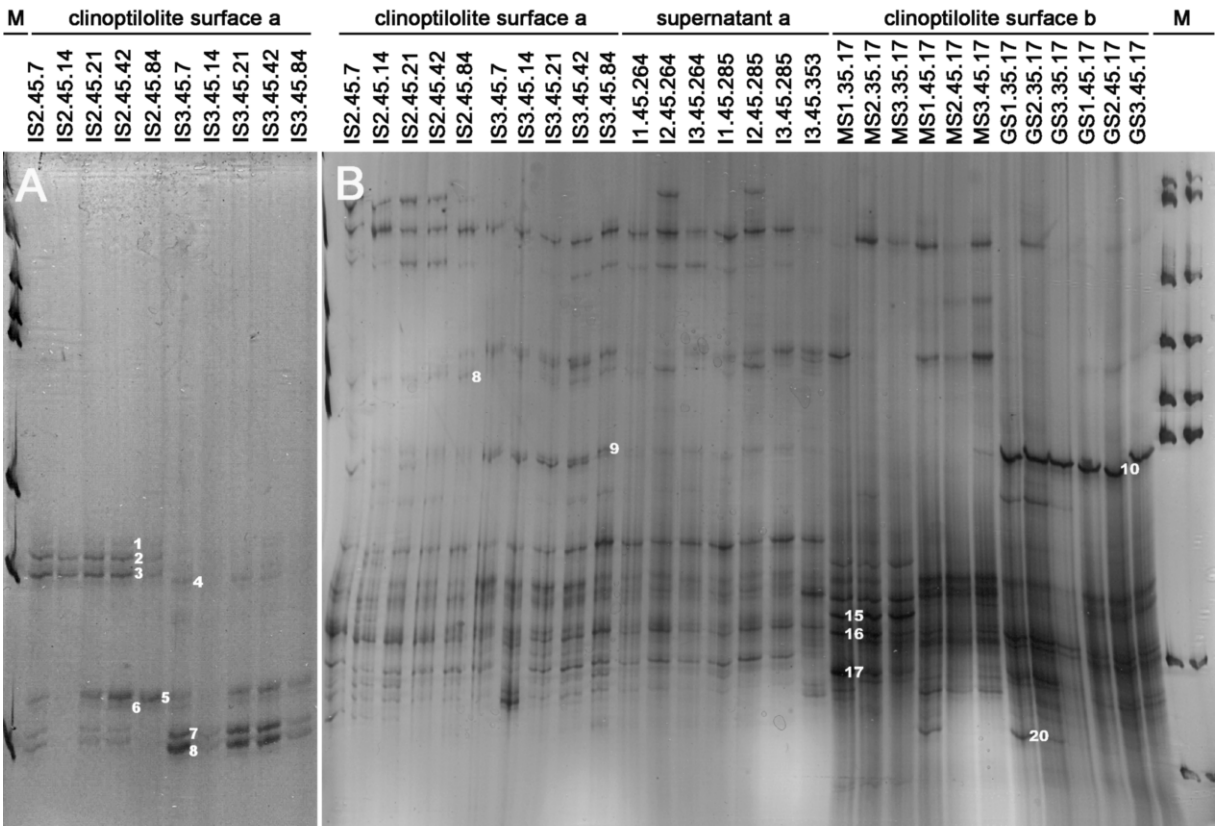

Fig. III-4 Non-denaturating polyacrylamide gel from the SSCP analysis based on (A) archaeal *rrs* (16S rDNA gene) fragments and (B) bacterial *rrs* (16S rDNA gene) fragments of (a) continuously operated mono-grass silage fermentation exposed clinoptilolites (IS2/3), corresponding supernatants (I1-3) and of (b) batch-cultures fed with grass silage (GS) or model substrate (MS). (M: 1 kb DNA-ladder marker lanes; sample-identity: IS2/3 = bioreactors (*in sacco* sample); MS/GS = batch-substrate, 35/45 = fermentation temperature in [°C], 7-353 = fermentation time in [d]).

Bacterial fingerprints of activated clinoptilolite migulators surface and supernatant show comparable patterns, however, certain bands (B: 10, 11) only appeared in samples from activated clinoptilolite migulators surface from only one semi-continuously operated bioreactor (I3) and batch-cultivation on grass silage. Most differences in band patterns between samples from continuous fermentation and batch-cultivation were observed in the lower part of the gel and therefore most interesting for identification analyses. Regarding archaeal populations, differences

between bioreactor I2 and I3 were observed. While bands 1 to 3 (A) were dominant in bioreactor I2, they were almost vanishing in reactor I3. In return, bands 7 and 8 (A) intensified from I2 to I3. Both bioreactors had pH values ranging from 8.0 to 8.6 during sampling period, but the initial VOA/TIC value was much higher for I3 (3.63) compared to I2 (0.94). High contents of VFA in I3 were affecting the sampling period from day 7 to 21 and presumably changed the archaeal community composition.

Clustering the fingerprint patterns observed during SSCP analysis revealed three distinct clusters regarding the bacterial community (figure III-5, I-III). One cluster (I) was specific for grass silage fed batch-cultivation with relatively low similarity of < 58% when both cultivation temperatures are included. Nevertheless, patterns derived from cultivation at 45°C alone showed an high homogeneity (similarity of 96%). Interestingly, cluster I was not only different from the one found for model substrate fed batch-cultures, but also from patterns derived from bioreactors continuously operated with grass silage at 45°C. Replicates of model substrate grown populations formed the second cluster (II) with a similarity value of > 73%, unravelling two minor clusters for each cultivation temperature with similarities of > 80%. Highest band pattern similarity value (> 88%) was found for fingerprints from semi-continuous digestion of grass silage forming a third major cluster, which revealed no significant differences between clinoptilolite surface and total sludge (supernatant) originated patterns. Populations in the liquid phase and on the surface were probably foremost equally abundant, but within the major cluster, two more distinct ones were found for activated clinoptilolite migulator surfaces from bioreactor I2 (after *in sacco* incubation from day 7-21) and I3 (day 21-84) were observed with similarities of 88% and 90% respectively.

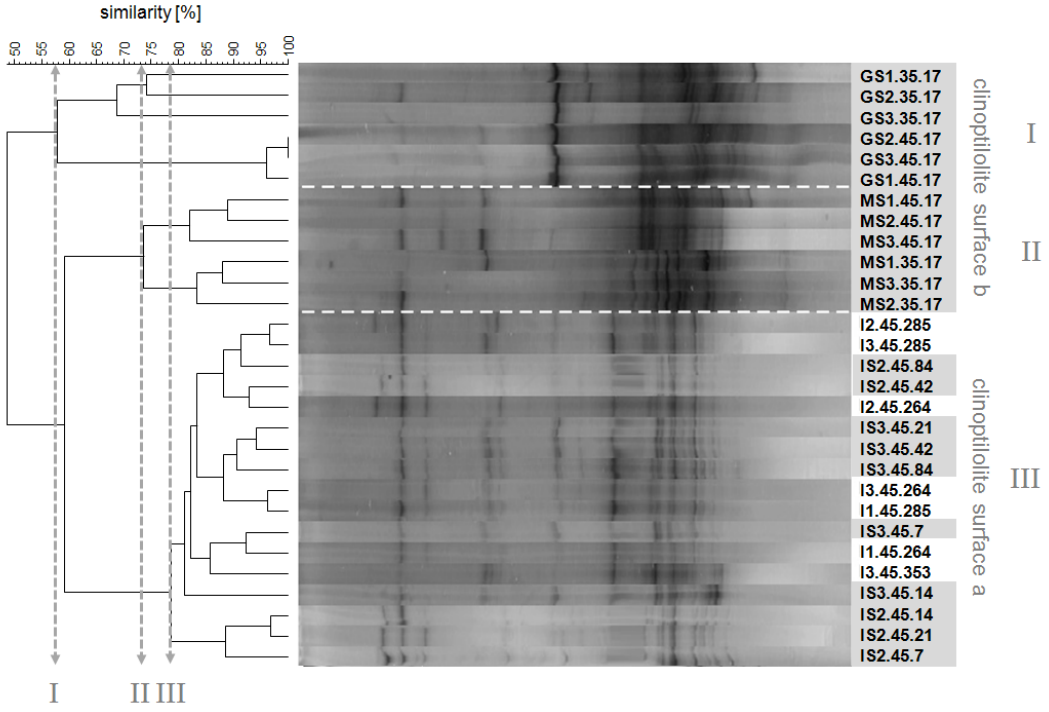

Fig. III-5 Clustering analysis generated dendrogram using band-based comparison (DICE; 1% tolerance, 1% optimisation, grouped by UPGMA) of anaerobic populations on activated clinoptilolite migulator surfaces (highlighted in grey) taken from batch-cultures (zeolite surface b) and continuous operated bioreactors (zeolite surface a and supernatant samples [highlighted in white]). Sample-identity: I2/3 = bioreactors (IS = *in sacco* sample); MS/GS = batch-substrate, 35/45 = fermentation temperature in [°C], 7-353 = fermentation time in [d]).

The colonisation of clinoptilolite surfaces collected from semi-continuously operated fermentation of grass silage was dominated by *Pseudomonas* spp. and *Methanoculleus* spp. At this, *Pseudomonas fluorescens (P. cellulosa)* and *P. putida*, producing cellulases and pectinases, were constantly identified over the total *in sacco* incubation time period, i.e. from day 7 to 84 at 45°C. Within the archaeal domain affiliations to only two genera were found, i.e. *Methanoculleus* spp. and *Methanolinea tarda*, both belonging to the order Methanomicrobiales. These observations match with the archaeal sequencing findings in this study, where *Methanoculleus* spp. was dominant within the order Methanomicrobiales, forming rods or sheathed rods. Amongst all 8 identified species, *M. bourgensis* was found over the total fermentation time (84 days). Data on the community composition of clinoptilolite-associated microorganisms (archaea and bacteria) are summarised in table III-1, sequences are available under the given accession numbers in the Materials and Methods section.

Tab. III-1 Identified clinoptilolite-associated microorganisms separated by SSCP analysis and direct sequencing from bioreactors semi-continuously operated with grass silage; Sample-identity: I2/3 = bioreactors (IS = *in sacco* sample); fermentation temperature during the sampling period: 45°C; 7-84 = day [d] of fermentation, when appearances were observed; band numbers are in accordance with band selection marked in figure 4 (see above).

fermentation			BLAST	organism	order	query	maximum
mode	time [d]	band	acc. no.			coverage [%]	identity [%]
continuous I3	7, 21	4	AY196674.1	*Methanoculleus bourgensis*	Methanomicrobiales	90	98
continuous I3	7, 21	4	EF118904.1	*Methanoculleus thermophilus*	Methanomicrobiales	90	98
continuous I3	7, 21	4	DQ787476.1	*Methanoculleus receptaculi* strain ZC-2,3	Methanomicrobiales	90	98
continuous I3	7, 21-42	7	AF107104	*Methanoculleus* sp. MAB2	Methanomicrobiales	92	99
continuous I3	7, 21-42	7	AY196674	*Methanoculleus bourgensis*	Methanomicrobiales	92	99
continuous I3	7, 21-42	7	DQ787476.1	*Methanoculleus receptaculi* strain ZC-2,3	Methanomicrobiales	92	98
continuous I3	7, 21-42	7	NR_028253.1	*Methanoculleus palmolei* DSM 4273	Methanomicrobiales	92	97
continuous I3	7, 21-42	7	AJ862839.1	*Methanoculleus thermophilus*	Methanomicrobiales	92	97
continuous I3	7, 21-42	7	AF095270.1	*Methanoculleus olentangyi*	Methanomicrobiales	92	96
continuous I3	7, 21-42	7	NR_028163.1	*Methanolinea tarda* NOBI-1	Methanomicrobiales	92	96
continuous I3	7, 21-42	8	AF107103.1	*Methanoculleus* sp. MAB1	Methanomicrobiales	96	99
continuous I3	7, 21-42	8	AY196674	*Methanoculleus bourgensis*	Methanomicrobiales	96	99
continuous I3	7, 21-42	8	DQ787476.1	*Methanoculleus receptaculi* strain ZC-2,3	Methanomicrobiales	96	98
continuous I3	7, 21-42	8	NR_028253.1	*Methanoculleus palmolei* DSM 4273	Methanomicrobiales	96	97
continuous I3	7, 21-42	8	NR_028163.1	*Methanolinea tarda* NOBI-1	Methanomicrobiales	96	96
continuous I2	42-84	1	AY196674	*Methanoculleus bourgensis*	Methanomicrobiales	90	99
continuous I2	42-84	1	EF118904	*Methanoculleus thermophilus* strain JB-1	Methanomicrobiales	90	98
continuous I2	42-84	1	DQ787476	*Methanoculleus receptaculi*	Methanomicrobiales	90	98
continuous I2	42-84	1	EU722338.1	*Methanoculleus marisnigri*	Methanomicrobiales	90	98
continuous I2	42-84	1	NR_028856	*Methanoculleus submarinus* strain Nankai-1	Methanomicrobiales	90	98
continuous I2	42-84	1	NR_028152.1	*Methanoculleus chikugoensis* MG62	Methanomicrobiales	90	98
continuous I2	42-84	1	NR_028253.1	*Methanoculleus palmolei* DSM 4273	Methanomicrobiales	90	98
continuous I2	7-84	3	AY196674	*Methanoculleus bourgensis*	Methanomicrobiales	90	98
continuous I2	7-84	3	EF118904	*Methanoculleus thermophilus* strain JB-1	Methanomicrobiales	90	98
continuous I2	7-84	3	DQ787476	*Methanoculleus receptaculi*	Methanomicrobiales	90	98
continuous I2	7-84	3	EU722338.1	*Methanoculleus marisnigri*	Methanomicrobiales	90	98
continuous I2	7-84	3	NR_028856	*Methanoculleus submarinus* strain Nankai-1	Methanomicrobiales	90	98
continuous I2	7-84	3	NR_028152.1	*Methanoculleus chikugoensis* MG62	Methanomicrobiales	90	98
continuous I2	7-84	3	NR_028253.1	*Methanoculleus palmolei* DSM 4273	Methanomicrobiales	90	98
continuous I2,3	7-84	9	FJ808611	*Clostridium* sp.	Clostridiales	96	92
continuous I2,3	7-84	17	JF432053	*Pseudomonas* sp.	Pseudomonadales	100	100
continuous I2,3	7-84	17	JF756250.1	*Pseudomonas lundensis* strain MFPB42A12-09	Pseudomonadales	100	100
continuous I2,3	7-84	17	HM854252.1	*Pseudomonas pelagia* strain KTT-14	Pseudomonadales	100	100
continuous I2,3	7-84	17	HM031486.1	*Pseudomonas pertucinogena* strain mol25	Pseudomonadales	100	100
continuous I2,3	7-84	17	FJ232608	*Pseudomonas fluorescens*	Pseudomonadales	100	100
continuous I2,3	7-84	17	AF173970	*Pseudomonas putida*	Pseudomonadales	100	100

2.3.4.2 Role of clinoptilolite-associated populations in biomass degradation

In order to analyse the role of microorganisms colonising activated clinoptilolite migulators on biomass degradation, hydrolytic enzyme activities were determined. Therefore, washed colonised activated clinoptilolite migulators were re-incubated in buffer on substrate according to their pre-cultivation, i.e. model substrate for/ or grass silage. Then, cellulase and xylanase activities were measured after certain time points throughout the re-incubation.(figure III-6). Highest hydrolytic enzyme activities (2.8 kU l^{-1}) were measured for colonized clinoptilolite samples taken from model substrate fermentations after 8 days of re-incubation at 35°C. When increased temperature (45°C) was applied, an individual maximum was reached (1.9 kU l^{-1}). Re-incubation in the presence of grass silage at 35°C led to 2.2 kU l^{-1} on average. As for model substrate, increased incubation temperature decreased hydrolytical enzyme activities (1.8 kU l^{-1} at day 27). The overall maximum was found for re-incubation on model substrate (35°C) at day 27 with 3.2 kU l^{-1} on average. Depicting xylanase and cellulase activities individually (data not shown), highest xylanase activities (around 1.5 to 1.6 kU l^{-1}) were found for both substrates (at day 8 for model substrate and day 27 for grass silage) at 45°C incubation temperature. In turn, maximum cellulase activities occurred during cultivation at 35°C ranging from 1.3 kU l^{-1} upon grass silage to 1.9 kU l^{-1} upon model substrate at day 8 and 27 respectively. As a result, cellulase activities pushed the maximum value of total hydrolytical enzyme activity towards the lower incubation temperature condition.

During cultivation pH was adjusted to 6.0 to 6.5 initially and at each sampling point. This pH range was not exceeded, except for batches re-incubated on model substrate at 45°C. Here, pH values were around 7.5 from day 8 to 27, which suggests that decreased hydrolytic enzyme activities from day 8 on where due to unstable pH conditions, possibly exceeding the optimal pH range for hydrolytic enzymes. Further feedings of model substrate or grass silage at day 28 could not provoke additional increases of enzyme activities (data not shown).

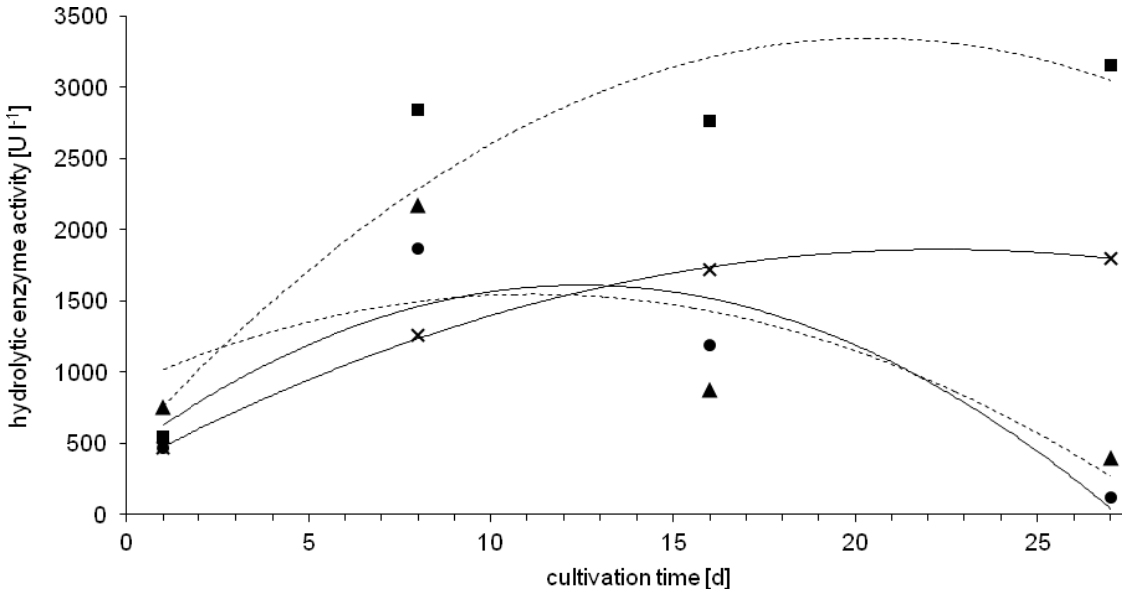

Fig. III-6 Hydrolytic enzyme activities (cellulase + xylanase) in [U l^{-1}] determined during during re-incubation of washed colonised clinoptilolites in a synthetic mineral medium on model substrate at 35°C (---■---) and 45°C (---▲---) or grass silage at 35°C (—●—) and 45°C (—×—) over a total time period of 27 days. Substrates were batch-wise fed at day 1. Standard deviations are below ±104 U l^{-1} for xylanase values and ±136 U l^{-1} for cellulase values.

Overall, bacteria immobilised on activated clinoptilolite migulators, washed and stored for more than 20 month, start production of hydrolytic enzymes only after a few days upon re-incubation. These results clearly demonstrated that clinoptilolite habituating functional microorganisms endure or gain a long-term revitalisation ability throughout immobilisation on clinoptilolites. Thus, bacteria cells are able to immediately start hydrolytic enzyme production when re-incubated in synthetic medium with model substrate at 35°C or grass silage at 45°C fermentation temperature.

For further characterisation of enzymes associated with clinoptilolite surfaces and degradation of grass silage, identification was realised through LC-MS peptide sequencing analysis and protein database searches. Hydrolytical active proteins secreted by clinoptilolite immobilised microorganisms after re-incubation were preselected by separation via gel electrophoresis on polyacrylamide gel matrix incorporating carboxymethylcellulose (CMC), lichenan or xylan. All three substrates for cellulases/hemicellulases were useful for detecting active enzymes, although

CMC delivered the sharpest protein bands compared to lichenan and was therefore preferred for enzyme separation. Samples were collected from batch-cultivated activated clinoptilolite migulator inhabiting anaerobic populations during re-incubation in synthetic mineral medium on model substrate or grass silage (table III-2). Sampling points were coordinated with positive enzyme activity findings. When lichenan was used, only exocellobiohydrolase II (3.2.1.91) and amylase (3.2.1.1) were identified throughout the total re-incubation period upon model substrate at 35°C. At day 1 several positive matches for grass silage fed batch-cultures re-incubated at 35°C appeared, i.e. cellulases (exocellobiohydrolases), hemicellulase (1,4-β-mannan-mannanohydrolase) and a sugar hydrolysing enzyme with molecular weights ranging from 47 to 149 kD exclusively related to *Paenibacillus polymyxa* strains from the division Firmicutes. At day 8 of re-incubation, where highest enzyme activities in batch-cultures fed with model substrate (at 35/45°C) and grass silage (at 35°C) were measured, mainly cellulolytic endo-1,4-1,3-β-D-glucan glucanohydrolase was identified (foremost related to *Paenibacillus* spp.). At day 8 of re-incubation, where highest enzyme activities in batch-cultures fed with model substrate (at 35/45°C) and grass silage (at 35°C) were measured, mainly cellulolytic endo-1,4-/1,3-β-D-glucanohydrolase was identified (foremost related to *Paenibacillus* spp.). At day 16, endoglucanase from *Paenibacillus* sp. was present in batch-cultures re-incubated at 45°C. Furthermore, endo-1,4-β-glucanase affiliated to *Symbiobacterium thermophilum* and isomerases of *Thermoanaerobacter pseudethanolicus* and *Fusobacterium nucleatum* were present. At day 27, xylose isomerases and glycoside hydrolase related to three genera from within the order Bacillales were identified, possibly indicating a shift towards carbohydrate conversion in succession to the former degradation of plant cell wall biopolymers. Besides positive matches for recalcitrant biomass degrading enzymes, flagellin of *Pseudomonas fluorescens* was found with highest score and sequence coverage (23%) from day 28 on to the end of the observation period at day 84 of the semi-continuously operated bioreactor experiment. These finding confirmed the positive identification of *P. fluorescens* (*P. cellulosa*) in the course of the community analysis.

Tab. III-2 Identification of hydrolases secreted by clinoptilolite immobilised microorganisms through SDS -PAGE with matrix incorporated CMC for activity staining. Active bands were excised and further analysed (LC-MS/MS, NCBI public database search with Mascot). Only hits with highest score are listed (except for samples collected at day 8 where ID was still reliable, but highest scores not reached). Samples were collected from batch-cultivated activated clinoptilolite migulator inhabiting microorganisms during re-incubation on model substrate (MS) or grass silage (GS) over a total time period of 27 days.

cultivation			gi-no.	EC no.	enzyme	mass [kD]	related organism	Score	peptides (unique)	sequence coverage
substrate	temp. [°C]	time [d]								
GS	35	1	308067135	3.2.1.55	arabinosidase	~57	*Paenibacillus polymyxa* E681	113	2 (2)	7
GS	35	1	308071054	3.2.1.78	1,4-β-mannase B	~149	*Paenibacillus polymyxa* E681	160	2 (2)	2
GS	35	1	308067781	3.2.1.91	exocellobiohydrolase 3	~77	*Paenibacillus polymyxa* E681	775	24 (12)	18
GS	35	1	308069068	3.2.1.91	exocellobiohydrolase II	~108	*Paenibacillus polymyxa* E681	271	4 (4)	6
GS	35	1	310640531	3.2.1.91	exoglucanase A	~77	*Paenibacillus polymyxa* SC2	609	16 (10)	19
GS	35	1	308071411	4.2.2.2	pectate lyase 2	~47	*Paenibacillus polymyxa* E681	190	4 (3)	12
GS	35	1	308068567	3.2.1.3	glucosidase yic I	~87	*Paenibacillus polymyxa* E681	103	2 (2)	3
GS	35	8	146350814	3.2.1.4	endoglucanase	~62	*Paenibacillus* sp. KSM-N659	120	3 (3)	5
GS	35	8	4249556	3.2.1.4	endoglucanase	~33	*Humicola grisea var. Thermoidea*	129	3	9
GS	35	8	232219	3.2.1.4	endoglucanase A	~77	*Paenibacillus lautus*	168	4 (3)	5
MS	35	8	146350814	3.2.1.4	endoglucanase	~62	*Paenibacillus* sp. KSM-N659	120	3	2
MS	35	8	146350812	3.2.1.4	endoglucanase	~62	*Paenibacillus* sp. KSM-N440	115	2	3
MS	35	8	146350810	3.2.1.4	endoglucanase	~62	*Paenibacillus* sp. KSM-N145	115	2	3
MS	35	8	146350808	3.2.1.4	endoglucanase	~62	*Paenibacillus* sp. KSM-N115	115	2	3
MS	35	8	232219	3.2.1.4	endoglucanase A	~77	*Paenibacillus lautus*	168	3	5
MS	35	8	308069068	3.2.1.91	exocellobiohydrolase II	~108	*Paenibacillus polymyxa* E681	130	2	2
MS	35	8	310641984	3.2.1.3	glycoside hydrolase family 48	~110	*Paenibacillus polymyxa* SC2	130	2	2
GS	35	16	4249556	3.2.1.4	endoglucanase	~33	*Humicola grisea* var. Thermoidea	170	7 (4)	15
GS	35	16	16078876	3.2.1.4	endoxylanase	~47	*Bacillus subtilis* 168	72	4 (2)	4
MS	35	16	1170135	3.2.1.4	cellulase	~24	*Humicola insolens*	87	2	9
MS	35	16	146350814	3.2.1.4	endoglucanase	~62	*Paenibacillus* sp. KSM-N659	292	6	9
GS	45	16	51893813	3.2.1.4	endo-1,4-β-glucanase	~40	*Symbiobacterium thermophilum*	570	8	35
MS	45	16	146350812	3.2.1.4	endoglucanase	~62	*Paenibacillus* sp. KSM-N440	270	4	6
MS	45	16	146350810	3.2.1.4	endoglucanase	~62	*Paenibacillus* sp. KSM-N145	270	4	6
MS	45	16	146350808	3.2.1.4	endoglucanase	~62	*Paenibacillus* sp. KSM-N115	270	4	6
MS	45	16	308068047	5.3.1.9	glucose-6-phosphate isomerase	~50	*Paenibacillus polymyxa* E681	116	3	7
MS	45	16	167037114	5.3.1.9	glucose-6-phosphate isomerase	~50	*Thermoanaerobacter pseudethanolicus* ATCC 33223	79	2	6
MS	45	16	34763477	5.3.1.9	glucose-6-phosphate isomerase	~42	*Fusobacterium nucleatum* ATCC 49256	139	3	7
MS	45	16	253574746	5.3.1.4	L-arabinose isomerase	~55	*Paenibacillus* sp. D14	92	2	4
MS	35	27	232219	3.2.1.4	endoglucanase A	~77	*Paenibacillus lautus*	619	12 (8)	19
MS	35	27	310641984	3.2.1.3	glycoside hydrolase family 48	~110	*Paenibacillus polymyxa* SC2	305	10 (5)	5
MS	35	27	253574413	5.3.1.14	xylose isomerase	~49	*Paenibacillus sp.* D14	227	10 (4)	8
MS	35	27	1750124	5.3.1.14	xylose isomerase	~50	*Bacillus subtilis*	164	2	6
MS	35	27	310641984	3.2.1.3	glycoside hydrolase family 48	~110	*Paenibacillus polymyxa* SC2	305	5	5
MS	35	27	27227837	3.2.1.8	xylanase 5	~143	*Paenibacillus* sp. W-61	128	2 (2)	1
MS	35	27	261409352	5.3.1.5	xylose isomerase	~49	*Geobacillus* sp. Y412MC10	196	2	6

2.3.5 Discussion and Conclusion

Scanning electron and confocal laser scanning microscopy using FISH gave optical evidence of microbes preferring activated clinoptilolite surfaces as operational environment. Thereby, colonisation was not only observed on the surface of clinoptilolite particles, it also took place inside the porous framework as well. Observed cell morphologies and pili-formations on surfaces did match with findings of Jarrell (2011), who reported that Flagella and pili of *Methanococcus maripaludis* have a second and first role in surface attachment besides motility and cell-connecting functions and that those cells lacking such surface appendages were unable to attach efficiently to any surfaces. Regarding bacteria, hydrolytically active representatives in anaerobic processes are producing multi-enzyme complexes, i.e. cellulosomes for efficient cellulose and hemicellulose degradation (Schwarz 2001; Karita 1997). Here, the attachment to substrate surfaces, e.g. fibres of microcrystalline cellulose is realised by protuberances with dimensions up to 550 nm in length and between 50 nm and 300 nm in width (Bayer 1998), that were also observed in our study. Furthermore, FISH-labeling confirmed dense biofilm formation on and inside clinoptilolite particles by bacteria exclusively. Though archaeal colonisers were detected during community analysis, archaea-specific probing did not lead to corresponding detection signals, which was rather a methodological problem, than real evidence for the absence of methanogens.

Cluster- and sequencing analyses were useful tools for the verification of microbial populations associated with clinoptilolite surfaces. Amongst them, *Clostridium* sp. was identified, a genus involving several species producing hemicellulolytic and cellulolytic enzyme activity such as *Clostridium cellolyticum, C. aerotolerans* or *C. xylanolyticum* (van Gylswyk and van der Toorn 1987). Additionally *Pseudomonas fluorescens*, a Gram-negative, rod-shaped mesophilic species was identified, that produces noncomplexed, cell free cellulolytic enzymes (Kim 1987) and is therefore also referred to as *P. cellulosa* (Dees 1995). Colonisers affiliated to the archaeal domain were throughout dominated by the order Methanomicrobiales. This group uses the hydrogenotrophic pathway to generate methane that allows faster growth rates than acetogenotrophically growing archaea, which in turn probably led to the dominant appearance of the genera *Methanoculleus* and *Methanolinea*. *Methanoculleus* sp. was also observed to appear in association with increased

methane production from model substrate for maize upon trace metal supplementation (Pobeheim 2010b). Among coccoid methanogens, which grow on H_2-CO_2, formate and some secondary alcohols, *Methanoculleus marisnigri* was identified, although this morphology could not be observed in microscopy approaches. Cells are usually 1 to 2 µm in diameter and have optimum growth conditions at mesophilic temperatures and slightly alkaline pH values (Maestrojuán 1990). In addition, *Methanolinea tarda* represents another mesophilic methane-producing archaeon using H_2 and formate for growth (Imachi 2008). In contrast to most indications observed in other studies, all methanogenic species we found, were identified under mild thermophilic conditions.

Enzyme identification complemented the community analysis revealing a broad spectrum of cellulolytical enzymes and related organisms that belonged to the genera *Bacillus* sp., *Clostridium* sp. and *Paenibacillus* sp.. Generated peptide sequences via LC-MS resulted in 36 positive hits covering up several important enzymes for the degradation of plant cell wall polymers. Additionally, a set of isomerases was found, that was affiliated to e.g. *Thermoanaerobacter pseudethanolicus*, a rod-shaped, spore forming, carbohydrate fermenting bacterium (Onyenwoke 2007) and *Fusobacterium nucleatum*, that is closely related to *Bacteroides* sp. and *Flavobacterium* sp. (Bolstad 1996). The conversion of D-glucose-6-phosphate to D-fructose-6-phosphate mediated by isomerases represents an energy delivering step within the bacterial metabolism and was probably evolved subsequent to hydrolysis of complex polysaccharides. In addition, enzyme activity tests revealed a long-term revitalisation ability regarding cellulases and xylanases associated with clinoptilolite habituating microorganisms. Former experiments showed that such populations can be introduced to the fermentation process resulting in significantly increased methane productivity (Weiß 2010). In conclusion, activated clinoptilolites are eminently suited as natural carrier material for microorganisms acting as mineral bioregulators (migulators), potentially stabilising and enhancing the biogas production process from recalcitrant plant biomass.

2.3.6 Acknowledgement

This study has been funded by the Austrian Research Promotion Agency (FFG) and was kindly supported by IPUS GmbH (Austria) and collaborating institutes (FELMI, ZMF), which are gratefully announced.

2.3.7 References

Altschul, S.F., Madden, T.L., Schaffer, A.A., Zhang, J.H., Zhang, Z., Miller, W. and Lipman, D.J. (1997) Gapped BLAST and PSI-BLAST: a new generation of protein database search programs. *Nucleic Acids Research* **25** (17), 3389-3402.

Amann, R.I., Binder, B.J., Olson, R.J., Chisholm, S.W., Devereux, R. and Stahl, D.A. (1990) Combination of 16S rRNA-targeted oligonucleotide probes with flow cytometry for analyzing mixed microbial populations. *Applied and Environmental Microbiology* **56** (6), 1919-1925.

Bailey, M.J., Biely, P. and Poutanen, K. (1992) Interlaboratory Testing of Methods for Assay of Xylanase Activity. *Journal of Biotechnology* **23** 257-270.

Banks, C.J., Zhang, Y. Jiang, Y. and Heaven, S. (2012) Trace element requirements for stable food waste digestion at elevated ammonia concentrations. *Bioresource Technology* **104**, 127-135.

Bayer, E.A., Shimon, L.J.W., Shoham, Y. and Lamed, R. (1998) Cellulosomes - structure and ultrastructure. *Journal of Structural Biology* **124** 221-234.

Bolstad, A.I., Jensen, H.B. and Bakken, V. (1996) Taxonomy, biology and periodontal aspects of *Fusobacterium nucleatum*. *Clinical Microbiology Review* **9**, 55-71.

Bougrier, C., Dognin, D., Laroche, C. and Rivero, J.C. (2011) Effects of additives solutions of trace elements on anaerobic digestion of maize silage. *1st International Conference on Biogas Microbiology*. Leipzig, 09.14.-16., *Proceedings* **P-10**, 75.

Bruni, E., Jensen, A.P. and Angelidaki, I. (2010) Comparative study of mechanical, hydrothermal, chemical and enzymatic treatments of digested biofibers to improve biogas production. *Bioresource Technology* **101** (22), 8713-8717.

Dees, C., Ringelberg, D., Scott, T.C. and Phelps, T.J. (1995) Characterisation of the cellulose degrading bacterium NCIMB 10462. *Applied Biochemistry And Biotechnology* **51** 263-274.

Goodwin, J.A.S., Wase, D.A.J. and Forster, C.F. (1990) Effects of nutrient limitation on the anaerobic up flow sludge blanket reactor. *Enzyme and MicrobialTechnology* **12**, 877-884.

Gorby, Y.A., Yanina, S., Mclean, J.S., Rosso, K.M., Moyles, D., Dohnalkova, A., Beveridge, T.J., Chang, I.S., Kim, B.H., Kim, K.S., Culley, D.E., Reed, S.B., Romine, M.F., Saffarini, D.A., Hill, E.A., Shi, L., Elias, D.A., Kennedy, D.W., Pinchuk, G., Watanabe, K., Ishii, S., Logan, B., Nealson, K.H. and Fredrickson, J.K. (2006) Electrically conductive bacterial nanowires produced by *Shewanella oneidensis* strain MR-1 and other microorganisms. *Proceedings of the National Academy of Sciences*, USA **103** (30), 11358-11363.

Holper, J., Lesjak, M., Heinzel, U., Boos, B., (2005) Zeolith in der Biogasgewinnung. Sonn. 05450052.5 [EP 1 577 269 A1], Patent Styria, Austria.

Jarrell, K.F., Stark, M., Nair, D.B. and Chong, J.P.J. (2011) Flagella and pili are both necessary for efficient attachment of *Methanococcus maripaludis* to surfaces. *FEMS Microbiology Letters* **319** (1), 44-50.

Karita, S., Sakka, K., and Ohmiya, K. (1997) Cellulosomes, cellulase complexes, of anaerobic microbes: their structure models and functions. In: Onodera, R., Itabashi, H., Ushida, K., Yano, H. and Sasaki, Y. (eds.), Japan Science Society Tokyo/Karger, Basel. *Rumen Microbes and Digestive Physiology in Ruminants* **14**, 47–57.

Kang, D., Gho, Y.S., Suh, M. and Kang, C. (2002) Highly sensitive and fast protein detection with Coomassie Brilliant Blue in sodium dodecyl sulfate-polyacrylamide gel electrophoresis. *Bulletin of the Korean Chemical Society* **23** (11), 1511-1512.

Laemmli, U.K. (1970) Cleavage of structural proteins during the assembly of the head of bacteriophage T4. *Nature* **227** 680-685.

Lebuhn, M., Liu, F., Heuwinkel, H. and Gronauer, A. (2008) Biogas production from mono-digestion of maize silage-long-term process stability and requirements. *Water Science and Technology* **58** (8), 1645-1651.

Lowry, O.H., Rosebrough, N.J., Farr, A.L. and Randall, R.J. (1951) Protein measurement with the Folin-Phenol reagents. *J Biol.Chem* **193** 265-275.

Maestrojuán, G.M., Boone, D.R., Xun, L., Mah, R.A. and Zhang, L. (1990) Transfer of *Methanogenium bourgense, Methanogenium marisnigri, Methanogenium olentangyi*, and *Methanogenium thermophilicum* to the Genus *Methanoculleus* gen. nov., Emendation of *Methanoculleus marisnigri* and *Methanogenium*, and Description of New Strains of *Methanoculleus bourgensis* and *Methanoculleus marisnigri*. *Int. J. Systematic Bacteriology* **40** (2), 117-122.

Onyenwoke, R.U., Vadim, V.K., Anatolly, M.L. and Wiegel, J. (2007) *Thermoanaerobacter pseudethanolicus* sp. nov., a thermophilic heterotrophic anaerobe from Yellowstone National Park. *International Journal of Systematic and Evolutionary Microbiology* **57**, 2191–2193.

Pobeheim,H., Munk,B., Johansson,J., and Guebitz,G.M. (2010) Influence of trace elements on methane formation from a synthetic model substrate for maize silage. *Bioresource Technology* **101** (2), 836-839.
Pobeheim,H., Munk,B., Mueller,H., Berg,G., and Guebitz,G.M. (2010) Characterization of an anaerobic population digesting a model substrate for maize in the presence of trace metals. *Chemosphere* **80** (8), 829-836.

Shevchenko, A., Wilm, M., Vorm, O., and Mann, M. (1996) Mass Spectrometric Sequencing of Proteins from Silver-Stained Polyacrylamide Gels. *Analytical Chemistry* **68** (5), 850-858.

Stahl, D.A. and Amann, R. (1996) Development and application of nucleic acid probes. In: Stackebrandt,E. and Goodfellow,M. (eds), *Nucleic Acid Techniques in Bacterial Systematics* 205-248, John Wiley & Sons Ltd., Chichester.

Takashima, M. and Speece, R.E. (1989) Mineral nutrient requirements for high-rate methane fermentation of acetate at low SRT. *Journal of the Water Pollution Control Federation* **61**, 1645–1650.

Van Gylswyk, N.O. and van der Toorn, J.J.T.K. (1986) Enumeration of *Bacteroides succinogenes* in the rumen of sheep fed maize-straw diets. *FEBS Letters* **38** (4), 205-209.

Weiß, S., Tauber, M., Somitsch, W., Meincke, R., Müller, H., Berg, G. and Guebitz, G.M. (2010) Enhancement of biogas production by addition of hemicellulolytic bacteria immobilised on activated zeolite. *Water Research* **44** (6), 1970-1980.

Weiß, S., Zankel, A., Lebuhn, M., Petrak, S., Somitsch, W. and Guebitz, G.M. (2011) Investigation of mircroorganisms colonising activated zeolites during anaerobic biogas production from grass silage. *Bioresource Technology* **102** (6), 4353-4359.
Wichern, M., Gehring, T., Fischer, K., Andrade, D., Luebken, M., Koch, K., Gronauer, A. and Horn, H. (2009) Monofermentation of grass silage under mesophilic conditions: Measurements and mathematical modeling with ADM 1. *Bioresource Technology* **100** (4), 1675-1681.

Yu, Y., Lee, C., Kim, J. and Hwang, S. (2005) Group-specific primer and probe sets to detect methanogenic communities using quantitative real-time polymerase chain reaction. *Biotechnology and Bioengineering* **89** (6), 670-679.

Zverlov, V.V., Hiegl, W., Köck, D.E., Kellermann, J., Köllmeier, T. and Schwarz, W.H. (2010) Hydrolytic bacteria in mesophilic and thermophilic degradation of plant biomass. *Engineering in Life Sciences* **10** (6), 528-536.

General conclusion

The anaerobic microbial micro cosmos on the natural carrier material zeolite (i.e. clinoptilolite) was investigated by using a combination of sophisticated microscopy techniques, molecular fingerprinting methods and proteomics. Scanning electron (SEM) and confocal laser scanning microscopy (CLSM) gave optical evidence of microbes preferring clinoptilolite surfaces as operational environment, showing biofilm formation and microbial cell morphology and taxonomic relationships. Furthermore, cluster- and sequencing analyses verified microbial populations associated with clinoptilolites as well as differentiating specific microbial groups preferring the carrier material from substrate bound and inoculation liquid borne populations. Enzyme activity tests assaying clinoptilolite associated and free extracellular enzymes involved in the plant cell wall degradation process confirmed hydrolytically active cellulase, xylanase and even pectinase. This was not only documented during the ongoing fermentation experiments, but additionally after long-term storage of pre-colonised clinoptilolite particles revealing a strong revitalisation ability of the immobilised microbial populations. The enzymes identified during the proteomics approach elucidated the spectrum of hydrolytically active enzymes including several types of exo- and endo-acting extracellular enzymes produced by anaerobic and facultative anaerobic microorganisms. Information about the functional role of microbial colonisers was complementing the community analyses through data base acquired comparisons of related microbial enzyme producers that were also identified via the DNA-based screening.

The cell adhesion to the surface of clinoptilolites and their influence on growth and enzyme synthesis as operational environment during subsequent fermentation stages were studied extensively. Herein, the colonisation of clinoptilolite particles by microorganisms was demonstrated, revealing spontaneous adhesion preferentially to sheltered topographic depression sides such as pits of the cratered surface, but also area wide biofilm formation was observed. Two dominant cell morphologies were present (i) long rod-shaped cells which occurred as single cells and (ii) shorter bacillary cells developing anchoring and cell-to-cell connecting pili and formed dense biofilm-like aggregations.

Confocal laser scanning microscopy using FISH did further help to investigate the localisation of clinoptilolite associated microbes. DNA-based probes and three-

dimensional reconstruction of clinoptilolite particles in powdery form proved that the colonisation was not only taking place on external surfaces, but also inside the nano-porous clinoptilolite structure as bacteria-specific signals were detected throughout the entire particle thickness as confirmed by scanning the specimen in layers. It is likely that bacteria entered voids and channels of the regularly formed framework as performed by cations. The molecular community screening unravelled information about the populations and concrete microbial participants involved in the natural colonisation process. (i) Populations found on clinoptilolites were forming a distinct cluster as confirmed by comparative fingerprint pattern analysis, i.e. zeolite associated population's fingerprint was significantly different from that one of populations found on substrate fibre surfaces or the inoculation liquid, which showed the most complex fingerprints with the highest number of bands, i.e. microorganisms. From this it follows that only a specific group left the free roaming consortium to settle down on clinoptilolite surfaces, apart from those conquering grass silage based plant material. (ii) Colonies adherent to clinoptilolite surfaces were composed of well known cell wall degrading fermentative bacteria representatives of the orders Clostridiales, Bacteroidales, Bacillales and Pseudomonadales on the one hand and methanogenic archaea of the hydrogenotrophic order Methanomicrobiales known to be predominant in biogas-producing communities due to their comparatively fast growth rates on the other. This neighbouring existence argues for the syntrophy (e.g. cross-feeding of hydrogen) between members of both domains, which are naturally co-existing in biogas-producing consortia and evidentially co-aggregated on clinoptilolites as well. Thus clinoptilolites serve as an exclusive operational environment in the biogas production process.

In addition, cultivation experiments attempted to force the enrichment of hydrolytic populations out of a natural mixed biogas consortium in order to enhance the hydrolysis of recalcitrant biomass during the fermentation process. It was shown that cellulolytic and hemicellulolytic populations within mixed fermentative microbial communities could be enforced by substrate determination using the hemicellulose xylan, which is most abundant in rural plant cell walls. Hence it can be concluded that the interaction of hydrolytic bacteria with certain substrates predisposes their growth and regulates the biosynthesis of their enzymes, leading to an induction of hydrolytic enzymes responding to the carbon source provided. The specific development of a hydrolytic population was confirmed by cluster analyses revealing a fingerprint

significantly distinctive from the natural bacteria community composition. Foremost abundant were the genera *Bacteroides*, *Azospira* and a broad spectrum of diverse *Clostridium* species. It was furthermore possible to use clinoptilolite as carrier material by a plain immobilisation strategy. Enriched cultures were collected through centrifugation and re-suspended in a medium containing clinoptilolite in powdery form. This led to a proper mixture of microorganisms and clinoptilolite particles. The immobilisation was completed by air-drying of the re-collected material, which could be straightforwardly stored and used. Introducing this microbial-advanced mineral in laboratory batch experiments led to a significant increase of methane yields during the fermentation of simple xylan powder from a natural source compared to the addition of microorganisms-free clinoptilolite. Since increased methane production was correlated with risen concentrations of acetic acid as revealed by high performance liquid chromatography, it can be concluded that the acetogenic fermentation phase, i.e. acetogenesis was enforced as a result of an enhanced hydrolysis rate due to additionally introduced pre-cultured xylanolytical bacteria. Going down the way, two scenarios are assumable to explain the resulting methane formation after this change in the fermentation process: (i) either higher methane formation was due to the direct conversation of acetic acid in the terms of the acetoclastic methanogenesis pathway or (ii) acetic acid was not consumed but accumulated, which would argue for the second possible final conversion step depending on hydrogen for the direct hydration of carbon dioxide, i.e. the hydrogenotrophic pathway. However, this strategy demonstrates an easy form of application that offers a great potential for exerting an influence during the ongoing fermentation process, although further investigations on complex natural substrates including crystalline cellulose and lignocelluloses are required to study the absolute efficiency of microbial-advanced clinoptilolite composites. The application of supplemental introduced immobilised bacteria might reduce the need for substrate pre-treatments or even expands the spectrum of accessibility to recalcitrant agricultural biomass and residues for an economic use in the production of biogas. It can finally be concluded that trace metal activated clinoptilolites are eminently suited as natural carriers for microorganisms, potentially enhancing the methane production process from recalcitrant plant biomass.

References

Amann, R.I., Ludwig, W. and Schleifer, K.-H. (1995) Phylogenetic identification and *in situ* detection of individual microbial cells without cultivation. *Microbiological Reviews* **59**, 143-169.

Ames, L.L. (1960) The cation sieve properties of clinoptilolite. *American Mineralogist* **45**, 689-700.

Ames, L.L. (1961) Cation sieve properties of the open zeolite, chabazite, mordenite, erionite and clinoptilolite. *American Mineralogist* **46**, 1120-1131.

Ames, L.L. (1964) Some zeolite equilibria with alkali metal cations. *American Mineralogist* **49**, 127-145.

Amon, T., Amon, B., Kryvoruchko, V., Zollitsch, W., Mayer, K., Gruber, L. (2007) Biogas production from maize and dairy cattle manure – influence of biomass composition on the methane yield. *Agriculture, Ecosystems and Environment* **118**, 173-182.

Amon, T., Kryvoruchko, V., Amon, B., Moitzi, G., Lyson, D., Hackl, E., Jeremic, D., Zollitsch, D. and Pötsch, E. (2003) Optimierung der Biogaserzeugung aus den Energiepflanzen Mais und Kleegras. *Bundesministerium für Land- und Forstwirtschaft, Umwelt- und Wasserwirtschaft* **77**, 1-10.

Angelidaki, I., Ellegaard, L. and Ahring, B. K. (1993) A mathematical model for dynamic simulation of an anaerobic digestion of complex substrates: focusing on ammonia inhibition. *Biotechnology and Bioengineering*, **42** (2), 159-166.

Armbruster, T. and Gunter, M.E. (2001) Crytal structures of natural zeolites. In: Bish, D.L. and Ming, D.W. (eds.) Natural Zeolites: occurrence, properties, applications. *Reviews in Mineralogy and Geochemistry* **45**, 1-57.

Aspinall, G.O. (1981) In: Tanner, W., Loewus, F.A. (eds.) Plant carbohydrates – Extracellular Carbohydrates. *Encyclopaedia of Plant Physiology*, New Series **13**B, 3-8.

Azuma, J.-I., Takahashi, N. And Koshijima, T. (1981) Isolation and characterisation of lignin-carbohydrate complexes from the milled-wood lignin fraction of Pinus densiflora Sieb et Zucc. *Carbohydrate Research* **93**, 91-104.

Barrer, R.M., Papadopoulos, R. and Rees, L.V.C. (1967) Exchange of sodium in clinoptilolite by organic cations. *Journal of Inorganic and Nuclear Chemistry* **29**, 2047-2063.

Barrer, R.M. (1978) Cation-exchange equilibria in zeolites and feldspathoids. In: Sand, L.B. and Mumpton, F.A. (eds.) *Natural Zeolites: occurrence, properties, use*. Pergamon, New York, 385-395.

Bayer, E.A., Chanzy, H., Lamed, R. And Shoham, Y. (1998) Cellulose, cellulases and cellulosomes. *Current Opinion in Structural Biology* **8**, 548-557.

Baykal, B.B. and Guven, D.A. (1997) Performance of clinoptilolite alone and in combination with sand filters for removal of ammonia peaks from domestic wastewater. *Water Science Technology* **35**, 47-54.

Biely, P., Vršanská, M. and Krátký, Z. (1980) Xylan-degrading enzymes of the yeast *Cryptococcus albidus* – identification and cellular localisation. *European Journal of Biochemistry* **108**, 313-321.

Biely, P., MacKenzie, C.R., Puls, J. and Schneider, H. (1986) Cooperativity of esterases and xylanases in the enzymatic degradation of acetyl xylan. *Bio/Technology* **4**, 731-733.

Biswas, J., Chowdhury, R. and Bhattacharya, P. (2005) Kinetic studies of biogas generation using municipal waste as feed stock. *Enzyme and Microbial Technology.*, **38**, 493-503.

Blanchard, G., Maunaye, M. and Martin, G. (1984) Removal of heavy metals from water by means of natural zeolites. *Water Research* **18**, 1501-1507.

Bowie, M.R. Barker, J.M. and Peterson, S.L. (1987) Comparison of selected zeolite deposits of Arizona, New Mexico and Texas. *Special Paper - State of Arizona, Bureau of Geology and Mineral Technology* **4**, 90-105.

Breck, D.W. (1974) Zeolite molecular sieves – structure, chemistry and use. John Wiley and Sons, New York, 771 p.

Brett, C. and Waldron, K. (1990) In: *Physiology and Biochemistry of Plant Cell Walls*. London: Unwin Hyman, 72.

Caldwell, D.E., Korber, D.R. and Lawrence, J.R. (1992) Confocal laser microscopy and digital image analysis in microbial ecology. In: Marhall, K.C. (ed.) *Advances in microbial ecology* **12**. Plenum Press, New York, 1-67.

Candrian, U. (2005) Polymerase chain reaction in food microbiology. *Journal of Microbiological Methods* **23**, 89-103.

Claeyssens, M. and Aerts, G. (1992) Characterisation of cellulolytic activities in commercial *Trichoderma reesei* preparations: an approach using small, chromogenic substrates. *Bioresource Technology* **39**, 143-146.

Chesson, A. and Forsberg, C.W. (1988) In: Hobson, P.N. (ed.) *The Rumen Microbial Ecosystem*. New York, Elsevier Applied Science, 251-283.

Constant, M. Naveau, H., Ferrero, G. L. and Nyns, E. J. (1989) Biogas - end-use in the European community. *Elsevier Science Publisher*, New York, 1-346.

Crosland-Taylor, P.J. (1953) A device for counting small particles suspended in a fluid through a tube. *Nature* **171**, 37-38.

Debzi, E. M., Chanzy, H., Sugiyama, J., Tekely, P. and Excoffier, G. (1991) The Iα to Iβ transformation of highly crystalline cellulose by annealing in various mediums. *Macromolecules* **24**, 6816-6822.

Devinny, J. S. (1999) *Biofiltration for air pollution control.* Deshusses M. A., Webster T. S. (eds.), CRC Lewis, Boca Raton, Florida, USA.

Diaper, J.P., Tither, K. and Edwards, C. (1992) Rapid assessment of bacterial viability by flow cytometry, *Applied Microbiology and Biotechnology* **38**, 268-272.

Dubois, B., Gilles, K.A., Hamilton, J.K., Rebers, P.A. and Smith, F. (1956) Colorimetric method for determination of sugars and relative substances. *Analytical Chemistry* **28**, 350-360.

Eder, B. and Schulz, H. (2006) *Biogas Praxis: Grundlagen, Planung, Anlagenbau, Beispiele, Wirtschaftlichkeit*. Ökobuch, Staufen, Germany ISBN: 3-936896-13-5 **3**, 25.

Fengel, D. (1971) Ideas on ultrastructural organisation of cell-wall components. *Journal of Polymer Science* Part C **36**, 383-392.

Fischer, S.G. and Lerman, L.S. (1983) DNA fragments differing by single base-pair substitutions are separated in denaturing gradient gels: correspondence with melting theory. *Proceedings of the National Academy of Sciences*, USA **80**, 1579-1583.

Fodor, S.P., Rava, R.P., Huang, X.C., Pease, A.C., Holmes, C.P. and Adams, C.L. (1993) Multiplexed biochemical assays with biological chips. *Nature* **364**, 555-556.

Forsberg, C.W., Lam, K. (1977) Use of Adenosine 5'-Triphosphate as an indicator of the microbiota biomass in rumen contents. *Applied Environmental Microbiology* **33**, 528-537.

Freudenberg, K. (1968) The constitution and biosynthesis of lignin. In: Freudenberg, K. and Neish, A.C. (eds.) *Constitution and Biosynthesis of Lignin*. Springer, Berlin, 45-122.

Gabriel, D. and Deshusses, M.A. (2003) *Proceedings of the National Academy of Sciences*, USA **100**, 6308-6312.

Galindo, C., Ming, D.W., Morgan, A. and Pickering, K. (2000) Use of Ca-saturated clinoptilolite for ammonium from NASA's advanced life support wastewater system. In: Colella, C. and Mumpton, F.A. (eds.) De Frede, Naples, *Natural Zeolites for the Third Millenium*, 363-371.

Ghose, T.K. (1987) Measurement of cellulase activities. *Pure and Applied Chemistry* **59**, 257-268.

Gottardi, G. And Galli, E. (1985) Natural zeolites. Springer, Berlin, Heidelberg, New York, Tokyo, *Minerals and Rocks Series* **18**, XII-409 pp.

Grigorieva, L.V., Salata, O.V., Kolesnikov, V.G. and Malakhova, L.A. (1988) Effectiveness of the sorptive and coagulational removal of enteric bacteria and viruses from water. *Khimiya i Tekhnoliya Vody* **10**, 458-461.

Gunter, M.E., Armbruster, T., Kohler, T. and Knowles, C.R. (1994) Crystal structure and optical properties of Na- and Pb-exchanged heulandite-group zeolites. *American Mineralogist* **79**, 675-682.

Gürtler, V. and Stanisich, V.A. (1996) New approaches to typing and identification of bacteria using the 16S-23S rDNA spacer region. *Microbiology* **142**, 3-16.

Haigler, C.H. (1985) In: *Cellulose Chemistry and its Applications*. Nevell, T.P. and Zeronian, S.H. (eds.) Ellis Horwood Limited, Chichester, 30-83.

Halling-Soerensen, B. and Hjuler, H. (1992) Simultaneous nitrification and denitrification with an upflow fixed bed reactor applying clinoptilolite as media. *Water Treatment* **7**, 77-88.

Hammel, K.E., Jensen, K.A., Mozuch, M.D., Landucci, L.L., Tien, M. and Pease, E.A.J. (1993) Ligninolysis by a purified lignin peroxidase. *Journal of Biological Chemistry* **268**, 12274-12280.

Hammel, M., Fierobe, H.P., Czjzek, M., Kurkal, V., Smith, J.C., Bayer, E.A., Finet, S. and Receveur-Brechot, V. (2005) Structural basis of cellulosome efficiency explored by small angle X-ray scattering. *Journal of Biological Chemistry* **280,** 38562–38568.

Hayashi, K. (1991) PCR-SSCP: a simple and sensitive method for detection of mutations in a genomic DNA. *PCR Methods and Applications* **1**, 34-38.

Heller, M.C., Keoleian, G.A. and Volk, T.A. (2003) Life cycle assessment of a willow bioenergy cropping system. *Biomass Bioengery* **25**, 147-165.
Hespel, R.B. (1988) Microbial digestion of hemicelluloses in the rumen. *Microbiological Sciences* **5** (12), 362-265.

Higuchi, T., Ioto, Y., Shimada, M. and Kawamura, I. (1967) Chemical properties of milled wood lignin of grasses. *Phytochemistry* **6**, 1551-1556.

Higuchi, T. (1990) Lignin biochemistry: biosynthesis and biodegradation. *Wood Science and Technology* **24**, 23-63.

Howery, D.G. and Thomas, H.C. (1965) Ion-exchange on the mineral clinoptilolite. *Journal of Physical Chemistry* **69**, 531-537.

Jama, M.A. and Yucel, H. (1990) Equilibrium studies of sodium-ammonium, potassium-ammonium and calcium-ammonium exchanges on clinoptilolite zeolite. *Separation Science and Technology* **24**, 1393-1416.

Jarvis, M. (2003) Cellulose stacks up. *Science* **426**, 611-612.

Kalló, D. (2001) Application of natural zeolites in water and wastewater treatment. In: Bish, D.L. and Ming, D.W. (eds.) Natural Zeolites: occurrence, properties, applications. *Reviews in Mineralogy and Geochemistry* **45**, 519-550.

Kang, S.J. (1989) Characterisation of ammonium and zinc(2+) ion adsorption by Korean natural zeolites. *Han'guk Nonghwa Hackhoechi* **32**, 386-392.

Kesraoui-Ouki, S., Cheeseman, C.R. and Perry, R. (1994) Natural zeolite utilisation in pollution control: a review to applications to metal effluents. *Journal of Technology and Biotechnology* **59**, 121-126.

Kepner, R.L.J. and Pratt, J.R. (1994) Use of fluorochromes for direct enumeration of total bacteria in environmental samples: past and present. *Microbiological Reviews* **58**, 603-615.

Khan, A.W., Tremblay, D. and Le Duy, L. (1986) Assay of xylanase and xylosidase activities in bacterial and fungal cultures. *Enzyme and Microbial Technology* **8**, 373-377.

Kidby, D.K. and Davidson, D.J. (1973) A convenient ferricyanide estimation of reducing sugars in the nanomole range. *Analytical Biochemistry* **55**, 321-325.

Kuhad, R.C., Singh, A. and Eriksson, K.E. (1997) Microorganisms enzymes involved in the degradation of plant fiber cell walls. *Advances in Biochemical Engineering / Biotechnology* **57**, 45-125.
Lamport, D.T.A. (1970) Cell wall metabolism. *Annual Review of Plant Physiology* **21**, 235-270.

Lawrence, J.R., Korber, D.R., Hoyle, B.D., Costerton, J.W. and Caldwell, D.E. (1991) Optical sectioning of microbial biofilms. *Journal of Bacteriology* **173**, 6558-6567.

Lee, D.H., Zo, Y.-G. and Kim, S.J. (1996) Non-radioactive method to study genetic profiles of natural bacterial communities by PCR-single-strand-conformation polymorphism. *Applied Environmental Microbiology* **62**, 3112-3120.

Lever, M. (1972) A new reaction for colorimetric determination of carbohydrates next term. *Analytical Biochemistry* **47**, 273-279.

Lockhart, D.J., Dong, H., Byrne, M.C., Folletti, M.T., Gallo, M.V., Chee, M.S., Mittmann, M., Wang, C., Kobayashi, M., Horton, H. and Brown, E.L. (1996) Expression monitoring by hybridisation to high-density oligonucleotides arrays. *Nature Biotechnology* **14**, 1675-1680.

Loewenstein, W. (1954) The distribution of aluminium in the tetrahedra of silicates and aluminates. *American Mineralogist* **39**, 92-96.

Loizidou, M. and Townsend, R.P. (1987) Exchange of cadmium into the sodium and ammonium forms of the natural zeolite clinoptilolite, mordenite and ferrierite. *Journal of the Chemical Society, Dalton Transactions*, 1911-1916.

Lundquist, K., Simonson, R. and Tingsvik, K. (1983) Lignin-carbohydrate linkages in milled wood lignin preparations from spruce wood. *Svensk Papperstid*, 44-47.

Macchi, E. and Palma, A. (1969) Morphological studies on precipitated cellulose. *Die Makro-molekulare Chemie* **123**, 286-288.

Mazur, G.A., Medvid, G.K. and Grigora, T.I. (1984) Use of natural zeolites for increasing the fertility of light-textured soils. *Pochvovedenie* **10**, 70-77.

Meier, W.M., Olson, D.H. and Baerlocher, C. (1996) Atlas of zeolite structure types: 4th revised Edition. *Zeolites* **17**, 1-230.

Miller, G.L. (1959) Use of dinitrosalicylic acid reagent for determination of reducing sugar. *Analytical Chemistry* **31**, 426-428.

Ming, D.W. and Allen, E.R. (1999) Zeoponic substrates for space applications: advances in the use of natural zeolites for plant growth. In: Misaelides, P., Macásek, F., Pinnavaia, T.J. and Colella, C. (eds.) Natural microporous materials in environmental technology. Kluwer Academic, Dordrecht. *NATO Advanced Science Institute Series* E **362**, 157-176.

Ming, D.W. and Allen, E.R. (2001) Use of natural zeolites in agronomy, horticulture and environmental soil remediation. In: Bish, D.L. and Ming, D.W. (eds.) Natural Zeolites: occurrence, properties, applications. *Reviews in Mineralogy and Geochemistry* **45**, 619-654.

Morosoli, R., Bertrand, J.L., Mondou, F., Sharek, F. and Kluepfel, D. (1986) Purification and properties of a xylanase from *Streptomyces lividans*. *Biochemical Journal* **239**, 587-592.

Møller, H. B., Nielsen, A. M., Murto, M., Christensson, K., Rintala, J., Svensson, M., Seppälä, M., Paavola, T., Angelidaki, I. and Kaparaju, P. L. (2008) Manure and energy crops for biogas production - Status and barriers. *Accepeted for publication by Nordic council of Ministers, MJS – Milijöstrategier för jord- och skogsbruk*, Denmark.

Mukoyoshi, S.I., Azuma, J.L. and Koshijima, T. (1981) Lignin-carbohydrate complexes from compression wood of Pinus densiflora Sieb et Zucc. *Holzforschung* **35**, 233-240.

Mullis, K., Faloona, F., Scharft, S., Saiki, R., Horn, G. and Erlich, H. (1986) Specific enzymatic amplification of DNA *in vitro*: the polymerase chain reaction. *Cold Spring Harbor Symposia on Quantitative Biology* **51**, 263-273.

Nelson, N. (1944) A photometric adaptation of the Somogyi method for the determination of glucose. *Journal of Biological Chemistry* **153**, 375-380.

Nevell, T.P. and Zeronian, S.H. (1985) In: *Cellulose Chemistry and its Applications*. Nevell, T.P. and Zeronian, S.H. (eds.) Ellis Horwood Limited, Chichester, 15-29.

Nishiyama Y, Sugiyama J, Chanzy H, Langan P. (2003) Crystal structure and hydrogen bonding system in cellulose Ia from aynchrotron X-ray and neutron fiber diffraction. *Journal of the American Chemical Society* **125** (47), 14300–14306.

Notley SM, Pettersson B,Wagberg L. (2004) Direct measurement of attractive van der Waals' forces between regenerated cellulose surfaces in an aqueous environment. *Journal of the American Chemical Society* **126** (43), 13930–13931.

Noyola, A., Morgan-Sagastume, J. M. and López-Hernández, J. E. (2006). Treatment of biogas produced in anaerobic reactors for domestic wastewater: odor control and energy/resource recovery. *Reviews in Environmental Science and Bio/Technology* **5**, 93-114.

Ohmiya, K., Sakka, K., Kimura, T. and Morimoto, K. (2003) Application of microbial genes to recalcitrant biomass utilisation and environmental conservation. *Journal of Bioscience and Bioengineering* **95** (6), 549-561.

Oksanen, T. Pere, J., Paavilainen, L., Buchert, J. and Viikari, L. (2000) Treatment of recycled kraft pulps with *Trichoderma reesei* hemicellulases and cellulases. *Journal of Biotechnology* **78**, 39-48.

Olsen, G.J., Lane, D.J., Giovannoni, S.J., Pace, N.R. and Stahl, D.A. (1986) Microbial ecology and evolution: a ribosomal RNA approach. *Annual Review of Microbiology* **40**, 337-365.

Orita, M., Iwahana, H., Kanazawa, H., Hayashi, K. and Sekiya, T. (1989) Detection of polymorphisms of human DNA by gel electrophoresis as single-strand conformation polymorphisms. *Proceedings of the National Academy of Sciences*, USA **86**, 2766-2770.

O'Sullivan, A.C. (1997) Cellulose: the structure slowly unravels. *Cellulose* **4**, 173-207.

Otterstedt, J.E., Schoeman, B. and Sterte, J. (1989) Effective zeolites remove ammonia from sewage. *Kemisk Tidskrift* **101** (13), 49-56.

Pabalan, R.T. (1994) Thermodynamics of ion-exchange between clinoptilolite and aqueous solutions of Na^+/K^+ and Na^+/Ca^{2+}. *Geochimica et Cosmochimica Acta* **58**, 4573-4590.

Pabalan, R.T. and Bertetti, F.P. (1999) Experimental and modelling study of ion-exchange between aqueous solutions and the zeolite mineral clinoptilolite. *Journal of Solution Chemistry* **28**, 367-393.

Pabalan, R.T. and Bertetti, F.P. (2001) Cation-exchange properties of natural zeolites. In: Bish, D.L. and Ming, D.W. (eds.) Natural Zeolites: occurrence, properties, applications. *Reviews in Mineralogy and Geochemistry* **45**, 453-517.

Parham, W.E. (1984) Future perspectives for natural zeolites in agriculture and aquaculture. In: Pond, W.G. and Mumpton, F.A. (eds.) Westview, Boulder, Colorado. *Zeo-Agriculture: Use of Natural Zeolites in Agriculture and Aquaculture*, 283-285.

Park, J.T. and Johnson, M.J. (1949) A sub micro determination of glucose. *Journal of Biological Chemistry* **181**, 149-151.

Passaglia, E. and Azzolini, S. (1994) Italien zeolites in wastewater purification: influence of zeolite exchangeable cations on NH_4^+ removal from swine sewage. *Mater Engineering* **5**, 343-355.

Pauling, L. (1939) The nature of the chemical bond and the structure of molecules and crystals. Cornell University Press, Ithaca, New York, 420.

Power, E.G.M. (1996) RAPD typing in microbiology – a technical review. *Journal of Hospital Infection* **34**, 247-265.

Ploem, J.S. (1967) The use of a vertical illuminator with interchangeable dichroic mirrors for fluorescence microscopy with incident light. *Zeitschrift fur wissenschaftliche Mikroskopie und mikroskopische Technik* **68**, 129-142.

Redondo, R., Machado, V.C., Baeza, M., Lafuente, J. and Gabriel, D. (2008) On-line monitoring of gas-phase bioreactors for biogas treatment: hydrogen sulfide and sulfide analysis by automated flow systems. *Analytical and Bioanalytical Chemistry* **391** (3), 789-798.

Reischl, U. and Kochanowski, B. (1995) Quantitative PCR – a survey of the present technology. *Molecular Biotechnology* **3**, 55-71.

Resch, C., Braun, R. and Kirchmayr, R. (2008) The Influence of energy crop substrates on the mass-flow analysis and the residual methane potential at a rural anaerobic digestion plant. *Water Science Technology* **57** (1), 73-81.

Robson, L.M. and Chambliss, G.H. (1989) Cellulases of bacterial origin. *Enzyme and Microbial Technology* **11**, 626.

Rolfs, A., Schuller, I., Finckh, U. and Weber-Rolfs, I. (1992) Detection of single base changes using PCR. In: Rolfs, A., Schuller, I., Finckh, U. and Weber-Rolfs, I. (eds.) *PCR: clinical diagnostics and research*. Springer, Berlin, Heidelberg, New York, 149-167.

Roose-Amsaleg, C.L., Garnier-Sillam, E. and Harry, M. (2001) Extraction and purification of microbial DNA from soil and sediment samples. *Applied Soil Ecology* **18**, 47-60.

Rosenbaum, V. and Riesner, D. (1987) Temperature-gradient gel electrophoresis – Thermodynamic analysis of nuclei acids and proteins in purified form in cellular extracts. *Biophysical Chemistry* **26**, 235-246.

Saha, B.C. (2003) Hemicellulose bioconversion. *Journal of Industrial Microbiology and Biotechnology* **30** (5), 279-291.

Saiki, R.K., Scharf, S., Faloona, F., Mullis, K.B., Erlich, H.A. and Arnheim N. (1985) Enzymatic amplification of beta-globin genomic sequences and restriction site analysis for diagnosis of sickle cell anemia. *Science* **230** (4732), 1350–1354.

Sasaki, K. and Taylor, I.E.P. (1984) Specific labelling of cell-wall polysaccharides with myo-[2-H-3]-inositol during germination and growth of *Phaseolus vulgaris* L.. *Cell Physiology* **25**, 989-997.

Saulnier, L. and Thibault, J.-F. (1999) Review: ferulic acid and diferulic acids as components of sugar-beet pectins and maize bran heteroxylans. *Journal of the Science of Food and Agriculture* **79**, 396-402.

Schena, M., Shalon, D., Davis, R.W. and Brown, P.O. (1995) Quantitative monitoring of gene expression patterns with a complementary DNA microarray. *Science* **270**, 467-470.

Schmidt, O. and Kebernik, U. (1988) A simple assay with dyed substrates to quantify cellulase and hemicellulase activity of fungi. *Biotechnology Techniques* **2**, 153-158.

Schöftner, R., Valentin, K., Schmiedinger, B., Trogisch, S., Haberbauer, M., Katzlinger, K., Schnitzhofer, W. and Weran, N. (2007) Monitoring und Benchmarks zur Etablierung eines Qualitätsstandards für die Verbesserung des Betriebs von Biogasanlagen und Aufbau eines österreichweiten Biogasnetzwerks. In: Paula, M. (ed.) Bundesministerium für Verkehr,Innovation und Technologie,Abteilung für Energie- und Umwelttechnologien. *Berichte aus Energie- und Umweltforschung* **45**, 1-132.

Schwarz, W., Chan, M., Breuil, C. and Saddler, J.N. (1988) Comparison of HPLC and colorimetric methods for measuring cellulolytic activity. *Applied Microbiology and Biotechnology* **28**, 398-403.

Schwarz,W.H. (2001) The cellulosome and cellulose degradation by anaerobic bacteria. *Applied Microbiology and Biotechnology* **56**, 634-649.

Schwarz, W.H., Bronnenmeier, K., GrSbnitz, F. and Staudenbauer, W.L. (1987) Activity staining of cellulases in polyacrylamide gels containing mixed linkage beta-glucans. *Analytical Biochemistry* **164** (1), 72-77.

Schwartz, D.C. and Cantor, C.R. (1984) Separation of yeast chromosome-sized DNAs by pulsed field gradient gel electrophoresis. *Cell* **37** (1), 67–75.

Selvakumar, N., Ding, B.C. and Wilson, S.M. (1997) Separation of DNA strands facilitates detection of point mutations by PCR-SSCP. *Biotechnology* **22**, 604-606.

Semmens, M.J. and Seyfarth, M. (1978) The selectivity of clinoptilolite for certain heavy metals. In: Sand, L.B. and Mumpton, F.A. (eds.) *Natural Zeolites: occurrence, properties, use*. Pergamon, Oxford, 517-526.

Sheppard, R.A. (1985) Death Valley-Ash Meadows zeolite deposit, California and Nevada. In: Clays and Zeolites – Los Angeles, California to Las Vegas, Nevada. *International Clay Conference Field Trip Guidebook*, 51-55.

Sheppard, R.A. and Hay, R.L. (2001) Formation of zeolites in open hydrologic systems. In: Bish, D.L. and Ming, D.W. (eds.) Natural Zeolites: occurrence, properties, applications. *Reviews in Mineralogy and Geochemistry* **45**, 261-273.

Shoham, Y., Lamed, R. and Bayer, E.A. (1999) The cellulosome concept as an efficient microbial strategy for the degradation of insoluble polysaccharides. *Trends in Microbiology* **7** (7), 275-281.

Somogyi, M. (1952) Notes on sugar determination. *Journal of Biological Chemistry* **195**, 19-23.

Söldner, F., Garcia Barquero, C., Tricas Aizpun, A., van Honacker, H., Ciupek, A., Rapacz, P., Vu Duc, H, Leinemann, F., Butler, V., Poinelli, M., Winkler, W., Hodson, P., Deurwaarder, E., Barreiro Hurle, J., Wrzesinska, M., Codrea, C., Bernard-Brunet, P., Buatas Costa, E., Chiron, D., Haag, M., Gialoglou, K., Lonza, L., Nemry, F., Schosger, J.-P., Jensen, P. (2011) *Report of the European expert group on future transport fuels*.

Stahl, D.A. and Capman, W.C. (1994) Applications of molecular genetics to the study of microbial communities. *NATO ASI Series* **35**, 193-206.

Stephen, A.M. (1983) In: Aspinall, G.O. (ed.) Academic Press, Orlando, Florida. *The Polysaccharides* **2**, 97.

Stugger, S. (1948) Fluorescence microscope examination of bacteria in soil. *Canadian Journal of Research* **26**, 188-193.

Sun, Y. and Cheng, J. (2002) Hydrolysis of lignocellulosic materials for ethanol production: a review. *Bioresource Technology* 83, 1-11.

Tarasevich, Y.I. (1994) Natural, modified and semisynthetic sorbents in water-treatment processes. *Khimiya i Tekhnoliya Vody* **16**, 626-640.

Taylor, D.L., and Salmon, E.D. (1989) Basic fluorescence microscopy. In: Wang, Y.-L. and Taylor, D.L. (eds.) Fluorescence microscopy of living cells in culture. Part A: fluorescent analogs, labelling cells and basic microscopy. *Methods in cell biology* **29**. Academic Press, San Diego, California, 207-237.

Tien, M. and Kirk, T.K. (1983) Lignin-degrading enzyme from Phanerochaete chrysosporium: purification, characterisation and catalytic properties of a unique H_2O_2-requiring oxygenase. *Proceedings of the National Academy of Sciences*, USA **81**, 2280-2284.

Torres, (1999) Ion-exchange between Cd^{2+} solution and clinoptilolite material. Materials Research Society, *12th International Zeolite Conference*, 2371-2377.

Townsend, R.P. and Loizidou, M. (1984) Ion-exchange properties of natural clinoptilolite, ferrierite and mordenite – sodium-ammonium equilibria*. Zeolites* **4**, 191-195.

Uellendahl, H., Wang, G., Møller, H., Jørgensen, U., Skiadas, I. V., Gavala, H. N. and Ahring, B. K. (2008) Energy balance and cost-benefit analysis of biogas production from perennial energy crops pretreated by wet oxidation. *5th International Symposium on Anaerobic Digestion of Solid Wastes and Energy Crops*, May 25 - 28, Hammamet, Tunisia.

Vadas, P. A., Barnett, K. H. and Undersander, D. J. (2008) Economics and energy of ethanol production from alfalfa, corn and switchgrass in the upper Midwest, USA. *Bioenergy Research* **1**, 44-55.

Van Soest, P.J. (1982) Nutritional Ecology of the ruminant. O and B Books, Corvallis, Oregon, 1-374.

Vaneechoutte, M. H., De Beenhouwer, G. Claeys, G. Verschraegen, A. De Rouck, N. Paepe, A. Elaichouni, and F. Portaels. (1993) Identification of *Mycobacterium* species with amplified rDNA restriction analysis. *Journal of Clinical Microbiology* **31**, 2061–2065.

Vaneechoutte, M. H. (1996) DNA fingerprinting techniques for microorganisms. *Molecular Biotechnology* **6**, 115-142.

Verlhac, C., Dedier, J. and Chanzy, H. (1990) Availability of surface hydroxyl groups in Valonia and bacterial cellulose. *Journal of Polymer Science* Part A: Polymer Chemistry **28**, 1171-1177.

Versalovic, J., Koeuth, T. and Lupski, J.R. (1991) Distribution of repetitive DNA sequences in eubacteria and application to fingerprinting of bacterial genomes. *Nucleic Acid Research* **19**, 6823-6831.

Von Wintzingerode, F., Göbel, U.B. and Stackebrandt, E. (1997) Determination of microbial diversity in environmental samples: pitfalls of PCR-based rRNA analysis. *FEMS Microbiological Reviews* **21**, 213-219.

Vos, P. Hoger, R., Bleeker, M., Reijans, M., van de Lee, T., Hornes, M., Frijters, A., Pot, J., Peleman, J., Kuiper, M. and Zabeau, M. (1995) AFLP: a new technique for DNA fingerprinting. *Nucleic Acids Research* **23** (21), 4407-4414.

Vucinic, D.R. (1998) Thermodynamics of the ion-exchange reactions on calcium-clinoptilolite. In: Atak, S. Onal, G. and Celik, M. (eds.) Innovations Mineral Coal Process. *Innovations in Mineral and Coal Processing: Proceedings of the 7th International Mineral Processing Symposium*, 809-814.

Waffenschmidt, S. and Janeicke, L. (1987) Assay of reducing sugars in the nanomole range with 2,2-bicinchoninate. *Analytical Biochemistry* **165**, 337-340.

Wagner, R. (1994) The regulation of ribosomal RNA synthesis and bacterial cell growth. *Archives of Microbiology* **161**, 100-109.

Wallace, G., Chesson, A., Lomax, J.A. and Jarvis, M.C. (1991) Lignin-carbohydrate complexes in graminaceous cell walls in relation to digestibility. *Animal Feeding Science and Technology* **32**, 193-199.

Watanabe, T. And Koshijima, T. (1988) Evidence for an ester linkage between lignin and glucuronic acid in lignin-carbohydrate complexes by DDQ-oxidation. *Agricultural Biology and Chemistry* **52**, 2953-2955.

Welsh, J. and McClelland, M. (1990) Fingerprinting genomes using PCR with arbitrary primers. *Nucleic Acid Research* **25**, 7212-7218.

Wilkie, K.C.B. (1979) The hemicelluloses of grasses and cereals. *Advances in Carbohydrate Chemistry and Biochemistry* **36**, 215-264.

Wirtanen, G, Storgårds, E., Saarela, M., Salo, S. and Mattila-Sandhom, T. (2000) Detection of biofilms in the food and beverage industry. In: Walker, J., Surman, S. and Jass, J. (eds.) *Industrial biofouling – detection, prevention and control*. Wiley, Chichester, 175-204.

Wiselogel, A., Tyson, S. and Johnson, D. (1996) Biomass feedstock resources and composition. In: Wyman, C.E. (ed.), *Handbook on Bioethanol: Production and Utilization*. Taylor and Francis, Washington, DC, 105-118.

Wolfenden, R. and Snider, M.J. (2001) The depth of chemical time and the powder of enzyme as catalysts. *Accounts of Chemical Research* **34**, 938-945.

Wong, D.W.S. (2009) Structure and action mechanism of ligninolytic enzymes*. Applied Biochemistry and Biotechnology* **157**, 174-209.

Wood, T.M. (1975) Properties and modes of action of cellulases. *Biotechnology and Bioengineering Symposium* **5**, 111-137.

Woodcock, K. E. and Gottlieb, M. (2004) *Kirk-Othmer encyclopedia.* John Wiley and Sons, Hoboken, NJ, USA **12**, 377-386.

Woodcock, C. and Sarko, A. (1980) Packing analysis of carbohydrates and polysaccharides: Molecular and crystal structure of native ramie cellulose. *Macromolecules* **13**, 1183-1187.

Yadvika, S., Sreekrishnan, T. R., Kohli, S. and Rana, V. (2004) Enhancement of biogas production from solid substrates using different techniques – a review. *Bioresource Technology* **95**(1), 1-10.

Zhang, Y.H.P. and Lynd, L.R. (2004) Toward an aggregated understanding of enzymatic hydrolysis of cellulose: non-complexed cellulase systems. *Biotechnology and Bioengineering* **88**, 797-824.

Zhang, Y.H.P. and Lynd, L.R. (2005) Determination of the number-average degree of polymerisation of cellodextrins and cellulose with application to enzymatic hydrolysis. *Biomacromolecules* **6**, 1510-1515.

Zhang, Y.H.P., Himmel, M.E. and Mielenz, J.R. (2006) Outlook for cellulase improvement: Screening and selection strategies. *Biotechnology Advances* **24**, 452-481.

Acknowledgment

Grateful acknowledgement is made for giving me the great opportunity to realise my doctoral thesis in a field of science, which is not only fascinating to me, but motivating so many scientists all over the world and which is of such utmost importance to all mankind – the generation of energy by sustainable and renewable means in the course of the ongoing energy source and power supply revolution.

Thank you

Prof. Georg M. Gübitz for being a wise mentor and supervisor.
Prof. Gabriele Berg for leading my way here to the beautiful city of Graz.

This work was not possible without the contribution of extraordinary co-workers.

Thank you very much for your fantastic work

Armin Zankel, Doris Steifer, Magdalena Kaml, Massimiliano Cardinale,
Michael Lebuhn and Ruth Birner-Grünberger

Since social foundations cannot be appreciated enough, I would like to say many thanks to the whole working group and the members of our unique office “V-max”.

Special thanks go to

Annemarie Marold, David Reinsberger, Herbert Pobeheim, Stefan Liebminger
and Teresa Flock

Without you, my day-to-day work would not have been so pleasant and amusing at so many times. Thanks for your support and kindness.

Last but not least, I would like to thank my parents, Sigrid and Hans-Joachim Weiß for always believing in me and supporting my ambitions. Susanne, my wonderful sister, I thank you so much for keeping me from giving up.

Remo, my dearest friend – You are always with me, wherever I go.

Declaration

I declare that I have authored this thesis independently, that I have not used other than the declared sources / resources and that I have explicitly marked all material which has been quoted either literally or by content from the used sources.

Graz, 18.02.2012

Stefan Weiß

Appendum